

**UCLA**

**UCLA Electronic Theses and Dissertations**

**Title**

The Role of Lipids in Pulmonary Alveolar Proteinosis

**Permalink**

<https://escholarship.org/uc/item/8ck3p8sw>

**Author**

Lee, Elinor

**Publication Date**

2020

Peer reviewed|Thesis/dissertation

UNIVERSITY OF CALIFORNIA

Los Angeles

The Role of Lipids in Pulmonary Alveolar Proteinosis

A dissertation submitted in partial satisfaction of the  
requirements for the degree Doctor of Philosophy  
in Molecular, Cellular, and Integrative Physiology

by

Elinor Lee

2020

© Copyright by

Elinor Lee

2020

## ABSTRACT OF THE DISSERTATION

### The Role of Lipids in Pulmonary Alveolar Proteinosis

by

Elinor Lee

Doctor of Philosophy in Molecular, Cellular, and Integrative Physiology

University of California, Los Angeles, 2020

Professor Elizabeth (Tarling) Aguiar Vallim, Chair

Pulmonary alveolar proteinosis (PAP) is a rare lung syndrome that has no cure and no FDA approved therapies. It is characterized by the accumulation of surfactant within alveoli due to disruption of granulocyte-macrophage colony stimulating factor (GM-CSF) signaling. The pathogenic mechanism that underlies PAP remains unknown. Early studies suggested that PAP resulted from dysfunction in phospholipid homeostasis that led to the accumulation of phospholipid-enriched surfactant. However, more recent studies suggest that PAP pathogenesis is driven by changes in cholesterol homeostasis that may be linked to alveolar macrophages. The



goal of this dissertation is to investigate the molecular mechanisms that lead to lipid dysregulation in PAP.

First, we examined the lipid content of both alveolar macrophages and type 2 epithelial cells, two primary cells involved in surfactant homeostasis in a mouse model of PAP (*Abcg1*<sup>-/-</sup> mice). Compared to wildtype animals, *Abcg1*<sup>-/-</sup> mice had increased lipid deposition in both alveolar macrophages and type 2 epithelial cells, suggesting both cells are involved in the pathogenesis of PAP. Next, we observed that PAP patients who were treated with a cholesterol-lowering agent, statin, demonstrated improvements in their lung disease. We then treated *Csf2rb*<sup>-/-</sup> mice, another PAP mouse model, with a statin and found that they had improvement in their lung disease due to increased efflux of cholesterol from alveolar macrophages. Finally, we utilized lipidomic analysis and mass spectrometry to measure lipid composition of PAP alveolar macrophages. We found that compared to non-PAP alveolar macrophages, PAP alveolar macrophages were enriched in phosphatidylcholine (PC) and cholesterol ester (CE). Furthermore, clinical improvement in treated PAP patients was associated with a decrease in PC and CE classes, indicating that levels of these lipids correlated with the severity of the disease.

Our studies demonstrate that disruption of both phospholipid and cholesterol homeostasis contributes to the pathogenesis of PAP. This new mechanistic insight has provided us with a better understanding of the pathophysiology of PAP and will be instrumental in our endeavor to find novel therapeutic targets and ultimately a cure for these patients.

The dissertation of Elinor Lee is approved.

Tomas Ganz

Karen Reue

Peter Tontonoz

Thomas Vallim

Elizabeth (Tarling) Aguiar Vallim, Committee Chair

University of California, Los Angeles

2020

For my family, friends, and patients

## TABLE OF CONTENTS

|  |           |
|--|-----------|
| Abstract of the Dissertation.....  | ii        |
| List of tables and figures.....  | ix        |
| Acknowledgements.....  | xii       |
| Vita.....  | xvi       |
| <br>   |           |
| <b>Chapter: 1 Introduction.....</b>  | <b>1</b>  |
| Lipids are integral to lung function.....  | 2         |
| Pulmonary alveolar proteinosis is an important clinical problem to study.....          | 2         |
| Tight regulation of surfactant homeostasis is essential for normal lung function.....  | 5         |
| GM-CSF signaling plays a critical role in surfactant homeostasis.....                  | 8         |
| Disruption of cholesterol metabolism may be causing PAP.....                           | 9         |
| The dissertation.....  | 10        |
| References.....  | 13        |
| <br>   |           |
| <b>Chapter 2: ABCG1 regulates pulmonary surfactant metabolism in mice and men.....</b> | <b>20</b> |
| Abstract.....  | 21        |
| Introduction.....  | 21        |
| Materials and methods.....   | 22        |
| Results.....   | 24        |
| Discussion.....  | 30        |

|  |           |
|--|-----------|
| References.....  | 32        |
| Supplemental data.....   | 35        |
| <b>Chapter 3: Statin as a novel pharmacotherapy of pulmonary alveolar proteinosis.....</b>   | <b>41</b> |
| Abstract.....  | 42        |
| Introduction.....  | 43        |
| Results.....   | 43        |
| Discussion.....  | 45        |
| Methods.....   | 47        |
| References.....  | 48        |
| Supplementary information.....   | 51        |
| <b>Chapter 4: Alveolar macrophage lipid levels and plasma anti-GM-CSF antibodies correlate with disease improvement in patients with pulmonary alveolar proteinosis.....</b> | <b>57</b> |
| Abstract.....  | 59        |
| Introduction.....  | 60        |
| Materials and methods.....   | 62        |
| Results.....   | 65        |
| Discussion.....  | 70        |
| Figure legends.....  | 74        |
| References.....  | 84        |
| <b>Chapter 5: Conclusion.....</b>  | <b>87</b> |
| The study of PAP has led to important discoveries.....   | 88        |
| A dysregulation in phospholipid and cholesterol metabolism leads to PAP.....   | 89        |
| Future directions.....   | 94        |

|                         |     |
|-------------------------|-----|
| Concluding remarks..... | 99  |
| References.....         | 101 |

## LIST OF TABLES AND FIGURES

### Chapter 2

|             |   |    |
|-------------|---|----|
| Figure 2.1  | ABCG1 has a critical role in nonhematopoietic cells.....  | 25 |
| Table 2.1   | Altered lipid content of the lungs of bone-marrow transplanted mice.....  | 26 |
| Figure 2.2  | Mice with selective deletion of <i>Abcg1</i> in T2 cells have abnormal<br>surfactant and lamellar body homeostasis..... | 27 |
| Figure 2.3  | Disrupted lipid homeostasis and immunity in <i>Abcg1</i> <sup>T2-KO</sup> mice.....                                     | 28 |
| Figure 2.4  | ABCG1 is required for the synthesis and secretion of cholesterol and<br>phospholipids from A549 T2 cells.....           | 29 |
| Figure 2.5  | <i>Abcg1</i> <sup>-/-</sup> macrophages signal to wild-type T2 cells.....   | 30 |
| Figure 2.6  | Sequence polymorphisms in human <i>ABCG1</i> in patients with PAP.....  | 31 |
| Figure 2.7  | Reduced activation of ABCG1 by LXR in a patient with PAP.....   | 32 |
| Table 2.S1  | Characteristics of PAP patients.....  | 35 |
| Figure S2.1 | .....   | 36 |
| Figure S2.2 | .....   | 37 |
| Figure S2.3 | .....   | 38 |
| Figure S2.4 | .....   | 39 |
| Figure S2.5 | .....   | 40 |

### Chapter 3

|            |  |    |
|------------|--|----|
| Figure 3.1 | Resolution of PAP associated with oral statin therapy.....     | 44 |
| Figure 3.2 | Cholesterol accumulation in human PAP alveolar macrophages and |    |

|             |   |    |
|-------------|---|----|
|             | correction by statin.....   | 45 |
| Figure 3.3  | Statin therapy improves cholesterol efflux from macrophages and ameliorates PAP in <i>Csf2rb</i> <sup>-/-</sup> mice..... | 46 |
| Figure 3.4  | Proposed mechanisms for the pathogenesis and statin therapy of PAP....  | 47 |
| Figure S3.1 | .....   | 52 |
| Figure S3.2 | Statin therapy increases expression of SREBP2 targets in alveolar macrophages (AMs).....                                  | 53 |
| Table S3.1  | Serum cholesterol levels of case report patient over a 10 year period (2008-2017).....                                    | 54 |
| Table S3.2  | Lung mass in healthy people determined by quantitative chest computed topography densitometry.....                        | 55 |
| Table S3.3  | Lung mass in the patient (Case 1) determined by quantitative chest computed topography densitometry.....                  | 56 |

## Chapter 4

|            |  |    |
|------------|--|----|
| Figure 4.1 | High-resolution lipidomic profiling reveals an overall increase of all lipid classes in alveolar macrophages of PAP patients compared to nonPAP patients with phosphatidylcholine and cholesterol ester being the most abundant lipid classes in the majority of PAP patients..... | 78 |
| Figure 4.2 | There is a decreased amount of phosphatidylcholine and cholesterol ester in the alveolar macrophages of PAP patient who have received therapy, which appears to be related to improving disease.....   | 79 |
| Figure 4.3 | There is an increased amount of phosphatidylcholine and cholesterol ester  |    |



in the alveolar macrophages of PAP patient despite receiving therapy,  
which appears to be associated with worsening, unremitting disease.....80

|            |  |
|------------|--|
| Figure 4.4 | A decline in GM-CSF antibody levels correlates with clinical<br>improvement in PAP patients.....81   |
| Table 4.1  | Baseline characteristics of nonPAP and 4 individual PAP patients.....82                              |
| Table 4.2  | Baseline characteristics of patients with autoimmune PAP on various<br>experimental therapies.....83 |

## ACKNOWLEDGEMENTS

There's an African proverb that states, "it takes a village to raise a child". This saying is apropos to completing a thesis. This thesis would have not been possible without my village of family, friends, mentors, scientists, colleagues, and patients.

First and foremost, I would like to thank my thesis advisor, Elizabeth Tarling, for all of her guidance, support, and patience throughout my PhD. I appreciate all of the time and energy that she invested in me to help me grow as a scientist. She encouraged me to pursue things that interested me and either helped me bring these ideas into fruition or steered me in a different direction in order to better achieve my goals. Her passion for science is infectious, and I learned a lot by working with her.

I also want to thank my thesis committee members, Tomas Ganz, Karen Reue, Peter Tontonoz, and Thomas Vallim. They were incredibly supportive and encouraging throughout my PhD. They always had thoughtful comments, insights, and ideas that were invaluable and taught me how to think like a scientist. Meeting with them has been enjoyable and enlightening. I want to give a special thanks to Thomas Vallim for being my second lab mentor and really appreciate all of his time, energy, dedication, and enthusiasm throughout my PhD.

I am super grateful for my clinical mentor, Tisha Wang. Not only is she an outstanding clinician, but she is also a great educator, clinical researcher, patient advocate, and mentor. Her passion and dedication to this patient population is unrivaled, and it is humbling to work with her. She is an incredible role model, and I appreciate all of the opportunities I had through her, such as participating in PAP education days, being involved in clinical trials from start to finish, doing grand rounds, and writing book chapters. Additionally, I am thankful for the support of the

pulmonary division at UCLA, especially of Steven Dubinett, who has been supportive of my research career throughout my time at UCLA as a fellow and now as a member of the faculty.

I want to express my gratitude for the STAR program at UCLA. I am so grateful for Alan Fogelman, Linda Demer, Mitch Wong, Tamer Sallam, and the rest of the leadership for all of their support and guidance. I want to give a special thanks to Linda Demer for meeting with me and checking in on how I was doing throughout the years. I appreciate all of her wisdom and encouragement throughout the process. The monthly seminars and workshops were also helpful in developing my research skills and in my transitioning from a trainee into a faculty member.

Being part of the Molecular, Cellular, and Integrative Physiology department at UCLA has been an amazing experience. I want to especially thank Mark Frye for all of his support and Yesenia Rayos for her help throughout my whole PhD process. I have also met some great peers and colleagues within the program, who have been encouraging and provided me with advice in one way or another.

I am super grateful for the present and former members in the Tarling-Vallim lab for all of their help, patience, support, and encouragement. I truly feel like we have all become close friends. They made working in the lab enjoyable, and they are the ones who made some of the most challenging days more bearable. I have learned so much from them. I also want to express a special thanks to Peter Edwards for continuing to give great advice and thoughtful feedback

I want to thank Kevin Williams in the UCLA Lipidomics laboratory. He has been incredibly helpful and a wealth of knowledge in regards to everything lipidomics related. I really appreciated his patience and his willingness to be my springboard to bounce ideas off of him while optimizing our protocols.

I do really believe that collaboration is key to being successful in science, and I have had the fortune to work with amazing collaborators. I want to thank particularly Cormac McCarthy, who is now at University College Dublin, as well as Brenna Carey and Bruce Trapnell at Cincinnati Children's Hospital for all of their help and insight. I learned a lot through our conversations and was able to experience what true translational research looked like. Through them, I also was able to obtain the Rare Lung Disease Consortium grant and participate in wonderful opportunities like the Rare Disease Clinical Research Network Certificate Program, all of which have been integral to my development as a physician scientist in rare lung diseases.

I cannot express enough appreciation for all of the patients and their families for being willing to participate in our research studies. Their sacrifice has made this research possible. They are the main reason and inspiration for this thesis dissertation.

Finally, I want to thank my family for their unwavering love, support, and encouragement throughout my journey to pursue anything I want, even if it means being in school or training for more than 30 years. I am forever grateful.

Chapter 2 is a reprint of “ABCG1 regulates pulmonary surfactant metabolism in mice and men” from *J Lipid Res.* 2017 May; 58(5): 941-954. © the American Society for Biochemistry and Molecular Biology. Thomas Q de Aguiar Vallim, David J Merriott, Christopher N Goulbourne, Joan Cheng, Angela Cheng, Ayelet Gonen, Ryan M Allen, Elisa N D Palladino, David A Ford, Tisha Wang, Angel Baldan, and Elizabeth J Tarling are co-authors.

Chapter 3 is a reprint of “Statin as a novel pharmacotherapy of pulmonary alveolar proteinosis” from *Nat Commun.* 2018 Aug; 9(1): 3127 under the Creative Commons Attribution 4.0 International License. Cormac McCarthy, James P Bridges, Anthony Salles, Takuji Suzuki, Jason C Woods, Brian J Bartholmai, Tisha Wang, Claudia Chalk, Brenna C Carey, Paritha Arumugam, Kenjiro Shima, Elizabeth J Tarling, and Bruce C Trapnell are co-authors.

Chapter 4 is a version of “Alveolar macrophage lipid levels and plasma anti-GM-CSF antibodies correlate with disease improvement in patients with pulmonary alveolar proteinosis”, which is currently undergoing manuscript preparation to be submitted to a journal. Kevin J Williams, Cormac McCarthy, Claudia Chalk, Brenna Carey, Bruce C Trapnell, Thomas Q de Aguiar Vallim, Tisha Wang, and Elizabeth J Tarling are co-authors.

This research was supported in part by Rare Lung Disease Consortium Grant (U54HL127672), UCLA Pulmonary and Critical Care Medicine T32 grant (T32HL072752), UCLA Cardiovascular T32 grant (T32HL007895), and UCLA Specialty Training and Advanced Research (STAR) program.

## VITA

Elinor Lee

### EDUCATION

- 2017 – current      University of California, Los Angeles, Los Angeles, California  
Doctor of Philosophy – Molecular, Cellular, and Integrative Physiology
- 2007 – 2011      University of Cincinnati, College of Medicine, Cincinnati, OH  
Doctor of Medicine
- 2001 – 2005      Amherst College, Amherst, Massachusetts  
Bachelor of Arts, *Cum Laude* – Biology and English
- Fall 2003      Queen Mary, University of London (Butler University, Study Abroad)  
London, United Kingdom

### EMPLOYMENT

- 2018 – current      Clinical Instructor, Division of Pulmonary & Critical Care Medicine,  
David Geffen School of Medicine at University of California, Los Angeles
- 2016 – current      Fellow in Basic Science Research, Specialty Training and Research  
Program, UCLA Department of Medicine; Los Angeles, CA
- 2015 – 2018      Fellow Physician, Division of Pulmonary & Critical Care Medicine,  
UCLA Health System, Los Angeles, CA
- 2013 – 2015      Chief Medical Resident, Departments of Internal Medicine and Pediatrics,  
Baylor College of Medicine, Houston, TX
- 2011 – 2015      Resident Physician, Departments of Internal Medicine and Pediatrics,  
Baylor College of Medicine, Houston, TX
- 2005 – 2007      Postbaccalaureate Intramural Research Fellow, National Heart, Lung,  
and Blood Institute (NHLBI), National Institutes of Health, Bethesda, MD

### PUBLICATIONS (Please see ORCID 0000-0003-3008-8325 for full list of publications)

1. Lee E, Williams KJ, McCarthy C, Chalk C, Carey B, Trapnell BC, De Aguiar Vallim TQ, Wang T, Tarling EJ. “Alveolar macrophage lipid levels and plasma anti-GM-CSF antibodies correlate with improvements in patients with Pulmonary Alveolar Proteinosis”. Manuscript in preparation to be submitted.
2. Bonaventura A, Vecchie A, Wang T, Lee E, Cremer PC, Carey B, Rajendram P, Hudock KM, Korbee L, Van Tassell BW, Dagna L, Abbate A. “Targeting GM-CSF in COVID-19 pneumonia: rationale and strategies.” *Front Immunol.* 2020; 11: 1625.

3. McCarthy C, **Lee E**, Bridges JP, Sallesse A, Suzuki T, Woods JC, Bartholmai BJ, Wang T, Chalk C, Carey BC, Arumugam P, Shima K, Tarling EJ, Trapnell BC. “Statin as a novel pharmacotherapy of pulmonary alveolar proteinosis.” *Nat Commun.* 2018; 9(1): 3127
4. De Aguiar Vallim TQ, **Lee E**, Merriott DJ, Goulbourne CN, Cheng J, Cheng A, Gonen A, Allen RM, Palladino EN, Ford DA, Wang T, Baldan A, Tarling EJ. “ABCG1 regulates pulmonary surfactant metabolism in mice and men.” *J Lipid Res.* 2017; 58(5):941-954.

## PRESENTATIONS

1. **Lee E**, Morand P, Williams K, Wang S, Wang T, Vallim T, Tarling EJ. “Defining the lipidome of alveolar macrophages in pulmonary alveolar proteinosis”. Accepted to be presented in May 2020 at the American Thoracic Society Meeting, Philadelphia, PA
2. Wang T and **Lee E**. “The pulmonary alveolar proteinosis story: from the bedside to the bench to the community”. Oral presentation in January 2020 at pulmonary grand rounds at UT Southwestern, Dallas, TX
3. **Lee E**, McCarthy C, Bridges J, Woods J, Suzuki T, Carey B, Wang T, Trapnell T, Tarling E. ”An approach to precision medicine for pulmonary alveolar proteinosis”. Poster presentation in May 2019 at the American Thoracic Society Meeting, Dallas, TX
4. **Lee E**, Wang T, McCarthy C, Bridges J, Woods J, Suzuki T, Carey B, Wang T, Morand P, Trapnell B, Tarling EJ. “The role of statins in pulmonary alveolar proteinosis”. Poster presentation in March 2019 at the Deuel Conference, Dana Point, CA
5. **Lee E**. “The role of statins in autoimmune pulmonary alveolar proteinosis”. Oral presentation in October 2018 at the Fourteenth Annual Respiratory Disease Young Investigators’ Forum, Washington D.C.
6. **Lee E**, Wang T, McCarthy C, Bridges J, Trapnell B, Tarling EJ. “A potential approach to personalized medicine for PAP patients”. Poster presentation in Sept 2018 at the Rare Lung Diseases Conference and LAMposium, Cincinnati, OH
7. **Lee E**. “The role of lipid metabolism in pulmonary alveolar proteinosis”. Oral presentation in June 2017 at pulmonary grand rounds at UCLA, Los Angeles, CA
8. **Lee E**, Vallim TQ, Merriott D, Cheng J, Cheng A, Trapnell BC, Wang T, Tarling EJ “ABCG1 plays an important role in surfactant metabolism in pulmonary alveolar proteinosis”. Poster presentation in May 2017 at the American Thoracic Society Meeting, Washington D.C.
9. **Lee E**, Vallim TQ, Merriott D, Cheng J, Goulbourne CN, Barmak K, Ford DA, Baldan A, Wang T, Tarling EJ. “ABCG1 has a critical role in pulmonary type 2 cells and surfactant metabolism: implications for pulmonary alveolar proteinosis.” Poster presentation in September 2016 at the Rare Lung Diseases Conference and LAMposium, Cincinnati, OH

## **CHAPTER 1**

### **Introduction**



## **Lipids are integral to lung function**

The lungs are not typically considered as an organ with active lipid metabolism. The maintenance of lipid homeostasis, however, is paramount to the optimal function of the lungs, especially in the alveolar space where gas exchange occurs. This is highlighted by the fact that any disturbance in the amount or composition of surfactant, which is predominantly comprised of lipids, leads to respiratory conditions that range from more common ones, like chronic obstructive pulmonary disease, to rare ones, such as pulmonary alveolar proteinosis (1, 2). Furthermore, different lipids are also essential structural components, integral for energy storage, and play a role in various signaling functions during physiological processes. With the advent of more sophisticated and sensitive methods of measuring and analyzing lipid data, we are rapidly gaining insight into how important pulmonary lipids are to lung function and how dysregulation of lipid homeostasis may lead to pulmonary disease pathology.

## **Pulmonary alveolar proteinosis is an important clinical problem to study**

Pulmonary Alveolar Proteinosis (PAP) is a rare lung syndrome characterized by the accumulation of surfactant within the alveoli that affects about 6-7 people per million in the United States (3). The pathogenesis of this syndrome is heterogenous with various biochemical defects that ultimately lead to the accumulation of surfactant within the alveoli. PAP is categorized into primary, secondary, and congenital etiologies (4). Primary PAP is the most common form of disease that occurs either from elevated levels of neutralizing antibodies to granulocyte-macrophage colony stimulating factor or GM-CSF (autoimmune PAP) or from hereditary causes due to mutations in the GM-CSF receptor (hereditary PAP). Autoimmune PAP is the most common type of primary PAP, representing about 90% of all patients (5). There is a

critical threshold of neutralizing antibodies to GM-CSF, which is 100% sensitive and specific for the diagnosis of patients with autoimmune PAP; if the antibody level is below this value, the patient does not develop disease (6). Interestingly, the level of GM-CSF autoantibodies has not been reported to correlate with disease severity (7). Secondary PAP is associated with underlying diseases that secondarily affect alveolar macrophage number and function, such as hematologic malignancies, immunologic syndromes, infections, or toxic inhalational exposures. Congenital PAP is the rarest type and is caused by mutations in genes that are essential for surfactant production, such as surfactant protein B (SP-B), surfactant protein C (SP-C), and ATP-binding cassette subfamily A member 3 (ABCA3) (8).

The clinical course of PAP is heterogenous and ranges from spontaneous resolution to stable persistent disease to progressive deterioration leading to death or need for lung transplantation. Spontaneous resolution of PAP occurs in about 5-7% of cases (9-11). Pulmonary fibrosis and end stage lung disease develop in approximately 20% of patients with PAP; however, it remains unclear why patients develop fibrosis (12). Notably, there is no specific validated biomarker or method currently available to risk stratify patients who will develop progressive lung disease and/or fibrosis from those who will not.

Compared to non-PAP patients, PAP patients have increased healthcare utilization and costs, including increased outpatient visits, emergency room visits, and prolonged hospital stays. Additionally, the annual per-patient healthcare costs are five-fold higher compared to those of patients without PAP (3). These patients are susceptible to infections from common respiratory pathogens and opportunistic organisms, such as *Mycobacterium tuberculosis*, *Mycobacterium avium-intracellulare*, *Nocardia spp.*, *Pneumocystis jirovecii*, and *Aspergillus spp* (13-15). This has been attributed to the fact that PAP patients have malfunctioning macrophages and

neutrophils (16, 17). Historically, survival rate has been reported at 79%, 75% and 68% at 2, 5 and 10 years, respectively (18). The majority of deaths are related to respiratory failure, and a minority are caused by uncontrolled infections.

Currently, there is no cure or FDA approved therapy for PAP. Treatment is focused on managing symptoms and preventing progression of disease. Whole lung lavage (WLL) is the current standard of care. This entails placing a double lumen endotracheal tube under general anesthesia to ventilate one lung while filling and emptying the other lung with normal saline to remove lipid-loaded and proteinaceous surfactant. Five-year survival in PAP is about  $85\% \pm 5\%$  without therapy and about  $94\% \pm 2\%$  with WLL (18). Other therapy modalities that have been shown to reduce anti-GM-CSF levels and improve lung function include exogenous GM-CSF given subcutaneously or aerosolized, rituximab, and plasmapheresis (19-26). Although these newer approaches have shown promising results, further studies need to be performed to assess their efficacy and safety profiles in patients with PAP. Lung transplantation has been performed mainly in pediatric patients and patients with end stage fibrosis; however, there is concern for recurrence although the data are limited (27, 28). Lastly, experimental approaches involving currently available drugs have been recently discovered. Thiazolidinediones, which are a class of diabetic medications that also improve dyslipidemia, have been shown to ameliorate PAP disease severity in mice (29). An open-label, phase I clinical trial using this class of medication has been completed; however, results have yet to be published. More studies need to be done to determine if thiazolidinediones are indicated for the treatment of PAP.

## **Tight regulation of surfactant homeostasis is essential for normal lung function**

Surfactant is essential for breathing and gas exchange. It is a complex mixture composed of 80% phospholipids, 10% cholesterol, and 10% proteins that forms a thin film that lines the alveolar epithelium and lowers surface tension, preventing alveolar collapse and reducing the work of breathing (30). Furthermore, it is the first line of defense against the entry of harmful particles and pathogens through the lung, which has a large body surface area exposed to the environment (31, 32). Surfactant lipids and proteins are made in the type 2 epithelial cells, which are then packaged tightly into organelles called lamellar bodies (LB) and secreted into the thin fluid phase that lines the alveoli (33). Once the LB are secreted into the liquid phase, the surfactant unpacks and creates a highly organized network called tubular myelin that adsorbs to the air-liquid interface of the alveoli and forms the surface-active film (34). Some of the surfactant also becomes other structures, such as unilamellar and multilamellar vesicles, that also adsorb and make up the surface-active film.

Phosphatidylcholine (PC) is the predominant phospholipid present in surfactant with dipalmitoylphosphatidylcholine (DPPC) accounting for about 40-50% of the PC species (35, 36). The saturated fatty acid chains of DPPC allow for maximal packing in the surface-active film, enabling the reduction of surface tension to very low values at the end of expiration. PC is produced *de novo* in the endoplasmic reticulum (ER) of type 2 epithelial cells through the Kennedy pathway or the cytidine diphosphocholine (CDP):choline pathway (35, 37). Because *de novo* synthesis of PC is slow, about 55-75% of surfactant DPPC is generated by remodeling (33, 38-40). The remodeling pathway involves phospholipase A2 (PLA2), which generates lyso-PC that is then re-acetylated with saturated fatty acid species by lysosomal enzyme acyl CoA: lysophosphatidylcholine acyltransferase 1 (LPCAT1) (41). Interestingly, *PLA2*<sup>-/-</sup> mice do not

develop respiratory issues, but mice homozygous for a hypomorphic allele of *Lpcat1* have shown varying perinatal mortality from respiratory failure (42, 43). Cholesterol plays an essential role in modulating the structure of surfactant membranes (32, 44, 45). The origin of cholesterol in surfactant remains unclear. Earlier studies using iodine-labeled lipoproteins have demonstrated that the majority of pulmonary cholesterol is obtained from serum lipoproteins (46, 47). However, other studies utilizing [<sup>3</sup>H] cholesterol suggest that serum cholesterol is accumulated in the limiting membrane of the LB and not secreted into the alveolar space with other surfactant lipids (48). Rather, other cells, such as alveolar lipofibroblasts, may be supplying cholesterol to surfactant (49). Surfactant proteins are divided into two groups, hydrophobic and hydrophilic. Hydrophobic surfactant proteins B and C (SP-B and SP-C, respectively) are integral for formation and stabilization of the film during respiratory cycles, while hydrophilic surfactant proteins A and D (SP-A, and SP-D, respectively) are important in lung-defense related roles, recognizing and binding to pathogens (35).

Surfactant homeostasis is maintained by alveolar type 2 epithelial cells, which secrete and clear surfactant by recycling or degradation, and alveolar macrophages, which clear surfactant by catabolism (33). Alveolar type 2 epithelial cells secrete surfactant in response to stimulation, such as stretching and adenosine triphosphate (ATP) (50, 51). On the other hand, the surfactant pool size appears to influence the rate of catabolism although the exact molecular pathways involved remain unclear (52). About 20-30% of surfactant is catabolized by alveolar macrophages, while the majority is recycled or degraded by type 2 epithelial cells (37, 53). In type 2 epithelial cells, surfactant is re-internalized via clathrin-mediated endocytosis in response to the interaction of SP-A with its receptor, P63, on the type 2 epithelial cells (54). There is also GPR116, which is an orphan G protein-coupled receptor (GPCR), that behaves both as an

inhibitor of surfactant secretion and stimulator of surfactant reuptake in type 2 epithelial cells (55). Additionally, there is an ABCA3-mediated LB reuptake, demonstrating that some components of LB can be recycled via clathrin-independent pathways (56). ABCA3 is a member of the ATP-binding cassette (ABC) transporter superfamily of transmembrane proteins involved in transporting molecules across membranes. The internalized lipids and proteins are then transferred to the LB within the type 2 epithelial cells, where a portion is rapidly recycled to the cell surface, while another portion is targeted for actin-dependent degradation (36, 57, 58). In alveolar macrophages, there may be uptake of LB or transport of individual lipids by various lipid transporters, but the exact mechanism remains unclear (33). There are scavenger receptors, such as CD36, scavenger receptor class A, type 1 (SR-A1), and scavenger receptor class B, type 1 (SR-B1), that are found in the alveolar macrophages and may be directly involved in internalizing lipids (33).

Once lipids are taken up within the alveolar type 2 epithelial cells and alveolar macrophages, lipid transporters that are present in both cells may become activated to help maintain lipid homeostasis. Specifically, there are ABC transporters A1 and G1 (ABCA1 and ABCG1, respectively), which are part of the ABC transporter superfamily and transcriptionally regulated by liver X receptor (LXR), which senses the cellular levels of cholesterol (59, 60). ABCA1 is known to efflux phospholipid and cholesterol to lipid-free apolipoprotein, while ABCG1 is involved in efflux of cholesterol to high-density lipoprotein (HDL) (61-64). When oxysterols accumulate during cholesterol overload in the cells, they activate LXR, which then upregulates ABCA1 and ABCG1 to promote cholesterol efflux. Mice deficient in ABCA1 (*Abca1<sup>-/-</sup>*) or ABCG1 (*Abcg1<sup>-/-</sup>*) develop an age dependent pulmonary lipidosis with accumulation of phospholipids and cholesterol in the lungs, similar to PAP (54, 63, 65).

Interestingly, PAP patients have reduced expression of ABCG1 but increased expression of ABCA1 in their alveolar macrophages, suggesting that ABCG1 is the primary lipid transporter in these cells (66). The expression of these transporters has not been studied in type 2 epithelial cells of PAP patients.

### **GM-CSF signaling plays a critical role in surfactant homeostasis**

GM-CSF signaling has been shown to be crucial for surfactant homeostasis. In the lungs, type 2 epithelial cells secrete GM-CSF, which then interacts with its receptor on various cell types, including type 2 epithelial cells and alveolar macrophages (67, 68). The receptor is a heterodimer that consists of two subunits, an alpha subunit, which is the major GM-CSF binding subunit, and a beta subunit, which is the major signaling subunit (69-71). The disruption of GM-CSF signaling has been shown to cause impairment of surfactant catabolism and accumulation of surfactant in the lungs (72). Its role in surfactant recycling by type 2 epithelial cells remains unclear. Mice deficient in GM-CSF (*Csf2*<sup>-/-</sup>) or its receptor (*Csf2ra*<sup>-/-</sup> and *Csf2rb*<sup>-/-</sup>, which are mice deficient in the alpha and beta subunits of the GM-CSF receptor, respectively) will develop a PAP-like pulmonary histopathology and are used as mouse models to study PAP (73-75). When GM-CSF was expressed locally under the control of SP-C gene promoter in lung epithelial cells of *Csf2*<sup>-/-</sup> mice, the surfactant lipid and protein concentrations were corrected to normal levels (76). Furthermore, *Csf2rb*<sup>-/-</sup> mice had reversal of their PAP phenotype after bone marrow transplantation, suggesting that the lack of GM-CSF in alveolar macrophages is responsible for PAP in this model rather than the lack of GM-CSF in type 2 epithelial cells (77). Therefore, the majority of studies examining PAP focus on alveolar macrophages.

In type 2 epithelial cells, GM-CSF has been shown to enhance lung growth and induce type 2 cell hyperplasia (71). Its role in type 2 epithelial cell maturation has not yet been identified. In alveolar macrophages, GM-CSF has been identified as a key mediator of alveolar macrophage maturation, self-renewal, and population size (78, 79). Alveolar macrophages are derived from fetal monocytes in the yolk sac that seed the lung before birth and develop into mature alveolar macrophages after birth in response to GM-CSF signaling. PU.1 and peroxisome proliferator-activated receptor gamma (PPAR $\gamma$ ) have also been shown to be crucial transcription factors downstream from GM-CSF for the maturation of alveolar macrophages in order to prevent development of PAP (80-82). Throughout life, adult circulating monocytes minimally contribute to the steady-state alveolar macrophage pool, and the majority of the alveolar macrophages are locally regenerated from its own pool in the lungs (79, 83). Thus, without proper GM-CSF signaling, the alveolar macrophages are unable to self-maintain, mature, and function properly, including catabolize surfactant efficiently or effectively.

### **Disruption of cholesterol metabolism may be causing PAP**

In the past, the accumulation of surfactant in PAP was attributed to the impaired catabolism of phospholipids in alveolar macrophages (84-86). Recent studies have demonstrated, however, that the relative proportion of cholesterol to total phospholipids in surfactant was elevated in PAP mice compared to wild-type (WT) mice, while the relative proportion of saturated phosphatidylcholine to total phospholipids remained the same (29). Additionally, the alveolar macrophages from PAP mice have increased levels of esterified and free cholesterol but minimal changes in the level of triglycerides, free fatty acids, and phospholipid species compared to healthy counterparts (29). Furthermore, the addition of PAP patient-derived



surfactant to bone marrow-derived macrophages (BMDM) from WT versus PAP mice resulted in higher levels of total, free, and esterified cholesterol in the macrophages of PAP mice, while the addition of phospholipid-containing/cholesterol-free pharmaceutical surfactant to bone marrow derived macrophages from WT versus *Csf2<sup>-/-</sup>* mice demonstrated no difference between the two groups. Changes in the level of phospholipids within the alveolar macrophages were not measured. Previous studies have shown that PAP alveolar macrophages have altered expression of the cholesterol ABC transporters, ABCA1 and ABCG1, and of the nuclear receptor PPAR $\gamma$ , important mediators of cholesterol trafficking in macrophages (64, 66, 80). These data imply that an impairment in cholesterol homeostasis underlies the pathogenesis of PAP; however, the exact mechanism remains unknown.

### **The dissertation**

This dissertation investigates molecular mechanisms that lead to lipid dysregulation in PAP, describes for the first time the lipidome of PAP alveolar macrophages, identifies a potential novel biomarker that may be utilized in clinical setting, and proposes a novel pharmacotherapy for PAP. In order to accomplish this, we utilized samples from various PAP mouse models and autoimmune PAP patients. Our results confirm the heterogeneity of the disease process that has made it challenging not only to cure but also to treat. Additionally, our data suggest that it is not the impaired catabolism of only phospholipid or only cholesterol that drives PAP but the dysregulation of both phospholipid and cholesterol metabolism that leads to PAP.

Chapter 2 is a reprint of “ABCG1 regulates pulmonary surfactant metabolism in mice and men”, which was originally published in *Journal of Lipid Research*. In this study, we examined the role of ABCG1 in both type 2 epithelial cells and alveolar macrophages and demonstrated

that ABCG1 is critical for both surfactant and type 2 epithelial cell (T2 cell) homeostasis. We were able to create both macrophage-specific ABCG1-deficient mice and T2 cell-specific ABCG1-deficient mice. Consistent with prior studies, loss of ABCG1 led to increased deposition of lipids in alveolar macrophages. It also led to increased lamellar body content in type 2 epithelial cells as well as increased amounts of phospholipid and cholesterol in the alveolar space. Furthermore, we were able to identify polymorphisms in regulatory regions of the *ABCG1* locus that corresponded to a putative LXR response element in the alveolar macrophages from one PAP patient. The induction of *ABCG1* mRNA in response to LXR activation was reduced in the alveolar macrophages from the PAP patient. This suggests that this patient population may express polymorphisms that may affect the expression and/or function of ABCG1, thus contributing to the development of PAP.

Because the lack of ABCG1 leads to PAP, one could hypothesize that a therapy that increases expression and function of ABCG1 may be able to reverse the disease process. We were able to demonstrate this in Chapter 3 with statin therapy. Chapter 3 is a reprint of “Statin as a novel pharmacotherapy of pulmonary alveolar proteinosis” from *Nature Communications*. Here, we demonstrated a marked increase in cholesterol content in PAP alveolar macrophages as well as an increase in the ratio of cholesterol to total phospholipids in pulmonary surfactant of PAP patients. We also identified statin as a potential novel pharmacotherapy for PAP. Mice and patients with PAP had improvement in their lung disease with reduction of cholesterol levels in alveolar macrophages after being treated with oral statin therapy by increasing the expression of ABCA1 and ABCG1 and enhancing cholesterol efflux from alveolar macrophages. Our data support the novel paradigm that improving cholesterol homeostasis leads to improvement in PAP disease.

Although statin therapy improved disease in some of our PAP patients, it did not work for all of our PAP patients. Therefore, we wanted to better examine the lipid profile of alveolar macrophages with mass spectrometry to identify other lipid classes or species that may be involved and be used as novel targets for therapeutics in the future. Previous studies have examined lipid composition of alveolar macrophages but in a cruder fashion with colorimetric assays and thin layer chromatography. We present our findings in Chapter 4, which is entitled “Alveolar macrophage lipid levels and plasma anti-GM-CSF antibodies correlate with improvements in disease in patients with pulmonary alveolar proteinosis”. In this study, we not only defined the alveolar lipidome quantitatively in non PAP and PAP patients but also followed how the alveolar macrophage lipid content changes in response to treatment. Compared to non-PAP patients, PAP patients demonstrated high levels of PC, especially PC 16:0/16:0, and cholesterol ester (CE) classes in their alveolar macrophages. Furthermore, a decrease in PC and CE classes correlated with improvement in disease. Therefore, we could use the lipid profile to correlate disease severity. In light of the invasive and expensive nature of obtaining lavage fluid from patients, we sought to identify an alternative approach and found that relative plasma GM-CSF antibody levels may be a novel biomarker that can be utilized to correlate with disease severity. In autoimmune PAP patients, patients with improvement in their disease process had a reduction in anti-GM-CSF antibody titer; however, patients with unremitting disease did not show a decrease in antibody level until they underwent plasmapheresis to physically remove circulating antibody levels.

Chapter 5 is a concluding summary of the dissertation and discusses future directions for examining the mechanism of lipid dysregulation in PAP in order to identify other novel biomarkers and therapies for PAP as well as to advance the field of lung lipid biology.

## References

1. Agudelo CW, Samaha G, Garcia-Arcos I. Alveolar lipids in pulmonary disease. *Lipids Health Dis.* 2020;19(1):122.
2. Devendra G, Spragg R. Lung surfactant in subacute pulmonary disease. *Respir Res.* 2002;3(1):19.
3. McCarthy C, Avetisyan R, Carey BC, Chalk C, Trapnell BC. Prevalence and healthcare burden of pulmonary alveolar proteinosis. *Orphanet J Rare Dis.* 2018;13(1):129.
4. Trapnell BC, Nakata K, Bonella F, Campo I, Griese M, Hamilton J, et al. Pulmonary alveolar proteinosis. *Nat Rev Dis Primers.* 2019;5(1).
5. Trapnell BC, Whitsett JA, Nakata K. Pulmonary Alveolar Proteinosis. *N Engl J Med.* 2003;349:2527-39.
6. Uchida K, Nakata K, Carey B, Chalk C, Suzuki T, Sakagami T, et al. Standardized serum GM-CSF autoantibody testing for the routine clinical diagnosis of autoimmune pulmonary alveolar proteinosis. *J Immunol Methods.* 2014;402(1-2):57-70.
7. Seymour JF, Doyle IR, Nakata K, Presneill JJ, Schoch OD, Hamano E, et al. Relationship of anti-GM-CSF antibody concentration, surfactant protein A and B levels, and serum LDH to pulmonary parameters and response to GM-CSF therapy in patients with idiopathic alveolar proteinosis. *Thorax.* 2003;58(3):252-7.
8. Whitsett JA, Weaver TE. Hydrophobic surfactant proteins in lung function and disease. *N Engl J Med.* 2002;347(26):2141-8.
9. Inoue Y, Trapnell BC, Tazawa R, Arai T, Takada T, Hizawa N, et al. Characteristics of a large cohort of patients with autoimmune pulmonary alveolar proteinosis in Japan. *Am J Respir Crit Care Med.* 2008;177(7):752-62.
10. Xu Z, Jing J, Wang H, Xu F, Wang J. Pulmonary alveolar proteinosis in China: a systematic review of 241 cases. *Respirology.* 2009;14(5):761-6.
11. Bonella F, Bauer PC, Griese M, Ohshimo S, Guzman J, Costabel U. Pulmonary alveolar proteinosis: new insights from a single-center cohort of 70 patients. *Respir Med.* 2011;105(12):1908-16.
12. Akira M, Inoue Y, Arai T, Sugimoto C, Tokura S, Nakata K, et al. Pulmonary Fibrosis on High-Resolution CT of Patients With Pulmonary Alveolar Proteinosis. *AJR Am J Roentgenol.* 2016;207(3):544-51.
13. Rosen SH, Castleman B, Liebow AA. Pulmonary alveolar proteinosis. *N Engl J Med.* 1958;258(23):1123-42.

14. Witty LA, Tapson VF, Piantadosi CA. Isolation of mycobacteria in patients with pulmonary alveolar proteinosis. *Medicine (Baltimore)*. 1994;73(2):103-9.
15. Wang T, Lazar CA, Fishbein MC, Lynch JPr. Pulmonary alveolar proteinosis. *Semin Respir Crit Care Med*. 2012;33(5):498-508.
16. Shibata Y, Berclaz PY, Chroneos ZC, Yoshida M, Whitsett JA, Trapnell BC. GM-CSF regulates alveolar macrophage differentiation and innate immunity in the lung through PU.1. *Immunity*. 2001;15(4):557-67.
17. Uchida K, Beck DC, Yamamoto T, Berclaz PY, Abe S, Staudt MK, et al. GM-CSF autoantibodies and neutrophil dysfunction in pulmonary alveolar proteinosis. *N Engl J Med*. 2007;356(6):567-79.
18. Seymour JF, Presneill JJ. Pulmonary alveolar proteinosis: progress in the first 44 years. *Am J Respir Crit Care Med*. 2002;166(2):215-35.
19. Venkateshiah SB, Yan TD, Bonfield TL, Thomassen MJ, Meziane M, Czich C, et al. An open-label trial of granulocyte macrophage colony stimulating factor therapy for moderate symptomatic pulmonary alveolar proteinosis. *Chest*. 2006;130(1):227-37.
20. Tazawa R, Trapnell BC, Inoue Y, Arai T, Takada T, Nasuhara Y, et al. Inhaled granulocyte/macrophage-colony stimulating factor as therapy for pulmonary alveolar proteinosis. *Am J Respir Crit Care Med*. 2010;181(12):1345-54.
21. Tazawa R, Ueda T, Abe M, Tatsumi K, Eda R, Kondoh S, et al. Inhaled GM-CSF for Pulmonary Alveolar Proteinosis. *N Engl J Med*. 2019;381(10):923-32.
22. Kavuru MS, Malur A, Marshall I, Barna BP, Meziane M, Huizar I, et al. An open-label trial of rituximab therapy in pulmonary alveolar proteinosis. *Eur Respir J*. 2011;38(6):1361-7.
23. Soyez B, Borie R, Menard C, Cadranel J, Chavez L, Cottin V, et al. Rituximab for autoimmune alveolar proteinosis, a real life cohort study. *Respir Res*. 2018;19(1):74.
24. Kavuru MS, Bonfield TL, Thomassen MJ. Plasmapheresis, GM-CSF, and alveolar proteinosis. *Am J Respir Crit Care Med*. 2003;167(7):1036-7.
25. Garber B, Albores J, Wang T, Neville TH. A plasmapheresis protocol for refractory pulmonary alveolar proteinosis. *Lung*. 2015;193(2):209-11.
26. Luisetti M, Rodi G, Perotti C, Campo I, Mariani F, Pozzi E, et al. 2009. *Eur Respir J*. Plasmapheresis for treatment of pulmonary alveolar proteinosis;33(5):1220-2.
27. Hamvas A, Noguee LM, Mallory GB, Jr. , Spray TL, Huddleston CB, August A, et al. Lung transplantation for treatment of infants with surfactant protein B deficiency. *J Pediatr*. 1997;130(2):231-9.

28. Parker LA, Novotny DB. Recurrent alveolar proteinosis following double lung transplantation. *Chest*. 1997;111(5):1457-8.
29. Sallese A, Suzuki T, McCarthy C, Bridges J, Filuta A, Arumugam P, et al. Targeting cholesterol homeostasis in lung diseases. *Sci Report*. 2017;7(1):10211-4.
30. Nkadi PO, Merritt TA, Pillers DA. An overview of pulmonary surfactant in the neonate: genetics, metabolism, and the role of surfactant in health and disease. *Mol Genet Metab*. 2009;97(2):95-101.
31. Daniels CB, Orgeig S. Pulmonary surfactant: the key to the evolution of air breathing. *News Physiol Sci*. 2003;18:151-7.
32. Pérez-Gil J. Structure of pulmonary surfactant membranes and films: the role of proteins and lipid-protein interactions. *Biochim Biophys Acta*. 2008;1778(7-8):1676-95.
33. Lopez-Rodriguez E, Gay-Jordi G, Mucci A, Lachmann N, Serrano-Mollar A. Lung surfactant metabolism: early in life, early in disease and target in cell therapy. *Cell Tissue Res*. 2017;367:721-35.
34. Nag K, Munro JG, Hearn SA, Rasmusson J, Petersen NO, Possmayer F. Correlated atomic force and transmission electron microscopy of nanotubular structures in pulmonary surfactant. *J Struct Biol*. 1999;126(1):1-15.
35. Cañadas O, Olmeda B, Alonso A, Pérez-Gil J. Lipid-Protein and Protein-Protein Interactions in the Pulmonary Surfactant System and Their Role in Lung Homeostasis. *Int J Mol Sci*. 2020;21(10):3708.
36. Agassandian M, Mallampalli RK. Surfactant phospholipid metabolism. *Biochim Biophys Acta*. 2013;1831(3):612-25.
37. Goss V, Hunt AN, Postle AD. Regulation of lung surfactant phospholipid synthesis and metabolism. *Biochim Biophys Acta*. 2013;1831(2):448-58.
38. Post M, Batenburg JJ, Schuurmans EA, Van Golde LM. The rate-limiting step in the biosynthesis of phosphatidylcholine by alveolar type II cells from adult rat lung. *Biochim Biophys Acta*. 1982;712(2):390-4.
39. Mason RJ, Nellenbogen J. Synthesis of saturated phosphatidylcholine and phosphatidylglycerol by freshly isolated rat alveolar type II cells. *Biochim Biophys Acta*. 1984;794(3):392-402.
40. den Breejen JN, Batenburg JJ, van Golde LM. The species of acyl-CoA in subcellular fractions of type II cells isolated from adult rat lung and their incorporation into phosphatidic acid. *Biochim Biophys Acta*. 1989;1002(3):277-82.

41. Harayama T, Shindou H, Shimizu T. Biosynthesis of phosphatidylcholine by human lysophosphatidylcholine acyltransferase 1. *J Lipid Res.* 2009;50(9):1824-31.
42. Uozumi N, Kume K, Nagase T, Nakatani N, Ishii S, Tashiro F, et al. Role of cytosolic phospholipase A2 in allergic response and parturition. *Nature.* 1997;390(6660):618-22.
43. Bridges JP, Ikegami M, Brilli LL, Chen X, Mason RJ, Shannon JM. LPCAT1 regulates surfactant phospholipid synthesis and is required for transitioning to air breathing in mice. *J Clin Invest.* 2010;120(5):1736-48.
44. Bernardino de la Serna J, Perez-Gil J, Simonsen AC, Bagatolli LA. Cholesterol rules: direct observation of the coexistence of two fluid phases in native pulmonary surfactant membranes at physiological temperatures. *J Biol Chem.* 2004;279(39):40715-22.
45. Turley SD, Andersen JM, Dietschy JM. Rates of sterol synthesis and uptake in the major organs of the rat in vivo. *J Lipid Res.* 1981;22(4):551-69.
46. Hass MA, Longmore WJ. Regulation of lung surfactant cholesterol metabolism by serum lipoproteins. *Lipids.* 1980;15(6):401-6.
47. Pietra GG, Spagnoli LG, Capuzzi DM, Sparks CE, Fishman AP, Marsh JB. Metabolism of 125I-labeled lipoproteins by the isolated rat lung. *J Cell Biol.* 1976;70(1):33-46.
48. Orgeig S, Daniels CB. The roles of cholesterol in pulmonary surfactant: insights from comparative and evolutionary studies. *Comp Biochem Physiol A Mol Integr Physiol.* 2001;129(1):75-89.
49. Torday JS, Rehan VK. On the evolution of the pulmonary alveolar lipofibroblast. *Exp Cell Res.* 2016;340(2):215-9.
50. Haller T, Ortmayr J, Friedrich F, Völkl H, Dietl P. Dynamics of surfactant release in alveolar type II cells. *Proc Natl Acad Sci U S A.* 1998;95(4):1579-84.
51. Patel AS, Reigada D, Mitchell CH, Bates SR, Margulies SS, Koval M. Paracrine stimulation of surfactant secretion by extracellular ATP in response to mechanical deformation. *Am J Physiol Lung Cell Mol Physiol.* 2005;289(3):L489-L96.
52. Kramer BW, Ikegami M, Jobe AH. Surfactant phospholipid catabolic rate is pool size dependent in mice. *Am J Physiol Lung Cell Mol Physiol.* 2000;279(5):L842-L8.
53. Rider ED, Ikegami M, Jobe AH. Localization of alveolar surfactant clearance in rabbit lung cells. *Am J Physiol.* 1992;263((2 Pt 1)):L201-L9.
54. Bates SR, Tao JQ, Collins HL, Francone OL, Rothblat GH. Pulmonary abnormalities due to ABCA1 deficiency in mice. *Am J Physiol Lung Cell Mol Physiol.* 2005;289(6):L980-L9.

55. Brown K, Filuta A, Ludwig MG, Seuwen K, Jaros J, Vidal S, et al. Epithelial Gpr116 regulates pulmonary alveolar homeostasis via Gq/11 signaling. *JCI Insight*. 2017;2(11):e93700.
56. Bates SR, Tao JQ, Schaller S, Fisher AB, Shuman H. Lamellar body membrane turnover is stimulated by secretagogues. *Am J Physiol Lung Cell Mol Physiol*. 2000;278(3):L443-L52.
57. Jain D, Dodia C, Fisher AB, Bates SR. Pathways for clearance of surfactant protein A from the lung. *Am J Physiol Lung Cell Mol Physiol*. 2005;289(6):L1011-L8.
58. Wissel H, Lehfeldt A, Klein P, Müller T, Stevens PA. Endocytosed SP-A and surfactant lipids are sorted to different organelles in rat type II pneumocytes. *Am J Physiol Lung Cell Mol Physiol*. 2001;281(2):L345-L60.
59. Costet P, Luo Y, Wang N, Tall AR. Sterol-dependent transactivation of the ABC1 promoter by the liver X receptor/retinoid X receptor. *J Biol Chem*. 2000;275(36):28240-5.
60. Kielar D, Dietmaier W, Langmann T, Aslanidis C, Probst M, Naruszewicz M, et al. Rapid quantification of human ABCA1 mRNA in various cell types and tissues by real-time reverse transcription-PCR. *Clin Chem*. 2001;47(12):2089-97.
61. Oram JF, Heinecke JW. ATP-binding cassette transporter A1: a cell cholesterol exporter that protects against cardiovascular disease. *Physiol Rev*. 2005;85(4):1343-72.
62. Bodzioch M, Orsó E, Klucken J, Langmann T, Böttcher A, Diederich W, et al. The gene encoding ATP-binding cassette transporter 1 is mutated in Tangier disease. *Nat Genet*. 1999;22(4):347-51.
63. Kennedy MA, Barrera GC, Nakamura K, Baldan A, Tarr P, Fishbein MC, et al. ABCG1 has a critical role in mediating cholesterol efflux to HDL and preventing cellular lipid accumulation. *Cell Metab*. 2005;1(2):121-31.
64. Cavelier C, Lorenzi I, Rohrer L, von Eckardstein A. Lipid efflux by the ATP-binding cassette transporters ABCA1 and ABCG1. *Biochim Biophys Acta*. 2006;1761(7):655-66.
65. Baldan A, Tarr P, Vales CS, Frank J, Shimotake TK, Hawgood S, et al. Deletion of transmembrane transporter ABCG1 results in progressive pulmonary lipodosis. *J Biol Chem*. 2006;281:29401-10.
66. Thomassen MJ, Barna BP, Malur AG, Bonfield TL, Farver CF, Malur A, et al. ABCG1 is deficient in alveolar macrophages of GM-CSF knockout mice and patients with pulmonary alveolar proteinosis. *J Lipid Res*. 2007;48(12):2762-8.
67. Cakarova L, Marsh LM, Wilhelm J, Mayer K, Grimminger F, Seeger W, et al. Macrophage tumor necrosis factor-alpha induces epithelial expression of granulocyte-macrophage colony-stimulating factor: impact on alveolar epithelial repair. *Am J Respir Crit Care Med*. 2009;180(6):521-32.



68. Rosas M, Gordon S, Taylor PR. Characterisation of the expression and function of the GM-CSF receptor alpha-chain in mice. *Eur J Immunol.* 2007;37(9):2518-28.
69. Gearing DP, King JA, Gough NM, Nicola NA. Expression cloning of a receptor for human granulocyte-macrophage colony-stimulating factor. *EMBO J.* 1989;8(12):3667-76.
70. Hayashida K, Kitamura T, Gorman DM, Arai K, Yokota T, Miyajima A. Molecular cloning of a second subunit of the receptor for human granulocyte-macrophage colony-stimulating factor (GM-CSF): reconstitution of a high-affinity GM-CSF receptor. *Proc Natl Acad Sci U S A.* 1990;87(24):9655-9.
71. Huffman Reed JA, Rice WR, Zsengeller ZK, Wert SE, Dranoff G, Whitsett JA. GM-CSF enhances lung growth and causes alveolar type II epithelial cell hyperplasia in transgenic mice. *Am J Physiol.* 1997;273(4):L715-L25.
72. Bhattacharya P, Thiruppathi M, Elshabrawy HA, Alharshawi K, Kumar P, Prabhakar BS. GM-CSF: An immune modulatory cytokine that can suppress autoimmunity. *Cytokine.* 2015;75(2):261-71.
73. Dranoff G, Crawford AD, Sadelain M, Ream B, Rashid A, Bronson RT, et al. Involvement of granulocyte-macrophage colony-stimulating factor in pulmonary homeostasis. *Science.* 1994;264(5159):713-6.
74. Robb L, Drinkwater CC, Metcalf D, Li R, Köntgen F, Nicola NA, et al. Hematopoietic and lung abnormalities in mice with a null mutation of the common beta subunit of the receptors for granulocyte-macrophage colony-stimulating factor and interleukins 3 and 5. *Proc Natl Acad Sci U S A.* 1995;92(21):9565-9.
75. Suzuki T, Shima K, Arumugam P, Ma Y, Black D, Chalk C, et al. Development and validation of Csf2ra gene-deficient mice as a clinically relevant model of children with hereditary pulmonary alveolar proteinosis. *Am J Respir Crit Care Med.* 2017;195:A4837.
76. Huffman JA, Hull WM, Dranoff G, Mulligan RC, Whitsett JA. Pulmonary epithelial cell expression of GM-CSF corrects the alveolar proteinosis in GM-CSF-deficient mice. *J Clin Invest.* 1996;97(3):649-55.
77. Nishinakamura R, Wiler R, Dirksen U, Morikawa Y, Arai K, Miyajima A, et al. The pulmonary alveolar proteinosis in granulocyte macrophage colony-stimulating factor/interleukins 3/5 beta c receptor-deficient mice is reversed by bone marrow transplantation. *J Exp Med.* 1996;183(6):2657-62.
78. Hamilton JA. GM-CSF in inflammation and autoimmunity. *Trends Immunol.* 2002;23(8):403-8.

79. Williams M, De Kleer I, Henri S, Post S, Vanhoutte L, De Prijck S, et al. Alveolar macrophages develop from fetal monocytes that differentiate into long-lived cells in the first week of life via GM-CSF. *J Exp Med*. 2013;210(10):1977-92.
80. Bonfield TL, Farver CF, Barna BP, Malur A, Abraham S, Raychaudhuri B, et al. Peroxisome proliferator-activated receptor-gamma is deficient in alveolar macrophages from patients with alveolar proteinosis. *Am J Respir Cell Mol Biol*. 2003;29(6):677-82.
81. Baker AD, Malur A, Barna BP, Ghosh S, Kavuru MS, Malur AG, et al. Targeted PPAR $\gamma$  deficiency in alveolar macrophages disrupts surfactant catabolism. *J Lipid Res*. 2010;51(6):1325-31.
82. Bonfield TL, Raychaudhuri B, Malur A, Abraham S, Trapnell BC, Kavuru MS, et al. PU.1 regulation of human alveolar macrophage differentiation requires granulocyte-macrophage colony-stimulating factor. *Am J Physiol Lung Cell Mol Physiol*. 2003;285(5):L1132-L6.
83. Hashimoto D, Chow A, Noizat C, Teo P, Beasley MB, Leboeuf M, et al. Tissue-resident macrophages self-maintain locally throughout adult life with minimal contribution from circulating monocytes. *Immunity*. 2013;38(4):792-804.
84. Griese M. Pulmonary surfactant in health and human lung diseases: state of the art. *Eur Respir J*. 1999;13(6):1455-76.
85. Ikegami M, Ueda T, Hull W, Whitsett JA, Mulligan RC, Dranoff G, et al. Surfactant metabolism in transgenic mice after granulocyte macrophage-colony stimulating factor ablation. *Am J Physiol*. 1996;270(4 Pt 1):L650-8.
86. Pison U, Wright JR, Hawgood S. Specific binding of surfactant apoprotein SP-A to rat alveolar macrophages. *Am J Physiol*. 1992;262:L412-7.

## **CHAPTER 2**

### **ABCG1 regulates pulmonary surfactant metabolism in mice and men**



Supplemental Material can be found at:  
<http://www.jlr.org/content/suppl/2017/03/06/jlr.M075101.DC1.html>

## ABCG1 regulates pulmonary surfactant metabolism in mice and men<sup>5</sup>

Thomas Q. de Aguiar Vallim,<sup>\*†,§,\*\*\*</sup> Elinor Lee,<sup>\*††</sup> David J. Merriott,<sup>1,†</sup> Christopher N. Goulbourne,<sup>§§</sup> Joan Cheng,<sup>†</sup> Angela Cheng,<sup>†</sup> Ayelet Gonen,<sup>\*\*\*</sup> Ryan M. Allen,<sup>2,†††</sup> Elisa N. D. Palladino,<sup>†††,§§§</sup> David A. Ford,<sup>†††,§§§</sup> Tisha Wang,<sup>\*††</sup> Ángel Baldán,<sup>†††</sup> and Elizabeth J. Tarling<sup>3,\*§,\*\*\*</sup>

Department of Medicine,<sup>\*</sup> Department of Biological Chemistry, David Geffen School of Medicine,<sup>†</sup> Molecular Biology Institute,<sup>§</sup> Johnson Comprehensive Cancer Center,<sup>\*\*</sup> and Division of Pulmonary and Critical Care Medicine,<sup>††</sup> University of California Los Angeles, Los Angeles, CA 90095; Columbia Nano Initiative Electron Microscopy Facility,<sup>§§</sup> Columbia University, New York, NY 10027; Department of Medicine,<sup>\*\*\*</sup> University of California San Diego, La Jolla, CA 92093; and Edward A. Doisy Department of Biochemistry and Molecular Biology<sup>†††</sup> and Center for Cardiovascular Research, School of Medicine,<sup>§§§</sup> Saint Louis University, St. Louis, MO 63104

ORCID ID: 0000-0002-0599-0432 (E.J.T.)

**Abstract** Idiopathic pulmonary alveolar proteinosis (PAP) is a rare lung disease characterized by accumulation of surfactant. Surfactant synthesis and secretion are restricted to epithelial type 2 (T2) pneumocytes (also called T2 cells). Clearance of surfactant is dependent upon T2 cells and macrophages. ABCG1 is highly expressed in both T2 cells and macrophages. ABCG1-deficient mice accumulate surfactant, lamellar body-loaded T2 cells, lipid-loaded macrophages, B-1 lymphocytes, and immunoglobulins, clearly demonstrating that ABCG1 has a critical role in pulmonary homeostasis. We identify a variant in the *ABCG1* promoter in patients with PAP that results in impaired activation of *ABCG1* by the liver X receptor  $\alpha$ , suggesting that ABCG1 basal expression and/or induction in response to sterol/lipid loading is essential for normal lung function. We generated mice lacking ABCG1 specifically in either T2 cells or macrophages to determine the relative contribution of these cell types on surfactant lipid homeostasis. **These results establish a critical role for T2 cell ABCG1 in controlling surfactant and overall lipid homeostasis in the lung and in the pathogenesis of human lung disease.**—de Aguiar Vallim, T. Q., E. Lee, D. J. Merriott, C. N. Goulbourne, J. Cheng, A. Cheng, A. Gonen, R. M. Allen, E. N. D. Palladino, D. A. Ford, T. Wang, Á. Baldán, and E. J. Tarling. *ABCG1 regulates pulmonary surfactant metabolism in mice and men.* *J. Lipid Res.* 2017. 58: 941–954.

**Supplementary key words** cholesterol • phospholipid • lung • pulmonary alveolar proteinosis • ATP binding cassette transporter G1

Surfactant is a complex mixture of lipids and proteins that forms a monolayer lining the alveolar sacs in the lungs to maintain surface tension and prevent the collapse of alveoli (1). Surfactant is composed of ~85% phospholipids [predominantly dipalmitoyl phosphatidylcholine (PC)], ~10% neutral lipids (mostly cholesterol), and ~5% proteins. The latter include surfactant proteins (SPs), SP-A, SP-B, SP-C, and SP-D. These proteins play critical roles in the formation, function, and metabolism of surfactant (2–5). SP-A and SP-D also play critical roles in the immune response to foreign antigens (3–6).

Surfactant lipids are synthesized and secreted by epithelial type 2 (T2) pneumocytes (also called T2 cells). Initially, lipids and SPs, SP-B and SP-C, are packed into lamellar bodies, specialized secretory organelles within T2 cells, prior to fusion with the plasma membrane and secretion into the hypophase of the alveoli (7). Other proteins recovered in surfactant, including SP-A and SP-D, are secreted

This work was supported, in part, by National Heart, Lung, and Blood Institute Grants HL116181 (to E.J.T.), HL122677 (to T.Q.d.A.V.), and HL107794 (to Á.B.); National Institute of General Medical Sciences Grant GM115553 (to D.A.F.); American Heart Association Grant-in-Aid 13BGIA17080038 (to E.J.T.); and Scientist Development Grant 14SDG18440015 (to T.Q.d.A.V.). The content is solely the responsibility of the authors and does not necessarily represent the official views of the National Institutes of Health.

The authors declare no conflicts of interest.

Manuscript received 23 January 2017 and in revised form 3 March 2017.

Published, JLR Papers in Press, March 6, 2017  
 DOI <https://doi.org/10.1194/jlr.M075101>

Copyright © 2017 by the American Society for Biochemistry and Molecular Biology, Inc.

This article is available online at <http://www.jlr.org>

Abbreviations: Ad-ABCG1, ABCG1 adenovirus; BAL, broncho-alveolar lavage; BM, bone marrow; HF/HG, high fat/high cholesterol; LXR, liver X receptor; PAP, pulmonary alveolar proteinosis; PC, phosphatidylcholine; PE, phosphatidylethanolamine; PG, phosphatidylglycerol; SP, surfactant protein; T2, type 2.

<sup>1</sup>Present address of D. J. Merriott: Department of Radiation-Oncology, Stanford School of Medicine, Stanford, CA 94305.

<sup>2</sup>Present address of R. M. Allen: Department of Medicine, Vanderbilt University Medical Center, Nashville, TN 37232.

<sup>3</sup>To whom correspondence should be addressed.

e-mail: [etarling@mednet.ucla.edu](mailto:etarling@mednet.ucla.edu)

<sup>5</sup>The online version of this article (available at <http://www.jlr.org>) contains a supplement.

through a different lamellar body-independent pathway (8). It is estimated that most of the surfactant phospholipids are synthesized in situ by T2 cells, whereas cholesterol is derived from serum lipoproteins with less than 1% being derived from de novo synthesis (9).

The mechanisms involved in subsequent clearing of the extracellular surfactant are not fully understood. It is known that both T2 cells and alveolar macrophages participate in the uptake of lipids from the alveolar hypophase in a process mediated by SP-A and SP-D (2, 8, 10). T2 cells recycle most of these lipids, repackaging them into lamellar bodies prior to resecretion. In contrast, surfactant phospholipids taken up by macrophages are thought to be catabolized. Intratracheal administration of radiolabeled dipalmitoyl PC suggests that T2 cells and macrophages contribute equally to surfactant uptake and/or degradation in vivo (11).

ABCG1 is a member of the ABC family of transmembrane transporters [reviewed in (12–15)]. ABCG1 has been shown to facilitate cholesterol efflux from cells to a variety of exogenous lipid acceptors that include LDL, phospholipid vesicles, phospholipid/apolipoprotein complexes, and mature HDL, but not lipid-poor apoA1 (16–23). We have demonstrated that ABCG1 localizes to intracellular organelles of the endosomal pathway, where it functions to regulate intracellular sterol homeostasis (24, 25). This is consistent with work from Sturek et al. (26), who reported that ABCG1 is important for pancreatic  $\beta$ -cell cholesterol homeostasis and insulin secretion.

*Abcg1*<sup>-/-</sup> mice have normal plasma lipid levels, but exhibit an age-related progressive pulmonary disease that has many of the properties associated with human respiratory distress syndromes, including lipidosis and chronic inflammation (27–30). Although the lungs of young mice (<6 weeks) appear visually normal, they are already accumulating small amounts of lipid. By the age of 6–8 months, the lungs of chow-fed *Abcg1*<sup>-/-</sup> mice are white as a result of lipid accumulation within macrophages and T2 cells and in the extracellular spaces (17, 27, 28, 30). The lungs of aged *Abcg1*<sup>-/-</sup> mice contain large numbers of lipid-loaded macrophages and 5-fold more T2 cells (28). Compared with T2 cells in wild-type mice, T2 cells in *Abcg1*<sup>-/-</sup> mice contain 5-fold more lamellar bodies that are both larger and more dense, consistent with intracellular accumulation of surfactant lipids that likely contributes to the overall pulmonary lipidosis (28). In addition, the lungs of *Abcg1*<sup>-/-</sup> mice show evidence of inflammation, as judged by increased lymphocytic infiltration, increased expression of cytokines, and the presence of chitinase-3-like crystals (27, 28, 30). All these changes are greatly accelerated when *Abcg1*<sup>-/-</sup> mice were fed a Western diet containing 21% fat and 0.2% cholesterol (17, 28). In contrast to the abnormalities of macrophages and T2 cells in the lungs of *Abcg1*<sup>-/-</sup> mice, endothelial cells and type 1 epithelial cells that line the alveoli appear normal, as determined by standard lipid staining techniques and electron microscopy (17, 28).

Taken together, these studies identified pivotal roles for ABCG1 in controlling pulmonary homeostasis in vivo (17, 27, 28, 30, 31). Interestingly, functional loss of two

other ABC transporters (ABCA3 and ABCA1) also results in pulmonary lipid abnormalities (32, 33). Loss of ABCA3 results in early postnatal death in both humans and mice due to the inability of *Abca3*<sup>-/-</sup> T2 cells to package surfactant into lamellar bodies and subsequently secrete these lipid organelles into the hypophase (33–35). In contrast, loss of ABCA1 (Tangier disease) results not only in >95% loss in plasma HDL in mice and humans, but also in a mild pulmonary lipidosis in mice (32). To our knowledge, pulmonary lipidosis has not been described in Tangier patients (36, 37).

In order to determine whether ABCG1 has a cell-autonomous function in T2 cells, we used bone marrow (BM) transplants to generate mice in which the lungs contained chimeric mixtures of wild-type and *Abcg1*<sup>-/-</sup> cells. Further, we generated mice lacking ABCG1 in either T2 cells (*Abcg1*<sup>T2-KO</sup>) or macrophages (*Abcg1*<sup>MAC-KO</sup>). Analyses of these various mice identify differential, but critical, roles for ABCG1 in both T2 cells and macrophages that affect pulmonary lipid and surfactant homeostasis and immunoglobulin levels.

## MATERIALS AND METHODS

### Mice

*Abcg1*<sup>fllox/fllox</sup> mice created on a C57BL6/J background [from Dr. Catherine Hedrick, La Jolla Institute for Allergy and Immunology (38)] were crossed with *Sftpc-Cre* mice [from Dr. Brigid Hogan, Duke University (39)] to obtain *Sftpc-Cre*<sup>+</sup> *Abcg1*<sup>fllox/fllox</sup> and control *Sftpc-Cre*<sup>-</sup> *Abcg1*<sup>fllox/fllox</sup> mice. *Abcg1*<sup>fllox/fllox</sup> mice were crossed with *LysM-Cre* mice (catalog 004781; Jackson Laboratory) to obtain *LysM-Cre*<sup>+</sup> *Abcg1*<sup>fllox/fllox</sup> and control *LysM-Cre*<sup>-</sup> *Abcg1*<sup>fllox/fllox</sup> mice. All mice used were 12-week-old males. Mice were fed a standard rodent chow diet (Purina 5001) until weaning. At weaning, mice were fed a high cholesterol diet containing 0.2% cholesterol and 21% calories from fat (D12079B; Research Diets) for 4 weeks. Mice were bred and maintained at the University of California Los Angeles in temperature-controlled pathogen-free conditions, under a 12 h light/dark cycle. All protocols involving mice were reviewed and approved by the University of California Los Angeles Animal Research Committee.

### BM chimera generation

*Abcg1*<sup>-/-</sup>/*LacZ* knock-in mice on a C57BL/6 background were maintained on a standard rodent diet (Purina 5001), as described (17, 28). For BM transplantation studies, recipient wild-type and *Abcg1*<sup>-/-</sup> mice (10 weeks old) were  $\gamma$ -irradiated with 900 rad before transplantation with cells ( $3 \times 10^6$ ) from 8- to 10-week-old donor male wild-type or *Abcg1*<sup>-/-</sup> animals via tail vein injection. After a 4 week recovery period, mice were fed a 21% fat and 0.2% cholesterol diet (Research Diets #D12079B) for 16 weeks.

### Histopathologic analysis and immunohistochemistry

Hematoxylin-eosin staining of paraffin-embedded lung sections was performed as described (17). Morphometric analysis of T2 cells was performed with Image Pro software (Media Cybernetics, Inc.). Oil red O and filipin staining of frozen lung sections was performed as described (40). Frozen lung sections were stained with antibodies for macrophages (anti-mac3 1:1,000; BD Biosciences) and T2 cells (anti-prosurfactant protein C 1:1,000; BD Biosciences). Filipin (25  $\mu$ g/ml) was added during overnight



Supplemental Material can be found at:  
<http://www.jlr.org/content/suppl/2017/03/08/jlr.M075101.DC1.html>

incubation of slides with antibodies. Immunostaining of adjacent sections in the absence of primary antibody was used as a negative control.

### Electron microscopy

Fixed tissues were incubated with 2.5% glutaraldehyde and 2% paraformaldehyde in 100 mM cacodylate buffer (pH 7.4) overnight. Samples were then treated with 1% osmium tetroxide in 100 mM cacodylate buffer for 1 h, washed in distilled water four times (10 min/wash), and then treated with 1–2% aqueous uranyl acetate overnight at 4°C in the dark. Samples were then washed and sequentially dehydrated with increasing concentrations of acetone (20, 30, 50, 70, 90, and 100%) for 30 min each, followed by three additional treatments with 100% acetone for 20 min each. Samples were then infiltrated with increasing concentrations of Spurr's resin (25% for 1 h, 50% for 1 h, 75% for 1 h, 100% for 1 h, 100% overnight at room temperature), and then incubated overnight at 70°C in a resin mold. Sections of 50–90 nm were cut on a Leica ultramicrotome with a diamond knife. Imaging then took place using an FEI Talos F200X operating at 200 kV.

### T2 pneumocyte isolation

Mouse lung cells were isolated as previously described (41), with some modifications. Lungs were perfused with PBS via the right ventricle. Lungs were inflated with enzyme solution [collagenase type I (450 U/ml; Roche Applied Science), dispase II (5 U/ml; StemCell Technologies), DNase I (0.33 U/ml; Sigma-Aldrich), and elastase (4 U/ml; Roche Applied Science)] for 3 min. Lungs were removed and minced into small pieces and incubated at 37°C for 25 min with shaking. Enzymatically digested samples were passed through needles and filtered through a 70 µm cell strainer (Fisher Scientific). After treatment with red blood cell lysis buffer, cells were filtered through a 40 µm cell strainer (Fisher Scientific) and resuspended in DMEM (Invitrogen) containing 10% FBS (Omega Scientific), 100 U/ml penicillin (Invitrogen), and 100 µg/ml streptomycin sulfate (Invitrogen). Hematopoietic cells were depleted from the lung cell suspension using the autoMACS separator with anti-mouse CD45 antibody-coated micro-beads according to the manufacturer's instructions (Miltenyi Biotech). Sorted CD45<sup>−</sup> lung cells were stained with phosphatidylethanolamine (PE)-anti-mouse epithelial cell adhesion molecule (EpCAM; eBioscience; catalog #12-5791-83; Clone G8.8) and Alex Fluor 488-anti-mouse Podoplanin/T1α (eBioscience; catalog #53-5381-82; Clone 8.1.1). T2 pneumocytes were classified as EpCAM<sup>hi</sup>/T1α<sup>−</sup>, as previously described (41).

### RNA isolation and analysis

RNA was isolated and analyzed by real-time quantitative (q) PCR, as described (40). Each qPCR assay was performed in triplicate using cDNA samples isolated from individual mice (n = 4–6 mice/group). Primer sets are available upon request. Values were normalized to 36B4.

### Immunoblotting

T2 cells and alveolar macrophages were isolated from mouse lung and broncho-alveolar lavage (BAL) fluid, respectively, as described, and lysed with RIPA buffer (Boston Bioproducts) containing protease inhibitors [25 µg/ml N-acetyl-L-leucyl-L-leucyl-L-norleucinal, 10 µg/ml leupeptin, 1 µg/ml pepstatin, and 1 mM phenylmethylsulfonyl fluoride (Sigma-Aldrich)]. Protein quantification was performed using BCA protein assay reagent (Thermo Fisher Scientific). Forty milligrams of protein per sample were loaded into SDS-PAGE and sequentially immunoblotted

with anti-ABCG1 antibody (1:1,000; catalog NB400-132; Novus Biologicals).

### Surfactant isolation

Pulmonary surfactant was isolated by BAL, as previously described (28). Briefly, tracheas were exposed and cannulated before the lungs were flushed three times with 1 ml aliquots of BAL buffer [10 mM Tris, 100 mM NaCl, and 0.2 mM EGTA (pH 7.2)]. The aliquots were combined and centrifuged (200 g, 5 min) to separate surfactant and alveolar cells.

### Lipid measurements

Plasma cholesterol and triglycerides were measured using an enzymatic kit (Wako Chemicals) according to the manufacturer's instructions. Tissue lipids were extracted into CHCl<sub>3</sub> by a modified Folch method, and quantitated using enzymatic kits for cholesterol, triglycerides, or phospholipid using the accompanying protocols (Wako Chemicals).

### Cholesterol and phospholipid analysis

Cells, BAL fluid, or lung tissue was snap-frozen in liquid nitrogen. Lung tissue was homogenized on ice in PBS. Cell suspensions, BAL fluid, or lung homogenates were subsequently subjected to modified Bligh-Dyer extraction (42) in the presence of lipid class internal standards, including eicosanoic acid, cholesteryl heptadecanoate, and 1,2-dieicosanoyl-*sn*-glycero-3-phosphocholine (43). Fatty acids were converted to their pentafluorobenzyl esters and subsequently quantified using GC-MS with negative-ion chemical ionization using methane as the reactant gas (44). For phospholipids, lipid extracts were diluted in methanol/chloroform (4/1, v/v) and molecular species were quantified by ESI-MS/MS on a triple quadrupole instrument (Thermo Fisher Quantum Ultra) using shotgun lipidomics methodologies (45). PC molecular species were quantified as sodiated adducts in the positive-ion mode using neutral loss scanning for 59.1 amu (collision energy = −28 eV). Neutral loss scanning for 368.5 amu (collision energy = −25 eV) was performed for quantification of sodiated CE molecular species in positive ion mode. Individual molecular species were quantified by comparing the ion intensities of the individual molecular species to that of the lipid class internal standard, with additional corrections for type I and type II [<sup>13</sup>C] isotope effects (45).

### A549 lipid analysis

Total lipids were extracted from 50 mg whole lung tissue and quantified, as previously described (17). A549 cells were seeded in 12-well plates (1 × 10<sup>6</sup> cells/well) and were infected overnight with either control GFP adenovirus, or adenovirus expressing ABCG1. Cells were then incubated in medium (0.2% BSA or 10% FBS) supplemented with 1 µCi/ml [<sup>14</sup>C]acetate (50–60 mCi/mmol) for the indicated time. Cells were washed two times in PBS and incubated in medium (0.2% BSA or 10% FBS) ± secretagogue mixture [100 µM ATP, 0.1 µM phorbol-12-myristate-13-acetate, and 20 µM terbutaline (46)]. After the indicated time, the cells were washed three times in PBS. Lipids were extracted from the medium and cells using the Bligh and Dyer method (42). Extracted lipids were dissolved in chloroform (100 µl), and aliquots (30 µl) were analyzed by thin-layer chromatography, as described (47, 48).

### Measurement of antibody titers

Total antibody titers were determined by chemiluminescent enzyme immunoassays, as previously described (49). In brief, capture antigens were coated on plates at 5 µg/ml in PBS overnight at 4°C [IgM (1:100 goat anti-mouse IgM; Sigma-Aldrich), IgG (1:400 goat anti-mouse IgG; Pierce Protein Biology), IgG1 (1:250

Supplemental Material can be found at:  
<http://www.jlr.org/content/suppl/2017/03/08/jlr.M075101.DC1.html>

goat anti-mouse IgG1; Jackson ImmunoResearch Laboratories), IgG (1:250 goat anti-mouse IgG2c; Jackson ImmunoResearch Laboratories), IgA (1:100 goat anti-mouse IgA; Sigma-Aldrich). Plates were blocked with 1% BSA in TBS, and serially diluted anti-serum or BAL fluid from individual mice was added. Plates were incubated for 1.5 h at room temperature. Bound immunoglobulin isotype levels were assessed with various anti-mouse Ig isotype-specific alkaline phosphatase conjugates using Lumi-Phos 530 (Lumigen, Southfield, MI) solution and a Dynex luminometer (Dynex Technologies, Chantilly, VA). Several secondary antibodies were used at dilutions of 1:30,000. These included alkaline phosphatase-labeled goat anti-mouse IgM ( $\mu$ -chain specific), goat anti-mouse IgG ( $\gamma$ -chain specific), and goat anti-mouse IgA ( $\alpha$ -chain specific) (all from Sigma-Aldrich). Specific controls were used for each specific antibody, and formal antibody dilution curves were determined in an initial study to identify the linear range of each antibody titer measurement. It was determined from these dilution curves that plasma samples could be optimally measured at 1:250 to 1:1,000 dilutions and BAL fluid samples could be optimally measured at 1:5 to 1:250 dilutions to yield concentrations within the linear detection range for each assay.

### Human alveolar macrophage analysis

Human BAL fluid was collected at the University of California Los Angeles, Division of Pulmonary and Critical Care Medicine from patients with pulmonary alveolar proteinosis (PAP) undergoing whole lung lavage. Enrolled patients included both men and women, aged 42–59 years, who had previously been diagnosed with PAP and presented for a medically necessary whole lung lavage (see supplemental Table S1 for a general characterization of the human subjects group studied). Pulmonary surfactant and alveolar macrophages were isolated by centrifugation (200 g, 5 min). Genomic DNA was isolated from alveolar macrophages using the DNeasy extraction kit (Qiagen) according to manufacturer's instructions. *ABCG1* regulatory regions were sequenced by Sanger sequencing (GENEWIZ, LLC). Primers are available on request.

### Treatment of human macrophages

Human macrophages were plated in 6-well plates in DMEM supplemented with 10% FBS, 100 U/ml penicillin, and 100  $\mu$ g/ml streptomycin sulfate (medium A) on day 0. On day 1, cells were placed in medium A in the presence or absence of 1  $\mu$ M GW3965 for 0, 0.5, 1, 2, 4, or 8 h. Cells were harvested in QIAzol (Invitrogen) and total RNA extracted according to the manufacturer's instructions. Gene expression was analyzed by real-time qPCR. Each qPCR assay was performed in triplicate using cDNA samples isolated from replicate wells ( $n = 3$  replicate wells per treatment and time point). Primer sets are available upon request. Values were normalized to 36B4.

### Statistical analysis

Significance was measured, as stated, by either one-way ANOVA followed by Bonferroni correction, two-way ANOVA followed by Bonferroni correction, or by Student's *t*-test.

### Study approval

Animal use was approved by the University of California Los Angeles and followed the National Institutes of Health *Guide for the Care and Use of Laboratory Animals*. All experiments were approved by the University of California Los Angeles Institute for Animal Care and Use Committee. Informed consent was obtained from human subjects for the use of BAL samples, with the approval of the Institutional Review Board for Medical Research at the University of California Los Angeles.

## RESULTS

### BM transplant studies identify an important role for ABCG1 expression in nonhematopoietic-derived cells

ABCG1 is highly expressed in T1 and T2 epithelial cells, interstitial and alveolar macrophages, and endothelial cells (17, 28, 40). Given the widespread expression of ABCG1 within the lung, it was not possible to determine which cell types contribute to the morphologic and lipid abnormalities observed in the lungs of *Abcg1*<sup>-/-</sup> mice (17, 28, 40). Previous studies indicated that accumulation of Oil red O-positive neutral lipids in the lung was greatly attenuated following BM transplantation of wild-type donor BM into recipient *Abcg1*<sup>-/-</sup> mice (30). This led to the proposal that the pulmonary lipidosis and inflammation were solely dependent on the presence of *Abcg1*<sup>-/-</sup> macrophages in the lungs of the recipient mice (30). Based on the high expression of ABCG1 in pulmonary T2 cells and the critical role these cells play in surfactant metabolism, we have reevaluated the role of ABCG1 in T2 cell function and pulmonary lipidosis.

In initial studies, we performed BM transplants using wild-type and *Abcg1*<sup>-/-</sup> mice as donors and/or recipients (Fig. 1A). This approach resulted in chimeric mice in which the lungs of the transplanted mice contain either: *i*) all *Abcg1*<sup>+/+</sup> cells (wild-type phenotype); *ii*) all *Abcg1*<sup>-/-</sup> cells (*Abcg1*<sup>-/-</sup> phenotype); *iii*) *Abcg1*<sup>+/+</sup> epithelial and endothelial cells and *Abcg1*<sup>-/-</sup> macrophages/lymphocytes (*Abcg1*<sup>M/L-KO</sup>); or *iv*) *Abcg1*<sup>+/+</sup> macrophages/lymphocytes and *Abcg1*<sup>-/-</sup> epithelial and endothelial cells (*Abcg1*<sup>EECKO</sup>). After BM transplantation, mice were allowed to recover for 4 weeks on a standard chow diet before being fed a high fat/high cholesterol (HF/HC) diet for 16 weeks (21% fat, 0.2% cholesterol) (Fig. 1A).

As expected, lungs of *Abcg1*<sup>+/+</sup> mice were morphologically normal and lacked any Oil red O-positive lipid droplets (supplemental Fig. S1A). In contrast, but consistent with earlier studies (17, 28), the lungs of mice containing *Abcg1*<sup>-/-</sup> macrophages exhibited reduced alveolar spaces, especially in the sub-pleural areas, as well as accumulation of Oil red O-positive cells (supplemental Fig. S1B, D). Importantly, histological analysis of the lungs of *Abcg1*<sup>EECKO</sup> chimeric mice (wild-type BM  $\rightarrow$  *Abcg1*<sup>-/-</sup> mice) indicates that they were structurally abnormal, despite the absence of Oil red O-positive cells (supplemental Fig. S1C). Table 1 shows that lung weights of *Abcg1*<sup>-/-</sup>, *Abcg1*<sup>M/L-KO</sup>, and *Abcg1*<sup>EECKO</sup> mice were increased by 82, 19, and 20%, respectively, in comparison to wild-type lungs. Further, the levels of free and esterified cholesterol as well as phospholipids were significantly increased in all three experimental groups (*Abcg1*<sup>-/-</sup> > *Abcg1*<sup>M/L-KO</sup> and *Abcg1*<sup>EECKO</sup>). These data indicate that abnormal lipid homeostasis occurs not only when pulmonary macrophages and/or lymphocytes lack ABCG1, but also when ABCG1 is deleted from epithelial T1 and T2 cells and endothelial cells (*Abcg1*<sup>EECKO</sup> mice).

### T2 cells lacking ABCG1 accumulate unesterified cholesterol

The finding that the lungs of *Abcg1*<sup>EECKO</sup> mice (containing wild-type macrophages/lymphocytes and *Abcg1*<sup>-/-</sup> epithelial



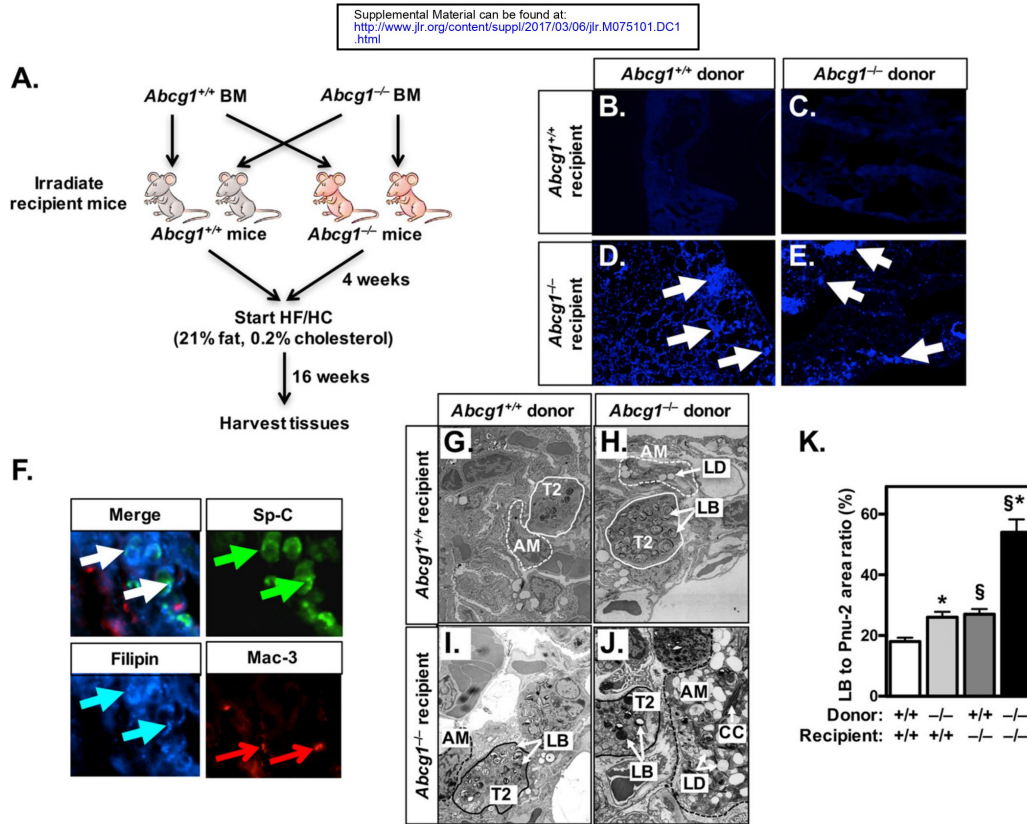


**Fig. 1.** ABCG1 has a critical role in nonhematopoietic cells. **A:** Schematic of BM transplantation studies. Wild-type and *Abcg1<sup>-/-</sup>* mice were irradiated and received BM from either wild-type or *Abcg1<sup>-/-</sup>* donor animals. After a 4 week recovery period, all mice were fed a HF/HC (21% fat, 0.2% cholesterol) diet for 16 weeks. **B–E:** Frozen lung sections (10  $\mu$ M) of BM-transplanted mice [as in (A)] were stained with filipin for the presence of free cholesterol. White arrows mark filipin-positive areas. Images are at 20 $\times$  magnification. **F:** Frozen lung sections (10  $\mu$ M) from *Abcg1<sup>EEG-KO</sup>* mice (*Abcg1<sup>-/-</sup>* mice receiving *Abcg1<sup>+/+</sup>* BM) were stained with antibodies for T2 cells (pro-SP-C; green arrows) and macrophages (Mac-3; red arrows), followed by staining with filipin (blue arrows) for free cholesterol. White arrows indicate areas of colocalization. Images are at 100 $\times$  magnification. **G–J:** Representative electron micrographs (original magnification: 9,900 $\times$ ) from BM-transplanted mice [as in (A)]. **K:** The relative area of lamellar bodies within each T2 cell was determined in electron micrographs ( $n = 32$ ) from each group of transplanted mice (G–J). Significance was measured by two-way ANOVA followed by Bonferroni correction. Data are expressed as mean  $\pm$  SEM. \* $P < 0.01$  wild-type versus *Abcg1<sup>-/-</sup>* donor; § $P < 0.01$  wild-type versus *Abcg1<sup>-/-</sup>* recipient. AM, alveolar macrophage; CC, cholesterol crystal; LB, lamellar body; LD, lipid droplet.

and endothelial cells) contained a high ratio of unesterified: total cholesterol (Table 1, column 3) was unexpected because excess unesterified cholesterol is generally toxic to cells and, hence, usually esterified and stored in lipid droplets (50). To determine whether unesterified cholesterol deposition (Table 1) localized to a specific cell type, we performed filipin staining using frozen lung sections from BM-transplanted mice. Filipin staining was only observed in the lungs of *Abcg1<sup>EEG-KO</sup>* and *Abcg1<sup>-/-</sup>* mice (Fig. 1D, E) suggesting that unesterified cholesterol was accumulating in endothelial and/or epithelial cells. Consequently, we obtained frozen sections from the lungs of *Abcg1<sup>EEG-KO</sup>* mice with filipin and antibodies against SP-C or Mac-3 that identify T2 cells and macrophages, respectively (Fig. 1F). The data show colocalization of filipin staining with SP-C

(Fig. 1F; white arrows). Thus, we conclude that the filipin-positive cells are T2 cells and that these cells have unusually high levels of unesterified cholesterol in the lungs of *Abcg1<sup>EEG-KO</sup>* mice fed a HF/HC diet.

#### Pulmonary *Abcg1<sup>-/-</sup>* T2 cells are abnormal in the presence of wild-type macrophages

We previously demonstrated that *Abcg1<sup>-/-</sup>* mice showed altered pulmonary surfactant metabolism, including increased lipid and protein levels in pulmonary surfactant recovered from BAL and abnormal T2 cells that contained increased numbers of enlarged electron-dense lamellar bodies (28). To our knowledge, it is not known whether these dramatic changes in T2 cells were a result of the loss of ABCG1 from T2 cells, macrophages, or both cell types.



Supplemental Material can be found at:  
<http://www.jlr.org/content/suppl/2017/03/08/jlr.M075101.DC1.html>

TABLE 1. Altered lipid content of the lungs of bone-marrow transplanted mice

|                          | Wild-type Recipient |                                   | <i>Abcg1</i> <sup>-/-</sup> Recipient |                                   |
|--------------------------|---------------------|-----------------------------------|---------------------------------------|-----------------------------------|
|                          | Wild-type Donor     | <i>Abcg1</i> <sup>-/-</sup> Donor | Wild-type Donor                       | <i>Abcg1</i> <sup>-/-</sup> Donor |
| Lung weight (mg)         | 41.2 ± 1.2          | 48.4 ± 1.4 <sup>a</sup>           | 50.7 ± 2.0 <sup>b</sup>               | 75.7 ± 2.4 <sup>a,b</sup>         |
| Lung lipids (μg/mg)      |                     |                                   |                                       |                                   |
| Total cholesterol        | 0.66 ± 0.1          | 2.56 ± 0.2 <sup>a</sup>           | 3.32 ± 0.6 <sup>b</sup>               | 8.34 ± 1.3 <sup>a,b</sup>         |
| Unesterified cholesterol | 0.46 ± 0.1          | 1.04 ± 0.1 <sup>a</sup>           | 2.84 ± 0.4 <sup>b</sup>               | 3.42 ± 0.4 <sup>b</sup>           |
| Esterified cholesterol   | 0.20 ± 0.1          | 1.52 ± 0.2 <sup>a</sup>           | 0.48 ± 0.2                            | 4.92 ± 1.4 <sup>a,b</sup>         |
| Phospholipids            | 1.86 ± 0.3          | 4.34 ± 0.4 <sup>a</sup>           | 6.50 ± 1.1 <sup>b</sup>               | 11.09 ± 2.7 <sup>a,b</sup>        |

Tissue lipid levels were determined as described in the Materials and Methods. Data are expressed as mean ± SEM (n = 4–6 mice/group). Significance was determined by two-way ANOVA followed by Bonferroni correction.

<sup>a</sup>P < 0.01 wild-type versus *Abcg1*<sup>-/-</sup> donor.

<sup>b</sup>P < 0.01 wild-type versus *Abcg1*<sup>-/-</sup> recipient.

Morphometric analysis of electron micrographs revealed that the T2 cells of *Abcg1*<sup>-/-</sup> mice had a 3-fold increase in lamellar bodies (Fig. 1J, K). These data are consistent with a prior study showing a 5-fold increase in lamellar bodies per T2 cell in the lungs of old whole-body *Abcg1*<sup>-/-</sup> mice (28). We now report that the T2 cells in both the *Abcg1*<sup>EECRKO</sup> (Fig. 1I, K) and *Abcg1*<sup>M/L-KO</sup> (Fig. 1H, K) chimeric mouse models contain a 47% increase in lamellar bodies. Taken together, these data suggest that ABCG1 plays critical cell-specific roles in both T2 cells and macrophages. It also suggests that T2 cell function can be modulated by signals from alveolar macrophages that lack ABCG1.

#### Specific loss of ABCG1 from T2 cells has broad effects on lung morphology and gene expression

The above studies do not allow us to attribute the observed abnormalities to individual cell types. To directly define the specific role and importance of ABCG1 in the lung, we first crossed *Abcg1*<sup>fllox/fllox</sup> mice with mice expressing *Sfptc-Cre* to generate mice in which ABCG1 was specifically deleted from T2 cells (*Abcg1*<sup>T2-KO</sup>). The fresh weight of lungs from *Abcg1*<sup>T2-KO</sup> mice was increased by 50%, as compared with *Abcg1*<sup>fllox/fllox</sup> mice (Fig. 2A) indicating that loss of ABCG1 from T2 cells has a dramatic effect on lung development and/or metabolism. This effect occurs even though T2 cells represent only ~15% of the cells in the lung and cover <5% of the alveolar surface (51). Further analysis of the lungs of *Abcg1*<sup>T2-KO</sup> mice indicated that they had altered histopathology consistent with sub-pleural proliferation (supplemental Fig. S2A), and did not stain with Oil red O, indicating that the tissue did not accumulate neutral lipids (supplemental Fig. S2B). Detailed morphometric analysis of multiple electron micrographs (n = 28) from the lungs of *Abcg1*<sup>fllox/fllox</sup> and *Abcg1*<sup>T2-KO</sup> mice demonstrates that the lungs of *Abcg1*<sup>T2-KO</sup> mice contain a 3-fold increase in the number of T2 cells (Fig. 2B, C) and a 2.5-fold increase in the number of lamellar bodies per T2 cell (Fig. 2B, D). In contrast, alveolar macrophages in the lungs of the *Abcg1*<sup>T2-KO</sup> mice appeared normal (Fig. 2B).

We performed positive selection followed by FACS to isolate cell populations highly enriched in either T2 or CD45<sup>+</sup> cells (Fig. 2E). T2 cells isolated from *Abcg1*<sup>T2-KO</sup> mice showed an approximate 75% decrease in both the *Abcg1* mRNA and protein (Fig. 2F, G). This effect was cell-type specific because *Abcg1* mRNA in CD45<sup>+</sup> cells was similar in

cells isolated from control *Abcg1*<sup>fllox/fllox</sup> and *Abcg1*<sup>T2-KO</sup> mice (Fig. 2H). Consistent with the observed increases in T2 cells and lamellar bodies in the lungs of *Abcg1*<sup>T2-KO</sup> mice (Fig. 2B–D), we noted a 2.8-fold increase in *Abca3* mRNA expression in freshly isolated T2 cells lacking *Abcg1* (Fig. 2I). *Abca1* mRNA levels were also increased (Fig. 2I), likely as compensation for the loss of *Abcg1*, as previously observed in *Abcg1*<sup>-/-</sup> mice (28). Isolated T2 cells lacking ABCG1 also displayed decreased mRNA levels corresponding to *Srebp-2* and *Srebp-2* target genes (*Fdps* and *Ldlr*) (Fig. 2J), suggesting increased levels of sterols in these cells. T2 cells lacking ABCG1 also showed increased expression of a number of inflammatory markers that included *Il1β*, *Il6*, and *Tnfα* (Fig. 2K). As expected, fold changes in mRNA levels in extracts from the whole lungs of *Abcg1*<sup>T2-KO</sup> were much smaller than the changes observed in isolated T2 cells lacking *Abcg1* (compare supplemental Fig. S3A–C to Fig. 2I–K).

#### Loss of ABCG1 from T2 cells increases surfactant and immunoglobulin levels

We have previously reported that the lungs of *Abcg1*<sup>-/-</sup> mice accumulate excess B-1a B cells and natural antibodies (52). We now demonstrate that BAL fluid from *Abcg1*<sup>T2-KO</sup> mice contains increased titers of IgG (Fig. 3A), IgG2c (Fig. 3B), and IgA (Fig. 3C). These changes were specific because the levels of IgG1 and IgM were similar in the lungs of *Abcg1*<sup>fllox/fllox</sup> and *Abcg1*<sup>T2-KO</sup> mice (Fig. 3D, E). Plasma immunoglobulin levels were unchanged in *Abcg1*<sup>T2-KO</sup> mice (supplemental Fig. S3D–F).

To determine whether the abnormalities observed in lamellar body and surfactant in *Abcg1*<sup>T2-KO</sup> mice were associated with disruptions in intracellular lipid homeostasis, we performed lipidomic analyses on BAL fluid and T2 cells. The data show that there were significant increases in total cholesterol, cholesteryl ester, and PC levels in the surfactant of *Abcg1*<sup>T2-KO</sup> mice (Fig. 3F). These increases corresponded to the 18:2 and 18:1 cholesterol ester species and the 32:1 and 34:1 PC species (Fig. 3G, H). In contrast, the lipid content of T2 cells or alveolar macrophages isolated from control and *Abcg1*<sup>T2-KO</sup> mice were not significantly different (supplemental Fig. S3G, H). However, the decreased levels of *Srebp-2* target genes suggest that despite minimal differences in total cellular cholesterol, there may still be changes in intracellular cholesterol distribution. Together

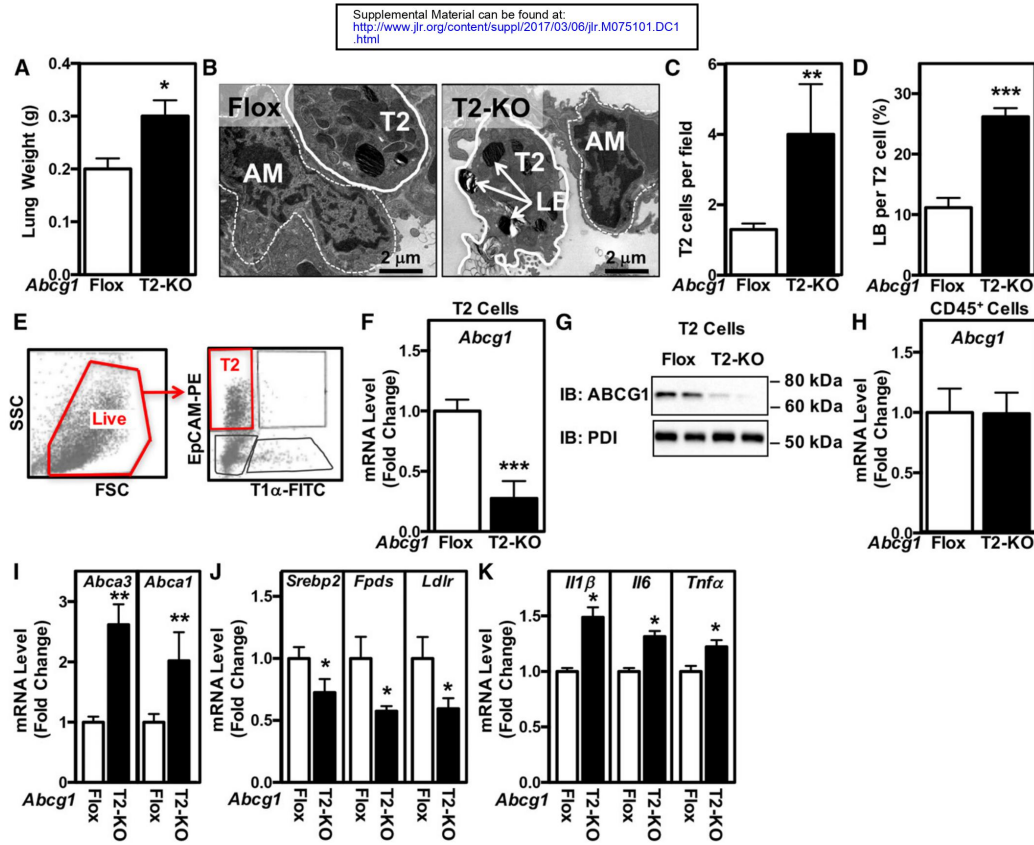


**Fig. 2.** Mice with selective deletion of *Abcg1* in T2 cells have abnormal surfactant and lamellar body homeostasis. **A:** The fresh weight of the lungs was increased in *Abcg1*<sup>T2-KO</sup> mice. **B:** Representative electron micrographs from *Abcg1*<sup>flox/flox</sup> and *Abcg1*<sup>T2-KO</sup> mice (original magnification: 17,400×). Increased T2 cell number (**C**) and relative area of lamellar bodies within each T2 cell (**D**). **E:** Flow cytometry gating strategy to identify T2 cells (defined as EpCAM<sup>hi</sup>T1α<sup>-</sup> cells). Single-cell suspensions of negatively selected CD45<sup>-</sup> cells were stained with fluorophore-conjugated antibodies and analyzed by flow cytometry. Among single cells, the live cells were selected for further analysis to identify T2 cells (EpCAM<sup>hi</sup>T1α<sup>-</sup>). **F:** *Abcg1* expression is significantly reduced in EpCAM<sup>hi</sup>T1α<sup>-</sup> T2 cells. **G:** ABCG1 protein is absent from EpCAM<sup>hi</sup>T1α<sup>-</sup> T2 cells. **H:** *Abcg1* expression is unchanged in CD45<sup>+</sup> cells isolated from *Abcg1*<sup>T2-KO</sup> mice. **I:** Increased *Abca3* and *Abca1* expression in EpCAM<sup>hi</sup>T1α<sup>-</sup> T2 cells. **J:** Decreased *Srebp-2*, *Fdps*, and *Ldlr* expression in EpCAM<sup>hi</sup>T1α<sup>-</sup> T2 cells. **K:** Increased *Il1β*, *Il6*, and *Tnfa* expression in EpCAM<sup>hi</sup>T1α<sup>-</sup> T2 cells. Significance was measured by Student's *t*-test. Data are expressed as mean ± SEM. \**P* < 0.05, \*\**P* < 0.01, \*\*\**P* < 0.001.

these data suggest that ABCG1 in T2 cells has a critical role that affects pulmonary and surfactant lipid homeostasis, as well as modulating the immune response.

#### Expression of ABCG1 in A549 cells alters lipid synthesis and secretion

The studies presented here demonstrate that ABCG1 plays a critical role in T2 cell biology and homeostasis. The human-derived A549 cell line exhibits a number of T2-like properties, including the presence of lamellar body-like organelles and the ABC transporter, ABCA3 (53). In addition, treatment of A549 cells with secretagogues increases secretion of lamellar bodies/phospholipids into the media (54). To determine whether ABCG1 affects synthesis and secretion of specific lipids, we infected A549 cells with control adenovirus or ABCG1 adenovirus (Ad-ABCG1). After 24 h, cells were incubated with <sup>14</sup>C-acetate for 6 h in medium

containing 0.2% BSA (data not shown) or 10% FBS prior to quantification of radioactive cell-associated lipids (Fig. 4A, B). The data of Fig. 4A, B show that overexpression of ABCG1 results in increased incorporation of <sup>14</sup>C-acetate into cholesterol (Fig. 4A, B; 46–52%), consistent with our earlier observation that overexpression of ABCG1 increases cholesterol synthesis genes (24, 55). Further, overexpression of ABCG1 increased incorporation of <sup>14</sup>C-acetate into FFA and DG (Fig. 4A; 71% and 74%, respectively), as well as PC (15%), PE (13%), PA/PS phospholipids (10%), and SM (20%) (Fig. 4B). The incorporation of <sup>14</sup>C-acetate into triacylglycerol, phosphatidylglycerol (PG), and PI remained largely unchanged (Fig. 4B). Similar results were seen with 0.2% BSA-containing medium (data not shown).

In a second series of experiments, we determined the role of ABCG1 in surfactant secretion. A549 cells were infected with control adenovirus or Ad-ABCG1, as in Fig. 4A, B.

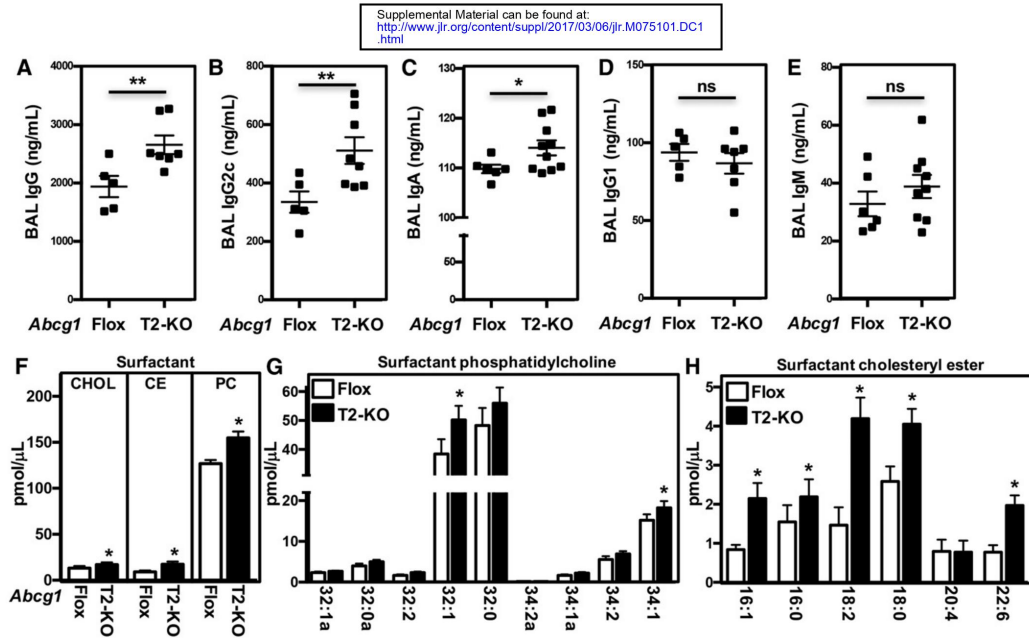


**Fig. 3.** Disrupted lipid homeostasis and immunity in *Abcg1*<sup>T2-KO</sup> mice. A–E: BAL fluid from *Abcg1*<sup>flox/flox</sup> and *Abcg1*<sup>T2-KO</sup> mice was diluted 1:5 to 1:250 and tested for binding to IgG (A), IgA (B), IgG2c (C), IgG1 (D), and IgM (E). ALP-conjugated antibodies were used for detection. Data are presented as mean antibody titer (ng/ml) ± SEM (n = 5–10 mice/genotype). F–H: Cholesterol, cholesteryl ester, and PC and their derivatives were quantified by ESI-MS/MS in BAL fluid from *Abcg1*<sup>flox/flox</sup> and *Abcg1*<sup>T2-KO</sup> mice. Data are presented as mean lipid level (pmol/μl) ± SEM (n = 3–6 mice/genotype). Significance was measured by Student's *t*-test. \**P* < 0.05, \*\**P* < 0.01.

After 24 h, cells were pulsed with <sup>14</sup>C-acetate for 4 h to label newly synthesized lipids. Cells were washed and chased for 2 h in medium containing either 0.2% BSA (supplemental Fig. S4A) or 10% FBS (Fig. 4C) in the presence or absence of a surfactant secretagogue cocktail (28). Consistent with the secretion of lamellar bodies, the cocktail increased secretion of PC (38%), PE (85%), SM (66%), and cholesterol (85%) into the medium (Fig. 4C; supplemental Fig. S4A, lanes 5, 6 vs. 1, 2 and lanes 7, 8 vs. 3, 4). ABCG1 overexpression increased secretion of both cholesterol (248%) and PC (33%), independent of whether the cells were incubated in lipid-free medium (supplemental Fig. S4A, 0.2% BSA; lanes 3, 4) or medium containing exogenous lipid acceptors (Fig. 4C, 10% FBS; lanes 3, 4).

Lastly, we determined the role of silencing ABCG1 on lipid secretion. A549 cells were transfected with a scrambled siRNA sequence or siRNA sequences targeted against *ABCG1* (Fig. 4D). Consistent with our observations in *Abcg1*<sup>T2-KO</sup> mice (Fig. 2I), silencing *ABCG1* in A549 cells resulted in compensatory increases in *ABCA1* and *ABCA3* mRNA (supplemental Fig. S4B). Silencing *ABCG1* in A549 cells resulted in increased total cellular cholesterol and phospholipids (Fig. 4E), and decreased cholesterol and phospholipid secretion into the medium (Fig. 4F).

#### *Abcg1*<sup>-/-</sup> macrophages modulate wild-type T2 cell surfactant homeostasis

Data from our BM transplant studies suggested that T2 cell function can be modulated by signals from alveolar

macrophages and/or lymphocytes that lack ABCG1. To test this hypothesis, we generated conditional KO mice in which ABCG1 was selectively deleted in macrophages using *LysM-Cre*. ABCG1 deletion in alveolar macrophages was confirmed by mRNA expression and Western blotting (Fig. 5A, B). As expected, and consistent with previous studies (28, 30, 40), *Abcg1*<sup>MAC-KO</sup> lungs displayed altered histopathology, increased proliferation in the sub-pleural space, and accumulation of Oil red O-positive macrophages (supplemental Fig. S5A, B). Morphological analysis of the lungs from *Abcg1*<sup>MAC-KO</sup> mice demonstrated the accumulation of giant alveolar macrophages filled with lipid droplets and cholesterol crystals (Fig. 5C). Upon closer inspection of individual micrographs, we noted that the T2 cells in the lungs of *Abcg1*<sup>MAC-KO</sup> mice were also enlarged with multiple irregularly shaped and electron dense lamellar bodies (Fig. 5D). Quantification of T2 cells and lamellar bodies demonstrated that *Abcg1*<sup>MAC-KO</sup> lungs have 4-fold more T2 cells (Fig. 5E), and each T2 cell contained 2.2-fold more lamellar bodies (Fig. 5F). These data suggest that the absence of ABCG1 specifically from macrophages also significantly impacts T2 lamellar body and surfactant homeostasis.

#### ABCG1 human variants in PAP

Overall, our data demonstrate that ABCG1 plays a critical role in normal T2 cell and surfactant homeostasis in mice. Importantly, we wanted to determine whether ABCG1 is important in pulmonary surfactant metabolism in humans. Chronic respiratory diseases are the third leading cause of



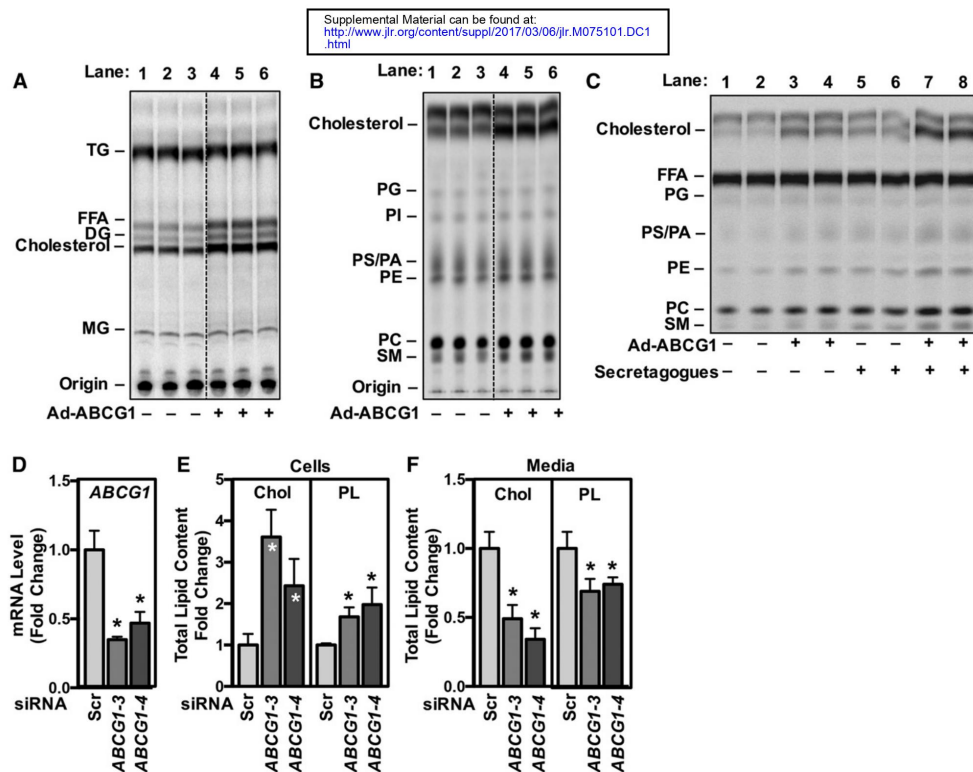


**Fig. 4.** ABCG1 is required for the synthesis and secretion of cholesterol and phospholipids from A549 T2 cells. **A, B:** A549 T2 cells were infected overnight with either control adenovirus or Ad-ABCG1. Cells were incubated with  $^{14}\text{C}$ -acetate in medium containing 10% FBS for 6 h before total cellular lipids were extracted and separated by thin-layer chromatography to determine levels of neutral lipids (**A**) and phospholipids (**B**). **C:** A549 T2 cells were infected as in (**A, B**). Cells were pulse labeled with  $^{14}\text{C}$ -acetate for 4 h, followed by a 2 h chase in medium containing 10% FBS in the presence or absence of a secretagogue cocktail (100  $\mu\text{M}$  ATP, 0.1  $\mu\text{M}$  phorbol-12-myristate-13-acetate, 20  $\mu\text{M}$  terbutaline). Total secreted lipids were extracted from the medium and separated by thin-layer chromatography to determine the levels of phospholipids. **D–F:** A549 T2 cells were transfected with a control scrambled siRNA sequence or siRNA sequences directed against *ABCG1*. **D:** Reduced *ABCG1* expression in A549 cells treated with *ABCG1* siRNA. Total cellular (**E**) and secreted (**F**) cholesterol and phospholipids were quantified by enzymatic assay according to manufacturer's instructions. Data are presented as mean  $\pm$  SEM ( $n = 6$  replicates/condition). Significance was measured by one-way ANOVA followed by Bonferroni correction.  $*P < 0.01$ .

death (56), and PAP is a rare disease caused by the accumulation of SPs and lipids in the pulmonary alveoli, resulting in respiratory distress (57, 58). Patients with autoimmune idiopathic PAP have reduced alveolar macrophage expression of *ABCG1* (59) and exhibit a remarkable resemblance to the phenotype observed in the lungs of *Abcg1*<sup>-/-</sup> mice. We hypothesized that polymorphisms in the human *ABCG1* locus may result in decreased ABCG1 function and, subsequently, altered pulmonary function.

We obtained human BAL samples from PAP patients undergoing whole lung lavage at the University of California Los Angeles. Information on the human subjects is detailed in supplemental Table S1. Genomic DNA isolated from patient alveolar macrophages was sequenced and compared with published reference sequences (NCBI). We found multiple sequence polymorphisms in one PAP patient, which correspond to a region containing a putative liver X receptor (LXR) response element (**Fig. 6A**) (60). LXR $\alpha$  is a well-known regulator of macrophage function

(61, 62). To determine whether this sequence polymorphism affected the response to LXR activation, we generated luciferase reporter genes in which the 2,000 bp upstream of the *ABCG1* transcriptional start site containing the published reference or mutated putative LXRE sequence were inserted upstream of the luciferase coding sequence (**Fig. 6B, C**). Plasmids containing these reporter genes and expression plasmids for LXR $\alpha$  and RXR $\alpha$  were transfected into HEK293 cells, and the cells treated for 24 h with either LXR and RXR agonists or vehicle. **Figure 6B** shows that LXR activation resulted in a significant increase in luciferase activity with the reference plasmid. However, no significant increase in luciferase activity was observed with the plasmid containing the mutated LXRE sequence (**Fig. 6C**). We next treated control or PAP patient macrophages with LXR $\alpha$  agonist for the indicated time period (**Fig. 7**). ABC transporter gene expression was determined by real-time qPCR. The data of **Fig. 7A** demonstrate that induction of *ABCG1* mRNA levels by a specific LXR $\alpha$

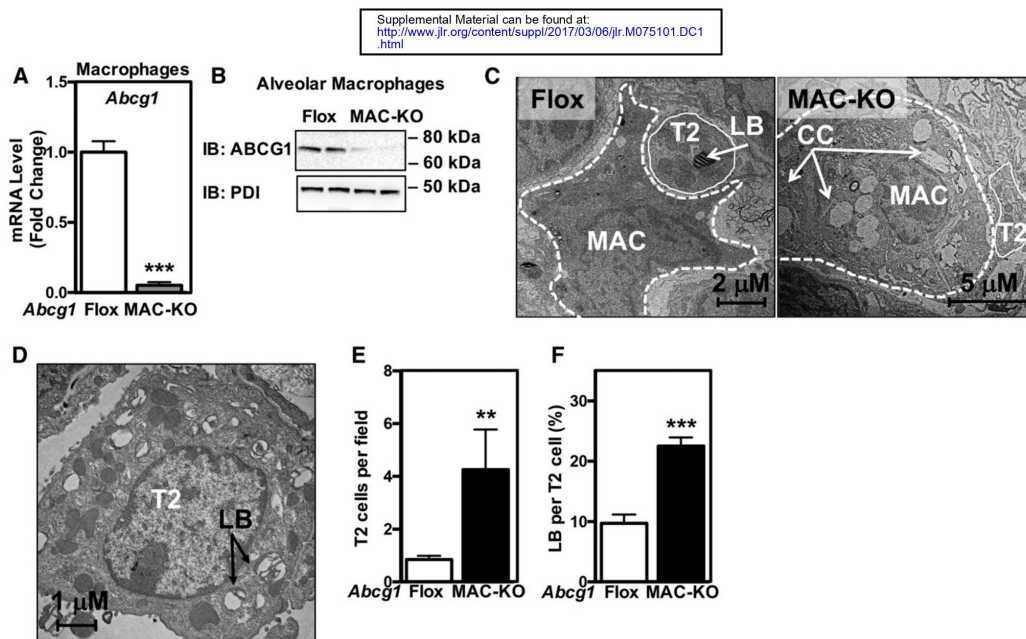


**Fig. 5.** *Abcg1*<sup>-/-</sup> macrophages signal to wild-type T2 cells. **A, B:** ABCG1 is absent in alveolar macrophages isolated from *Abcg1*<sup>MAC-KO</sup> mice. **A:** *Abcg1* expression in alveolar macrophages isolated from *Abcg1*<sup>flox/flox</sup> and *Abcg1*<sup>MAC-KO</sup> mice. **B:** ABCG1 protein in alveolar macrophages isolated from *Abcg1*<sup>flox/flox</sup> and *Abcg1*<sup>MAC-KO</sup> mice. **C:** Representative electron micrographs from *Abcg1*<sup>flox/flox</sup> and *Abcg1*<sup>MAC-KO</sup> mice (original magnification: 17,400 $\times$ ). **D:** Electron micrograph of a T2 cell from *Abcg1*<sup>MAC-KO</sup> mice (original magnification: 22,600 $\times$ ). Increased T2 cell number (**E**) and relative area of lamellar bodies within each T2 cell (**F**) in *Abcg1*<sup>MAC-KO</sup> mice. Data are expressed as mean  $\pm$  SEM (n = 4–6 mice/genotype). AM, alveolar macrophage; CC, cholesterol crystal; LB, lamellar body; T2, T2 cell. Significance was measured by Student's *t*-test. \*\**P* < 0.01, \*\*\**P* < 0.001.

agonist were significantly impaired in PAP patient macrophages (Fig. 7A), while minimal differences were noted in the induction of other LXR target genes, including *ABCA1*, *IDOL*, and *LPCAT3* (Fig. 7B–D). Together these data suggest that the sequence polymorphism identified within the *ABCG1* locus could be, in part, responsible for the reduced ABCG1 function observed in PAP patient macrophages (Fig. 7) (59).

## DISCUSSION

Improper pulmonary lipid homeostasis results in different respiratory syndromes, such as PAP, respiratory distress of the newborn, idiopathic pulmonary fibrosis, or chronic obstructive pulmonary disease (34, 35, 63–67). Studies in both patients and mice have identified GM-CSF, SP-B, SP-C, SP-D, *ABCA3*, *ABCA1*, and lysosomal acid lipase (LAL) as genes involved in some of these syndromes (32, 34, 35, 63, 65–67). We previously reported a severe lipidosis in the lungs of aged *Abcg1*<sup>-/-</sup> mice fed a normal chow diet (28). *Abcg1*<sup>-/-</sup> lungs accumulated foamy macrophages and abnormal T2 cells, and displayed massive deposition of cholesterol (both unesterified and esterified) and phospholipids. Additionally, severe signs of inflammation that included lymphocytic infiltration and increased expression of cytokines were observed in the lungs of *Abcg1*<sup>-/-</sup> mice.

Interestingly, this phenotype could be accelerated in younger animals by feeding a HF/HC diet (17).

An important question that remained to be established in those studies was the relative importance of alveolar macrophages and T2 cells for the development of the lung phenotype in *Abcg1*<sup>-/-</sup> mice. The presence of a *LacZ* knock-in cassette, under transcriptional control of the endogenous *Abcg1* promoter, allowed us to unequivocally identify both alveolar macrophages and T2 cells that normally express ABCG1 (17, 28). Wojcik et al. (30) previously reported that, following BM transplants, Oil red O deposition and cytokine induction in the murine lungs correlated with the presence of *Abcg1*<sup>-/-</sup> BM-derived cells, independent of the genotype of the recipient mice. However, we note that, in contrast to the study reported herein, the mice studied by Wojcik et al. (30) were not challenged with a HF/HC diet, were euthanized after only 9 weeks post-transplantation, and the lipid content of T2 cells was not reported.

Here we show that ABCG1 is critical for surfactant and T2 cell homeostasis. *Abcg1*<sup>T2-KO</sup> mice allowed us to specifically study the function of ABCG1 in T2 cells, while use of *Abcg1*<sup>MAC-KO</sup> and BM chimeras allowed us to study the contribution of ABCG1 in other lung cell types, such as macrophages. Our results are consistent with previous reports (30) that loss of ABCG1 expression in BM-derived cells leads to deposition of Oil red O-positive lipids (i.e., cholesteryl esters)

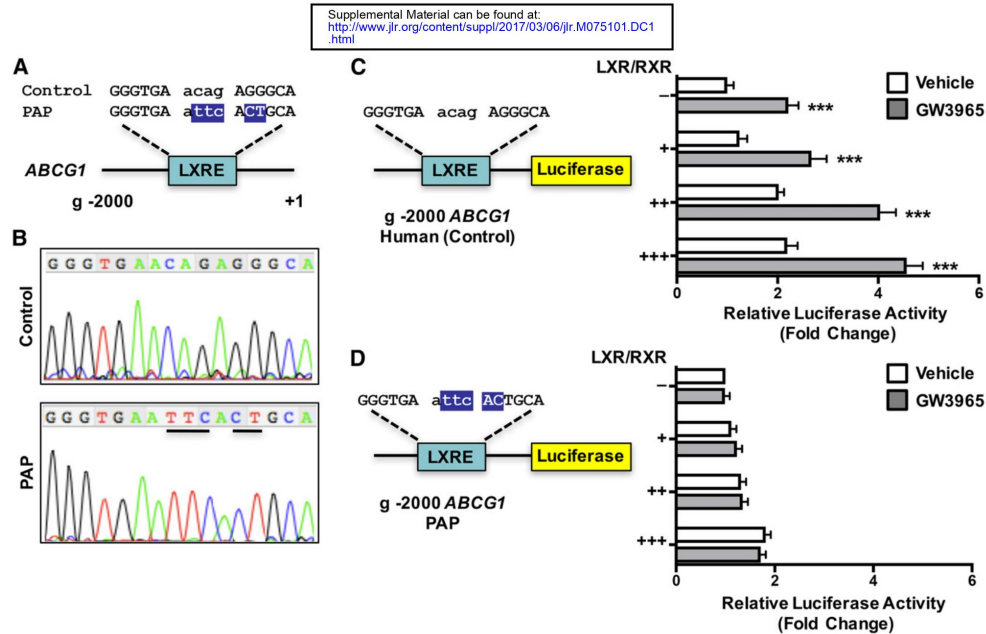


**Fig. 6.** Sequence polymorphisms in human *ABCG1* in patients with PAP. **A:** Genomic location of *ABCG1* sequence polymorphisms. **B:** Sequence trace from control or PAP patient showing sequence polymorphisms. **C, D:** The 2,000 bp upstream of the *ABCG1* transcriptional start site was cloned upstream of the luciferase gene from control and PAP patient genomic DNA. The reporter plasmid was transfected into CHO-K1 cells together with a  $\beta$ -galactosidase expression plasmid and increasing amounts of LXR $\alpha$  and RXR $\alpha$  expression plasmids in the presence or absence of LXR $\alpha$  agonist, GW3965 (1  $\mu$ M). Promoter activity was normalized to  $\beta$ -galactosidase activity. Data are presented as mean  $\pm$  SEM. Significance was measured by Student's *t*-test. \*\*\**P* < 0.001.

in pulmonary macrophages (supplemental Fig. S1, Table 1). In addition to these observations, we demonstrate that, under conditions of dietary challenge with a HF/HC diet, loss of ABCG1 function in alveolar T2 cells results in increased lamellar body content, and increased pulmonary phospholipids and unesterified cholesterol (Fig. 1, Table 1). These results highlight the importance of ABCG1 function not just in alveolar macrophages, but also in T2 cells. The data also suggest that loss of ABCG1 in either cell type results in phenotypic changes related to pulmonary lipid homeostasis. Therefore, perhaps not surprisingly, total loss of the transporter in the lungs (*Abcg1*<sup>-/-</sup> BM  $\rightarrow$  *Abcg1*<sup>-/-</sup> recipient mice) leads to a more severe phenotype (Fig. 1, supplemental Fig. S1, Table 1).

T2 cell-specific ABCG1-deficient mice accumulated abnormal electron-dense lamellar bodies, and had increased surfactant levels of cholesteryl ester, PC, and immunoglobulins (Figs. 2, 3). These data demonstrate that ABCG1 expression in T2 cells not only regulates T2 surfactant lipid homeostasis, but also immune response and immunoglobulins, consistent with previous reports that ABCG1 plays important roles in both lipid homeostasis and immunity (30, 38, 52, 68–74). Loss of ABCG1 in T2 cells compromises their ability to secrete and/or recycle surfactant lipids, resulting in hypertrophied cells that accumulate enlarged lamellar bodies [(28) and this study]. We have previously shown that continual uptake of cholesterol-rich surfactant by *Abcg1*<sup>-/-</sup> macrophages, coupled with impaired macrophage

cholesterol efflux, results in the generation of macrophage foam cells (28). These data strongly suggest that the phenotype observed in *Abcg1*<sup>-/-</sup> mice is the result of not only cell-specific events, but also complex interactions between the different pulmonary cell types, particularly alveolar macrophages and T2 cells.

LacZ staining of frozen sections from mice lacking ABCG1 revealed that ABCG1 is also expressed in endothelial cells and epithelial cells lining the bronchioles (17, 27, 28, 40). It is likely that alterations in these cells as a result of loss of ABCG1 expression may also contribute to the phenotype observed in the lungs of *Abcg1*<sup>-/-</sup> mice. Endothelial cells are known to produce and secrete numerous cytokines in response to a variety of stimuli [reviewed in (75)]. Some of these molecules have been described to modulate monocyte/macrophage migration and/or T2 cell proliferation in the lungs during inflammation or following tissue damage (75). The role of such crosstalk between endothelial cells and macrophages and T2 cells in the lungs remains to be elucidated.


To our knowledge, no functional mutations have been described in human *ABCG1*. However, Thomassen et al. (76) reported that a subgroup of patients with PAP showed a marked decrease in ABCG1 mRNA expression in alveolar macrophages recovered from BALs, compared with samples from healthy volunteers. This same group has also demonstrated that lentiviral overexpression of ABCG1 improves the lipid-loaded macrophage phenotype of *Gmcsf*<sup>-/-</sup> mice



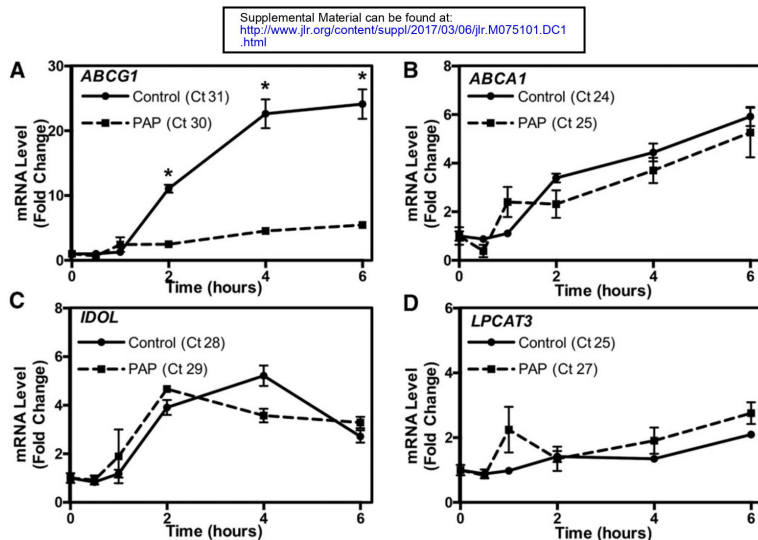


**Fig. 7.** Reduced activation of ABCG1 by LXR in a patient with PAP. A–D: Macrophages isolated from a PAP patient and non-PAP control were plated and treated with a specific LXR agonist (1  $\mu$ M GW3965) for the indicated time period. *ABCG1* (A), *ABCA1* (B), *IDOL* (C), and *LPCAT3* (D) activation by LXR. Gene expression was normalized to 36B4 and presented as fold changes. Data are presented as mean  $\pm$  SEM. Significance was measured by two-way ANOVA followed by Bonferroni correction. \* $P < 0.001$ .

(77). Importantly, we identified sequence polymorphisms in ABCG1 in one PAP patient that correspond to a putative LXR response element. We show that the normal induction of *ABCG1* mRNA in response to LXR activation was greatly attenuated in alveolar macrophages isolated from one PAP patient (Fig. 7). In contrast, induction of other LXR target genes, including *ABCA1*, *IDOL*, and *LPCAT3*, in control and patient-derived cells were not significantly different. These data suggest that polymorphisms that affect the expression and/or function of ABCG1 may result in an increased risk of pulmonary lipidosis and inflammation.

In summary, our results identify a critical role for ABCG1 in controlling T2 cell surfactant metabolism and pulmonary immunoglobulin levels. We also identify sequence polymorphisms in *ABCG1* in a human patient with PAP that impact the regulation of *ABCG1* expression by LXR. Our data suggest that a decline in pulmonary ABCG1 levels may affect the pathogenesis of PAP. Finally, the current studies support the proposal that altering intracellular cholesterol metabolism in T2 cells affects both surfactant secretion/recycling and pulmonary immunity. 

The authors thank Drs. Peter Edwards and Joseph Witztum, and members of the Tarling laboratory for critical reading of the manuscript. The authors thank Tony Mottino from the Department of Medicine at University of California Los Angeles for electron microscopy technical assistance. The authors would like to acknowledge Columbia University's Nanoscience Initiative (CNI) for the use of its shared facilities and the Fu Foundation School of Engineering and Applied Science and the Faculty of Arts and Sciences for their support of the CNI facilities.

## REFERENCES

- Schürch, S., M. Lee, and P. Gehr. 1992. Pulmonary surfactant: surface properties and function of alveolar and airway surfactant. *Pure Appl. Chem.* **64**: 1745–1750.
- Chander, A., and A. B. Fisher. 1990. Regulation of lung surfactant secretion. *Am. J. Physiol.* **258**: L241–L253.
- Haagsman, H. P., A. Hogenkamp, M. van Eijk, and E. J. A. Veldhuizen. 2008. Surfactant collectins and innate immunity. *Neonatology*, **93**: 288–294.
- McIntosh, J. C., A. H. Swyers, J. H. Fisher, and J. R. Wright. 1996. Surfactant proteins A and D increase in response to intratracheal lipopolysaccharide. *Am. J. Respir. Cell Mol. Biol.* **15**: 509–519.
- Wright, J. R. 2004. Host defense functions of pulmonary surfactant. *Biol. Neonate*. **85**: 326–332.
- Wright, J. R. 2005. Immunoregulatory functions of surfactant proteins. *Nat. Rev. Immunol.* **5**: 58–68.
- Weaver, T. E., C-L. Na, and M. Stahlman. 2002. Biogenesis of lamellar bodies, lysosome-related organelles involved in storage and secretion of pulmonary surfactant. *Semin. Cell Dev. Biol.* **13**: 263–270.
- Mason, R. J., M. C. Lewis, K. E. Edeen, K. McCormick-Shannon, L. D. Nielsen, and J. M. Shannon. 2002. Maintenance of surfactant protein A and D secretion by rat alveolar type II cells in vitro. *Am. J. Physiol. Lung Cell. Mol. Physiol.* **282**: L249–L258.
- Hass, M. A., and W. J. Longmore. 1979. Surfactant cholesterol metabolism of the isolated perfused rat lung. *Biochim. Biophys. Acta.* **573**: 166–174.
- Goerke, J. 1998. Pulmonary surfactant: functions and molecular composition. *Biochim. Biophys. Acta.* **1408**: 79–89.
- Gurel, O., M. Ikegami, Z. Chroneos, and A. Jobe. 2001. Macrophage and type II cell catabolism of SP-A and saturated phosphatidylcholine in mouse lungs. *Am. J. Physiol. Lung Cell. Mol. Physiol.* **280**: L1266–L1272.
- Baldán, A., P. Tarr, R. Lee, and P. A. Edwards. 2006. ATP-binding cassette transporter G1 and lipid homeostasis. *Curr. Opin. Lipidol.* **17**: 227–232.
- Baldán, A., D. D. Bojanic, and P. A. Edwards. 2009. The ABCs of sterol transport. *J. Lipid Res.* **50**: S80–S85.
- Tarr, P. T., E. J. Tarling, D. D. Bojanic, P. A. Edwards, and A. Baldán. 2009. Emerging new paradigms for ABCG transporters. *Biochim. Biophys. Acta.* **1791**: 584–593.

Supplemental Material can be found at:  
<http://www.jlr.org/content/suppl/2017/03/08/jlr.M075101.DC1.html>

15. Tarling, E. J., and P. A. Edwards. 2012. Dancing with the sterols: critical roles for ABCG1, ABCA1, miRNAs, and nuclear and cell surface receptors in controlling cellular sterol homeostasis. *Biochim. Biophys. Acta.* **1821**: 386–395.
16. Gelissen, I. C., M. Harris, K.A. Rye, C. Quinn, A. J. Brown, M. Kockx, S. Cartland, M. Packianathan, L. Kritharides, and W. Jessup. 2006. ABCA1 and ABCG1 synergize to mediate cholesterol export to apoA-I. *Arterioscler. Thromb. Vasc. Biol.* **26**: 534–540.
17. Kennedy, M. A., G. C. Barrera, K. Nakamura, A. Baldan, P. Tarr, M. C. Fishbein, J. Frank, O. L. Francone, and P. A. Edwards. 2005. ABCG1 has a critical role in mediating cholesterol efflux to HDL and preventing cellular lipid accumulation. *Cell Metab.* **1**: 121–131.
18. Klucken, J., C. Buchler, E. Orso, W. E. Kaminski, M. Porsch-Ozcurumez, G. Liebisch, M. Kapinsky, W. Diederich, W. Drobnik, M. Dean, et al. 2000. ABCG1 (ABC8), the human homolog of the *Drosophila* white gene, is a regulator of macrophage cholesterol and phospholipid transport. *Proc. Natl. Acad. Sci. USA.* **97**: 817–822.
19. Kobayashi, A., Y. Takanezawa, T. Hirata, Y. Shimizu, K. Misasa, N. Kioka, H. Arai, K. Ueda, and M. Matsuo. 2006. Efflux of sphingomyelin, cholesterol, and phosphatidylcholine by ABCG1. *J. Lipid Res.* **47**: 1791–1802.
20. Nakamura, K., M. A. Kennedy, A. Baldan, D. D. Bojanic, K. Lyons, and P. A. Edwards. 2004. Expression and regulation of multiple murine ATP-binding cassette transporter G1 mRNAs/isoforms that stimulate cellular cholesterol efflux to high density lipoprotein. *J. Biol. Chem.* **279**: 45980–45989.
21. Vaughan, A. M., and J. F. Oram. 2005. ABCG1 redistributes cell cholesterol to domains removable by high density lipoprotein but not by lipid-depleted apolipoproteins. *J. Biol. Chem.* **280**: 30150–30157.
22. Vaughan, A. M., and J. F. Oram. 2006. ABCA1 and ABCG1 or ABCG4 act sequentially to remove cellular cholesterol and generate cholesterol-rich HDL. *J. Lipid Res.* **47**: 2433–2443.
23. Wang, N., D. Lan, W. Chen, F. Matsuura, and A. R. Tall. 2004. ATP-binding cassette transporters G1 and G4 mediate cellular cholesterol efflux to high-density lipoproteins. *Proc. Natl. Acad. Sci. USA.* **101**: 9774–9779.
24. Tarling, E. J., and P. A. Edwards. 2011. ATP binding cassette transporter G1 (ABCG1) is an intracellular sterol transporter. *Proc. Natl. Acad. Sci. USA.* **108**: 19719–19724.
25. Tarling, E. J., and P. A. Edwards. 2016. Intracellular localization of endogenous mouse ABCG1 is mimicked by both ABCG1-L550 and ABCG1-P550-brief report. *Arterioscler. Thromb. Vasc. Biol.* **36**: 1323–1327.
26. Sturek, J. M., J. D. Castle, A. P. Trace, L. C. Page, A. M. Castle, C. Evans-Molina, J. S. Parks, R. G. Mirmira, and C. C. Hedrick. 2010. An intracellular role for ABCG1-mediated cholesterol transport in the regulated secretory pathway of mouse pancreatic beta cells. *J. Clin. Invest.* **120**: 2575–2589.
27. Baldán, A., A. V. Gomes, P. Ping, and P. A. Edwards. 2008. Loss of ABCG1 results in chronic pulmonary inflammation. *J. Immunol.* **180**: 3560–3568.
28. Baldán, A., P. Tarr, C. S. Vales, J. Frank, T. K. Shimotake, S. Hawgood, and P. A. Edwards. 2006. Deletion of the transmembrane transporter ABCG1 results in progressive pulmonary lipidosis. *J. Biol. Chem.* **281**: 29401–29410.
29. Out, R., M. Hoekstra, R. B. Hildebrand, J. K. Kruit, I. Meurs, Z. Li, F. Kuipers, T. J. C. Van Berkel, and M. Van Eck. 2006. Macrophage ABCG1 deletion disrupts lipid homeostasis in alveolar macrophages and moderately influences atherosclerotic lesion development in LDL receptor-deficient mice. *Arterioscler. Thromb. Vasc. Biol.* **26**: 2295–2300.
30. Wojcik, A. J., M. D. Skafien, S. Srinivasan, and C. C. Hedrick. 2008. A critical role for ABCG1 in macrophage inflammation and lung homeostasis. *J. Immunol.* **180**: 4273–4282.
31. Out, R., M. Hoekstra, K. Habets, I. Meurs, V. de Waard, R. B. Hildebrand, Y. Wang, G. Chimini, J. Kuiper, T. J. C. Van Berkel, et al. 2008. Combined deletion of macrophage ABCA1 and ABCG1 leads to massive lipid accumulation in tissue macrophages and distinct atherosclerosis at relatively low plasma cholesterol levels. *Arterioscler. Thromb. Vasc. Biol.* **28**: 258–264.
32. Bates, S. R., J. Q. Tao, H. L. Collins, O. L. Francone, and G. H. Rothblat. 2005. Pulmonary abnormalities due to ABCA1 deficiency in mice. *Am. J. Physiol. Lung Cell. Mol. Physiol.* **289**: L980–L989.
33. Fitzgerald, M. L., R. Xavier, K. J. Haley, R. Welti, J. L. Goss, C. E. Brown, D. Z. Zhuang, S. A. Bell, N. Lu, M. Mckee, et al. 2007. ABCA3 inactivation in mice causes respiratory failure, loss of pulmonary surfactant, and depletion of lung phosphatidylglycerol. *J. Lipid Res.* **48**: 621–632.
34. Bullard, J. E., S. E. Wert, J. A. Whitsett, M. Dean, and L. M. Noguee. 2005. ABCA3 mutations associated with pediatric interstitial lung disease. *Am. J. Respir. Crit. Care Med.* **172**: 1026–1031.
35. Shulenin, S., L. M. Noguee, T. Annilo, S. E. Wert, J. A. Whitsett, and M. Dean. 2004. ABCA3 gene mutations in newborns with fatal surfactant deficiency. *N. Engl. J. Med.* **350**: 1296–1303.
36. Francis, G. A., R. H. Knopp, and J. F. Oram. 1995. Defective removal of cellular cholesterol and phospholipids by apolipoprotein A-I in Tangier disease. *J. Clin. Invest.* **96**: 78–87.
37. Rogler, G., B. Trumbach, B. Klima, K. J. Lackner, and G. Schmitz. 1995. HDL-mediated efflux of intracellular cholesterol is impaired in fibroblasts from Tangier disease patients. *Arterioscler. Thromb. Vasc. Biol.* **15**: 683–690.
38. Cheng, H. Y., D. E. Gaddis, R. Wu, C. McSkimming, L. D. Haynes, A. M. Taylor, C. A. McNamara, M. Sorci-Thomas, and C. C. Hedrick. 2016. Loss of ABCG1 influences regulatory T cell differentiation and atherosclerosis. *J. Clin. Invest.* **126**: 3236–3246.
39. Okubo, T., P. S. Knoepfler, R. N. Eisenman, and B. L. Hogan. 2005. Nmyc plays an essential role during lung development as a dosage-sensitive regulator of progenitor cell proliferation and differentiation. *Development.* **132**: 1363–1374.
40. Tarling, E. J., D. D. Bojanic, R. K. Tangirala, X. Wang, A. Lovgren-Sandblom, A. J. Lusic, I. Bjorkhem, and P. A. Edwards. 2010. Impaired development of atherosclerosis in Abcg1<sup>-/-</sup> Apoe<sup>-/-</sup> mice: identification of specific oxysterols that both accumulate in Abcg1<sup>-/-</sup> Apoe<sup>-/-</sup> tissues and induce apoptosis. *Arterioscler. Thromb. Vasc. Biol.* **30**: 1174–1180.
41. Fujino, N., H. Kubo, T. Suzuki, C. Ota, A. E. Hegab, M. He, S. Suzuki, T. Suzuki, M. Yamada, T. Kondo, et al. 2011. Isolation of alveolar epithelial type II progenitor cells from adult human lungs. *Lab. Invest.* **91**: 363–378.
42. Blish, E. G., and W. J. Dyer. 1959. A rapid method for total lipid extraction and purification. *Can. J. Biochem. Physiol.* **37**: 911–917.
43. Demarco, V. G., D. A. Ford, E. J. Henriksen, A. R. Aroor, M. S. Johnson, J. Habibi, L. Ma, M. Yang, C. J. Albert, J. W. Lally, et al. 2013. Obesity-related alterations in cardiac lipid profile and nondipping blood pressure pattern during transition to diastolic dysfunction in male db/db mice. *Endocrinology.* **154**: 159–171.
44. Quehenberger, O., A. Armando, D. Dumlao, D. L. Stephens, and E. A. Dennis. 2008. Lipidomics analysis of essential fatty acids in macrophages. *Prostaglandins Leukot. Essent. Fatty Acids.* **79**: 123–129.
45. Han, X., and R. W. Gross. 2005. Shotgun lipidomics: electrospray ionization mass spectrometric analysis and quantitation of cellular lipidomes directly from crude extracts of biological samples. *Mass Spectrom. Rev.* **24**: 367–412.
46. Chintagari, N. R., N. Jin, P. Wang, T. A. Narasaraaju, J. Chen, and L. Liu. 2006. Effect of cholesterol depletion on exocytosis of alveolar type II cells. *Am. J. Respir. Cell Mol. Biol.* **34**: 677–687.
47. Sommerer, D., R. Süß, S. Hammerschmidt, H. Wirtz, K. Arnold, and J. Schiller. 2004. Analysis of the phospholipid composition of bronchoalveolar lavage (BAL) fluid from man and minipig by MALDI-TOF mass spectrometry in combination with TLC. *J. Pharm. Biomed. Anal.* **35**: 199–206.
48. White, T., S. Bursten, D. Federighi, R. A. Lewis, and E. Nudelman. 1998. High-resolution separation and quantification of neutral lipid and phospholipid species in mammalian cells and sera by multi-one-dimensional thin-layer chromatography. *Anal. Biochem.* **258**: 109–117.
49. Binder, C. J., S. Horkko, A. Dewan, M-K. Chang, E. P. Kieu, C. S. Goodyear, P. X. Shaw, W. Palinski, J. L. Witztum, and G. J. Silverman. 2003. Pneumococcal vaccination decreases atherosclerotic lesion formation: molecular mimicry between *Streptococcus pneumoniae* and oxidized LDL. *Nat. Med.* **9**: 736–743.
50. Chang, T-Y., C. C. Y. Chang, S. Lin, C. Yu, B-L. Li, and A. Miyazaki. 2001. Roles of acyl-coenzyme A: cholesterol acyltransferase-1 and -2. *Curr. Opin. Lipidol.* **12**: 289–296.
51. Castranova, V., J. Rabovsky, J. H. Tucker, and P. R. Miles. 1988. The alveolar type II epithelial cell: a multifunctional pneumocyte. *Toxicol. Appl. Pharmacol.* **93**: 472–483.
52. Baldan, A., A. Gonen, C. Choung, X. Que, T. J. Marquart, I. Hernandez, I. Bjorkhem, D. A. Ford, J. L. Witztum, and E. J. Tarling. 2014. ABCG1 is required for pulmonary B-1 B cell and natural antibody homeostasis. *J. Immunol.* **193**: 5637–5648.
53. Lieber, M., B. Smith, A. Szakal, W. Nelson-Rees, and G. Todaro. 1976. A continuous tumor-cell line from a human lung carcinoma with properties of type II alveolar epithelial cells. *Int. J. Cancer.* **17**: 62–70.



Supplemental Material can be found at:  
<http://www.jlr.org/content/suppl/2017/03/08/jlr.M075101.DC1.html>

54. Shapiro, D. L., L. L. Nardone, S. A. Rooney, E. K. Motoyama, and J. L. Munoz. 1978. Phospholipid biosynthesis and secretion by a cell line (A549) which resembles type II alveolar epithelial cells. *Biochim. Biophys. Acta.* **530**: 197–207.
55. Tarr, P. T., and P. A. Edwards. 2008. ABCG1 and ABCG4 are coexpressed in neurons and astrocytes of the CNS and regulate cholesterol homeostasis through SREBP-2. *J. Lipid Res.* **49**: 169–182.
56. Centers for Disease Control and Prevention. 2011. National Diabetes Fact Sheet, 2011. Accessed March 1, 2017, at <https://stacks.cdc.gov/view/cdc/13329>.
57. Carey, B., and B. C. Trapnell. 2010. The molecular basis of pulmonary alveolar proteinosis. *Clin. Immunol.* **135**: 223–235.
58. Trapnell, B. C., J. A. Whitsett, and K. Nakata. 2003. Pulmonary alveolar proteinosis. *N. Engl. J. Med.* **349**: 2527–2539.
59. Thomassen, M. J., B. P. Barna, A. G. Malur, T. L. Bonfield, C. F. Farver, A. Malur, H. Dalrymple, M. S. Kavuru, and M. Febbraio. 2007. ABCG1 is deficient in alveolar macrophages of GM-CSF knockout mice and patients with pulmonary alveolar proteinosis. *J. Lipid Res.* **48**: 2762–2768.
60. Sabol, S. L., H. B. Brewer, Jr., and S. Santamarina-Fojo. 2005. The human ABCG1 gene: identification of LXR response elements that modulate expression in macrophages and liver. *J. Lipid Res.* **46**: 2151–2167.
61. Hong, C., and P. Tontonoz. 2008. Coordination of inflammation and metabolism by PPAR and LXR nuclear receptors. *Curr. Opin. Genet. Dev.* **18**: 461–467.
62. Zelcer, N., and P. Tontonoz. 2006. Liver X receptors as integrators of metabolic and inflammatory signaling. *J. Clin. Invest.* **116**: 607–614.
63. Anderson, R. A., G. M. Bryson, and J. S. Parks. 1999. Lysosomal acid lipase mutations that determine phenotype in Wolman and cholesterol ester storage disease. *Mol. Genet. Metab.* **68**: 333–345.
64. Arai, T., E. Hamano, Y. Inoue, T. Ryushi, T. Nukiwa, M. Sakatani, and K. Nakata. 2004. Serum neutralizing capacity of GM-CSF reflects disease severity in a patient with pulmonary alveolar proteinosis successfully treated with inhaled GM-CSF. *Respir. Med.* **98**: 1227–1230.
65. Lian, X., C. Yan, L. Yang, Y. Xu, and H. Du. 2004. Lysosomal acid lipase deficiency causes respiratory inflammation and destruction in the lung. *Am. J. Physiol. Lung Cell. Mol. Physiol.* **286**: L801–L807.
66. Nogue, L. M. 2004. Alterations in SP-B and SP-C expression in neonatal lung disease. *Annu. Rev. Physiol.* **66**: 601–623.
67. Bewig, B., X. Wang, D. Kirsten, K. Dalhoff, and H. Schafer. 2000. GM-CSF and GM-CSF beta c receptor in adult patients with pulmonary alveolar proteinosis. *Eur. Respir. J.* **15**: 350–357.
68. Bensinger, S. J., M. N. Bradley, S. B. Joseph, N. Zelcer, E. M. Janssen, M. A. Hausner, R. Shih, J. S. Parks, P. A. Edwards, B. D. Jamieson, et al. 2008. LXR signaling couples sterol metabolism to proliferation in the acquired immune response. *Cell.* **134**: 97–111.
69. Draper, D. W., K. M. Gowdy, J. H. Madenspacher, R. H. Wilson, G. S. Whitehead, H. Nakano, A. R. Pandiri, J. F. Foley, A. T. Remaley, D. N. Cook, et al. 2012. ATP binding cassette transporter G1 deletion induces IL-17-dependent dysregulation of pulmonary adaptive immunity. *J. Immunol.* **188**: 5327–5336.
70. Draper, D. W., J. H. Madenspacher, D. Dixon, D. H. King, A. T. Remaley, and M. B. Fessler. 2010. ATP-binding cassette transporter G1 deficiency dysregulates host defense in the lung. *Am. J. Respir. Crit. Care Med.* **182**: 404–412.
71. Armstrong, A. J., A. K. Gebre, J. S. Parks, and C. C. Hedrick. 2010. ATP-binding cassette transporter G1 negatively regulates thymocyte and peripheral lymphocyte proliferation. *J. Immunol.* **184**: 173–183.
72. Whetzel, A. M., J. M. Sturek, M. H. Nagelin, D. T. Bolick, A. K. Gebre, J. S. Parks, A. C. Bruce, M. D. Skafien, and C. C. Hedrick. 2010. ABCG1 deficiency in mice promotes endothelial activation and monocyte-endothelial interactions. *Arterioscler. Thromb. Vasc. Biol.* **30**: 809–817.
73. Sag, D., C. Cekic, R. Wu, J. Linden, and C. C. Hedrick. 2015. The cholesterol transporter ABCG1 links cholesterol homeostasis and tumour immunity. *Nat. Commun.* **6**: 6354.
74. Sag, D., G. Wingender, H. Nowyhed, R. Wu, A. K. Gebre, J. S. Parks, M. Kronenberg, and C. C. Hedrick. 2012. ATP-binding cassette transporter G1 intrinsically regulates invariant NKT cell development. *J. Immunol.* **189**: 5129–5138.
75. Rao, R. M., L. Yang, G. Garcia-Cardena, and F. W. Lusinskas. 2007. Endothelial-dependent mechanisms of leukocyte recruitment to the vascular wall. *Circ. Res.* **101**: 234–247.
76. Thomassen, M. J., B. P. Barna, A. G. Malur, T. L. Bonfield, C. F. Farver, A. Malur, H. Dalrymple, M. S. Kavuru, and M. Febbraio. 2007. ABCG1 is deficient in alveolar macrophages of GM-CSF knockout mice and patients with pulmonary alveolar proteinosis. *J. Lipid Res.* **48**: 2762–2768.
77. Malur, A., I. Huizar, G. Wells, B. P. Barna, A. G. Malur, and M. J. Thomassen. 2011. Lentivirus-ABCG1 instillation reduces lipid accumulation and improves lung compliance in GM-CSF knock-out mice. *Biochem. Biophys. Res. Commun.* **415**: 288–293.

## ABCG1 regulates pulmonary surfactant metabolism in mice and men

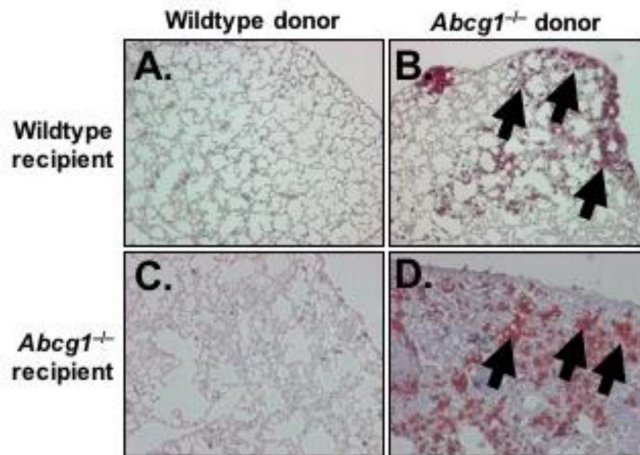
Thomas Q. de A. Vallim<sup>1,2,3,4</sup>, Elinor Lee<sup>1,5</sup>, David J. Merriott<sup>2,\*</sup>, Christopher N. Goulbourne<sup>6</sup>, Joan Cheng<sup>2</sup>, Angela Cheng<sup>2</sup>, Ayelet Gonen<sup>7</sup>, Ryan M. Allen<sup>8,#</sup>, Elisa N.D. Palladino<sup>8,9</sup>, David A. Ford<sup>8,9</sup>, Tisha Wang<sup>1,5</sup>, Ángel Baldán<sup>8</sup>, and Elizabeth J. Tarling<sup>1,3,4</sup>

Running Title: Dissecting the Pulmonary Lipidosis of *Abcg1*<sup>-/-</sup> Mice

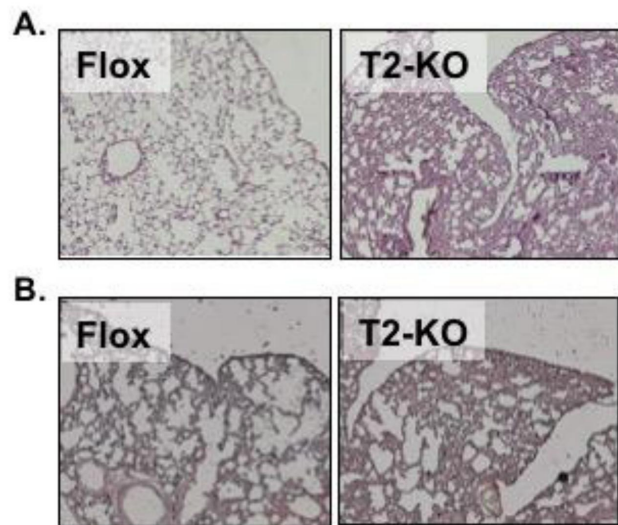
### Supplemental Data

#### Supplemental Table S1. Characteristics of PAP patients.

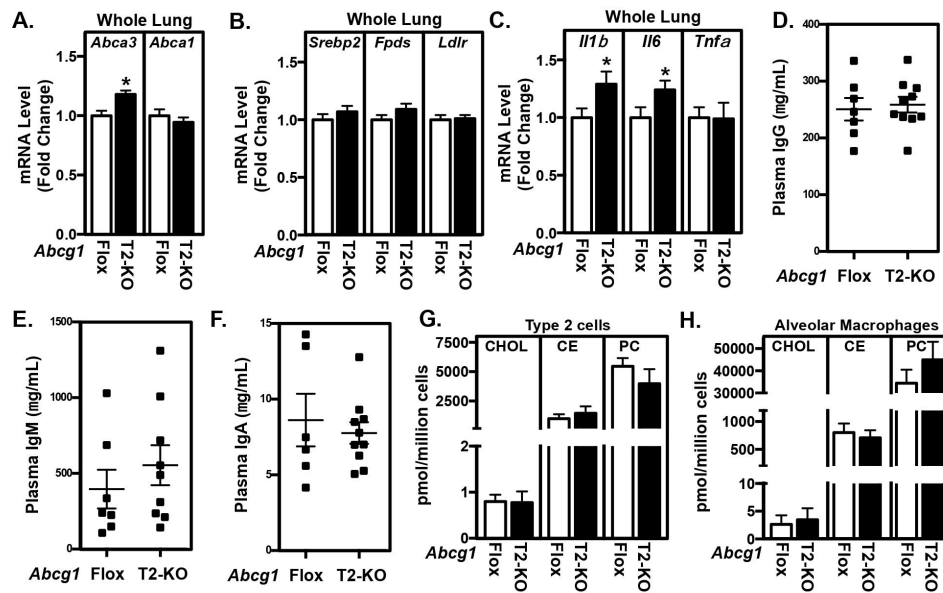
| Patient Characteristics | Cohort |
|-------------------------|--------|
| Number of subjects      | 7      |
| Males                   | 6      |
| Females                 | 1      |
| White                   | 4      |
| African-American        | 1      |
| Hispanic                | 2      |
| Median Age (yr)         |        |
| Male                    | 46.5   |
| Female                  | 50     |



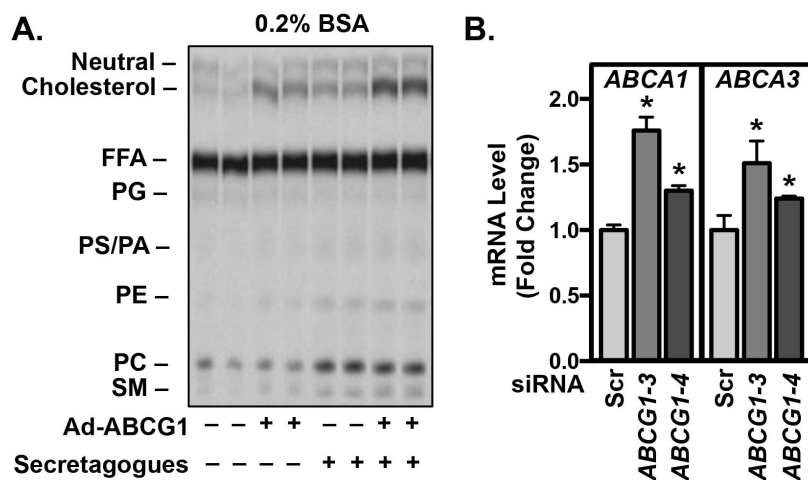
**Supplemental Figure S1.** (A-D) Frozen lung sections (10  $\mu$ M) from mice treated as in Figure 1 were stained with Oil red O to identify neutral lipids. Arrows indicate positively stained areas. (A) *Abcg1*<sup>+/+</sup> donor bone marrow (BM)  $\rightarrow$  *Abcg1*<sup>+/+</sup> recipient mice. (B) *Abcg1*<sup>-/-</sup> donor bone marrow (BM)  $\rightarrow$  *Abcg1*<sup>+/+</sup> recipient mice. (C) *Abcg1*<sup>+/+</sup> donor bone marrow (BM)  $\rightarrow$  *Abcg1*<sup>-/-</sup> recipient mice. (D) *Abcg1*<sup>-/-</sup> donor bone marrow (BM)  $\rightarrow$  *Abcg1*<sup>-/-</sup> recipient mice.



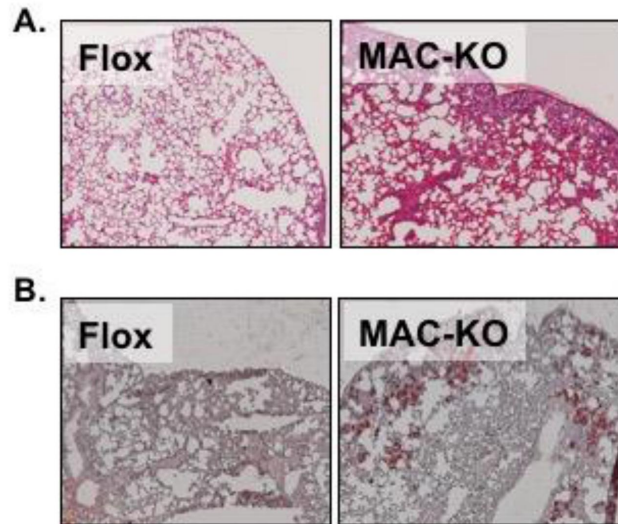
**Supplemental Figure S2.** Frozen lung sections (10  $\mu$ M) from *Abcg1<sup>FloX</sup>* (FloX) and *Abcg1<sup>T2-KO</sup>* (T2-KO) mice were stained with hematoxylin and eosin (**A**) or Oil red O (**B**).



**Supplemental Figure S3.** (A-C) Whole lung mRNA expression of (A) *Abca1* and *Abca3*, (B) *Srebp-2*, *Fdps*, and *Ldlr*, and (C) *Il1 $\beta$* , *Il6*, and *Tnfa* in *Abcg1<sup>f/f</sup>* (Flox) and *Abcg1<sup>T2-KO</sup>* (T2-KO) mice. Gene expression was normalized to 36B4 and presented as fold change. Data are expressed as mean mRNA level  $\pm$ SEM ( $n = 4-6$  mice/genotype). (D-F) Plasma was diluted 1:250-1:1000 and tested for binding to IgG (D), IgM (E) and IgA (F). HRP-conjugated antibodies were used for detection. Data are presented as mean antibody titer (ng/mL)  $\pm$ SEM ( $n = 3-6$  mice/genotype). (G-H) Cholesterol, cholesteryl ester, phosphatidylcholine and their derivatives were quantified by ESI-MS/MS in T2 cells (G) and alveolar macrophages (H) from *Abcg1<sup>f/f</sup>* and *Abcg1<sup>T2-KO</sup>* mice. Data are presented as mean lipid level (pmol/million cells)  $\pm$ SEM ( $n = 3-6$  mice/genotype). Significance was measured by Student's *t* test. \*  $p < 0.05$ .



**Supplemental Figure S4.** (A) A549 T2 cells were infected as in Figure 4. Cells were pulse labeled with  $^{14}\text{C}$ -acetate for 4 h, followed by a 2 h chase in media containing 0.2% BSA in the presence or absence of a secretagogue cocktail (100  $\mu\text{M}$  ATP, 0.1  $\mu\text{M}$  phorbol-12-myristate-13-acetate, 20  $\mu\text{M}$  terbutaline). Total secreted lipids were extracted from the media and separated by thin layer chromatography to determine the levels of phospholipids. (B) Increased *ABCA3* and *ABCA1* expression in A549 cells treated with *ABCG1* siRNA. Data are presented as mean  $\pm$ SEM ( $n = 6$  replicates/condition). Significance was measured by one-way ANOVA followed by Bonferroni correction. \*  $p < 0.05$ .



**Supplemental Figure S5.** Frozen lung sections (10  $\mu$ M) from *Abcg1<sup>Flox</sup>* (Flox) and *Abcg1<sup>MAC-KO</sup>* (MAC-KO) mice were stained with hematoxylin and eosin (**A**) or Oil red O (**B**).

## **CHAPTER 3**

### **Statin as a novel pharmacotherapy of pulmonary alveolar proteinosis**



ARTICLE

DOI: 10.1038/s41467-018-05491-z

OPEN

# Statin as a novel pharmacotherapy of pulmonary alveolar proteinosis

Cormac McCarthy<sup>1,2,3,4</sup>, Elinor Lee<sup>5,6</sup>, James P. Bridges<sup>2</sup>, Anthony Salles<sup>1,2</sup>, Takuji Suzuki<sup>1,2</sup>, Jason C. Woods<sup>3</sup>, Brian J. Bartholmai<sup>7</sup>, Tisha Wang<sup>5,6</sup>, Claudia Chalk<sup>1,2</sup>, Brenna C. Carey<sup>1,2</sup>, Paritha Arumugam<sup>1,2</sup>, Kenjiro Shima<sup>1,2</sup>, Elizabeth J. Tarling<sup>6,8</sup> & Bruce C. Trapnell<sup>1,2,3,4</sup>

Pulmonary alveolar proteinosis (PAP) is a syndrome of reduced GM-CSF-dependent, macrophage-mediated surfactant clearance, dysfunctional foamy alveolar macrophages, alveolar surfactant accumulation, and hypoxemic respiratory failure for which the pathogenic mechanism is unknown. Here, we examine the lipids accumulating in alveolar macrophages and surfactant to define the pathogenesis of PAP and evaluate a novel pharmacotherapeutic approach. In PAP patients, alveolar macrophages have a marked increase in cholesterol but only a minor increase in phospholipids, and pulmonary surfactant has an increase in the ratio of cholesterol to phospholipids. Oral statin therapy is associated with clinical, physiological, and radiological improvement in autoimmune PAP patients, and ex vivo statin treatment reduces cholesterol levels in explanted alveolar macrophages. In *Csf2rb*<sup>-/-</sup> mice, statin therapy reduces cholesterol accumulation in alveolar macrophages and ameliorates PAP, and ex vivo statin treatment increases cholesterol efflux from macrophages. These results support the feasibility of statin as a novel pathogenesis-based pharmacotherapy of PAP.

<sup>1</sup>Translational Pulmonary Science Center, Children's Hospital Medical Center, Cincinnati, OH, USA. <sup>2</sup>Division of Pulmonary Biology, Children's Hospital Medical Center, Cincinnati, OH, USA. <sup>3</sup>Division of Pulmonary Medicine, Children's Hospital Medical Center, Cincinnati, OH, USA. <sup>4</sup>Division of Pulmonary, Critical Care, and Sleep Medicine, University of Cincinnati College of Medicine, Cincinnati, OH, USA. <sup>5</sup>Division of Pulmonary and Critical Care Medicine, University of California Los Angeles, Los Angeles, CA, USA. <sup>6</sup>Department of Medicine, University of California Los Angeles, Los Angeles, CA, USA. <sup>7</sup>Department of Radiology, Mayo Clinic, Rochester, MN, USA. <sup>8</sup>Molecular Biology Institute, University of California Los Angeles, Los Angeles, CA, USA. Correspondence and requests for materials should be addressed to E.J.T. (email: [etarling@mednet.ucla.edu](mailto:etarling@mednet.ucla.edu)) or to B.C.T. (email: [Bruce.Trapnell@cchmc.org](mailto:Bruce.Trapnell@cchmc.org))

**P**ulmonary surfactant is composed of 80% polar lipids, primarily phosphatidylcholine, and multiple less-abundant phospholipid species, 10% neutral lipids, primarily free cholesterol with small amounts of triglycerides and free fatty acids, and 10% surfactant proteins<sup>1,2</sup>. Since cholesterol content regulates the fluidity and surface tension-lowering effects of surfactant, which are critical to alveolar stability and lung function, surfactant composition is tightly regulated<sup>3</sup>. Surfactant homeostasis is maintained by balanced secretion by alveolar epithelial type II cells and clearance via recycling and catabolism in these cells and by catabolism in alveolar macrophages<sup>4</sup>. Prior studies reporting the relative fractional composition of surfactant phospholipids is normal in pulmonary alveolar proteinosis (PAP) patients<sup>5</sup> and *Csf2*<sup>-/-</sup> mice<sup>6</sup>, led to a widely-held belief that surfactant accumulation in PAP is caused by impaired catabolism of phospholipids within alveolar macrophages<sup>7</sup>, however, to date, no such mechanism has been identified.

Alveolar macrophages require granulocyte/macrophage-colony-stimulating factor (GM-CSF) for maturation in the lungs and to enable surfactant clearance in vitro and in vivo<sup>8,9</sup>. Further, disruption of GM-CSF signaling by either GM-CSF autoantibodies as occurs in autoimmune PAP<sup>10–12</sup> or by *CSF2RA* or *CSF2RB* mutations as occurs in hereditary PAP<sup>13–15</sup> mediates pathogenesis in >90% of PAP patients. PAP has no approved pharmacotherapy and is currently treated by whole lung lavage (WLL), an invasive, inefficient procedure that is repeatedly required and not widely available. Based on the observation that impaired GM-CSF-dependent cholesterol clearance within alveolar macrophages drives reduction of macrophage-mediated surfactant clearance in *Csf2rb*<sup>-/-</sup> mice<sup>16</sup>, a validated animal model of human PAP<sup>17</sup>, here, we evaluate cholesterol content in human alveolar macrophages and pulmonary surfactant from PAP patients, and test cholesterol homeostasis as a novel target for development of pharmacotherapy of PAP.

## Results

**Statin therapy and resolution of autoimmune PAP lung disease.** We identified a 58-year-old woman with severe autoimmune PAP who responded poorly to WLL but improved dramatically on statin therapy. She initially presented with progressive dyspnea of insidious onset and a past medical history positive only for hypercholesterolemia. Pulmonary function testing revealed a forced vital capacity (FVC) of 74% of the predicted value and a diffusing capacity for carbon monoxide (DLCO) of 41% of predicted. A high-resolution computed tomogram (HRCT) of the chest revealed diffuse, ground glass opacification and septal thickening (Fig. 1a) and a lung biopsy identified histopathology typical of PAP (Fig. 1b). A serum GM-CSF autoantibody test<sup>18</sup> was abnormal (74 mcg/ml, normal <5.0 mcg/ml) and a STAT5-phosphorylation index<sup>13</sup> test indicated GM-CSF signaling was not detectable, thereby establishing a diagnosis of autoimmune PAP. Dyspnea and resting hypoxemia were treated with continuous low-flow oxygen. Multiple bilateral high-volume WLL treatments (each ~50 l saline/lung) were performed 1, 3, 7, 11, and 25 months after presentation with some symptomatic relief but no major effect on hypoxemia or supplemental oxygen requirement (Fig. 1d); radiographic abnormalities (Fig. 1a) and severely reduced DLCO (41–54% of predicted) persisted (Fig. 1f). GM-CSF autoantibody and STAT5-phosphorylation index tests remained abnormal at all times. Thirty-two months after presentation, statin therapy was initiated for hypercholesterolemia and lowered serum cholesterol as expected (Supplementary Table 1). Six months later, she experienced unanticipated improvement in dyspnea and elimination of her oxygen requirement (Fig. 1d), HRCT revealed reduced

pulmonary ground glass opacification (Fig. 1a) and 42 months after initiating statin therapy, the abnormal PAP-related surfactant accumulation had completely resolved as determined by two different, previously validated, quantitative computed tomography (CT)-based methods (categorical parenchymal-pattern assessment (CALIPER) and densitometry<sup>19–21</sup>). CALIPER analysis indicated the percentage lung parenchyma affected by PAP had declined from 32% to 0% during three and half years on statin therapy (Fig. 1a, c, Supplementary Tables 2, 3). Furthermore, at this time, the FVC increased to 100% of predicted and the DLCO increased to 80% of predicted (Fig. 1e, f). Thus, initiation of statin therapy was associated with sustained clinical and radiological improvement of PAP lung disease and WLL therapy was no longer required or administered.

Subsequently, we identified a 66-year-old female with unremitting, slowly progressive autoimmune PAP (serum GM-CSF autoantibody: 109.1 mcg/ml) who had not received WLL or other therapy of PAP. Three years after diagnosis, dyspnea on exertion was persistent, the DLCO was reduced to 69% of predicted, and HRCT revealed moderate PAP (Supplementary Fig. 1a). Independently, oral statin was initiated as therapy for hypercholesterolemia; after 4 months, dyspnea had resolved and after 1 year, she remained asymptomatic, the DLCO had normalized (85% of predicted), and CALIPER analysis indicated the percentage of lung parenchyma affected by PAP had declined from 38% to 15% (Supplementary Fig. 1a, b).

## Statins reduce alveolar macrophage cholesterol in PAP.

Prompted by the clinical improvement these patients experienced on statin therapy and the recent observation that loss of GM-CSF signaling disrupts cholesterol homeostasis in *Csf2rb*<sup>-/-</sup> mice<sup>16</sup>, we examined the alveolar material accumulating in autoimmune PAP by studying total surfactant lipids (i.e., polar and neutral together) rather than just the polar lipid fraction as had been done previously<sup>5</sup>. Alveolar macrophages from autoimmune PAP patients were foamy (Fig. 2a) and contained large amounts of free and esterified cholesterol and only a small increase in phospholipids (Fig. 2b, c). Importantly, the ratio of cholesterol to phospholipids in pulmonary surfactant was markedly increased (Fig. 2d). This latter observation has physiological implications, as cholesterol regulates surfactant fluidity<sup>22</sup> as well as diagnostic implications as its measurement could serve as an adjunct to the bronchoscopic evaluation of patients with ground glass opacification identified by chest CT examination.

To determine whether statin therapy may act via a direct effect on alveolar macrophages, PAP patient-derived foamy alveolar macrophages were exposed to statin therapy ex vivo for 24 hours and cholesterol content was measured. Statin treatment reduced cholesterol content by 40% compared with paired control cells (Fig. 2e). As statins inhibit 3-hydroxy-3-methylglutaryl-CoA reductase (HMGCR) thus reducing endoplasmic reticulum (ER) cholesterol levels resulting in increased expression of sterol regulatory element-binding protein-2 (*SREBP2*)<sup>23,24</sup>, we evaluated the effects of statin on this pathway in alveolar macrophages. Statin therapy increased expression of *SREBP2* (Fig. 2f) and its downstream target genes (Supplementary Fig. 2a) including neutral cholesterol ester hydrolase-1 (*NCEH1*) (Fig. 2f), an enzyme responsible for converting esterified cholesterol to free cholesterol, which facilitates cholesterol efflux. Because ATP-binding cassette transporter family members A1 and G1 (*ABCA1* and *ABCG1*, respectively) mediate cholesterol efflux from macrophages and their expression is abnormal in PAP<sup>25,26</sup>, we evaluated the effects of ex vivo statin exposure on *ABCG1/ABCA1* mRNA levels in PAP patient-derived alveolar macrophages. Statin increased mRNA transcript levels of both *ABCA1*

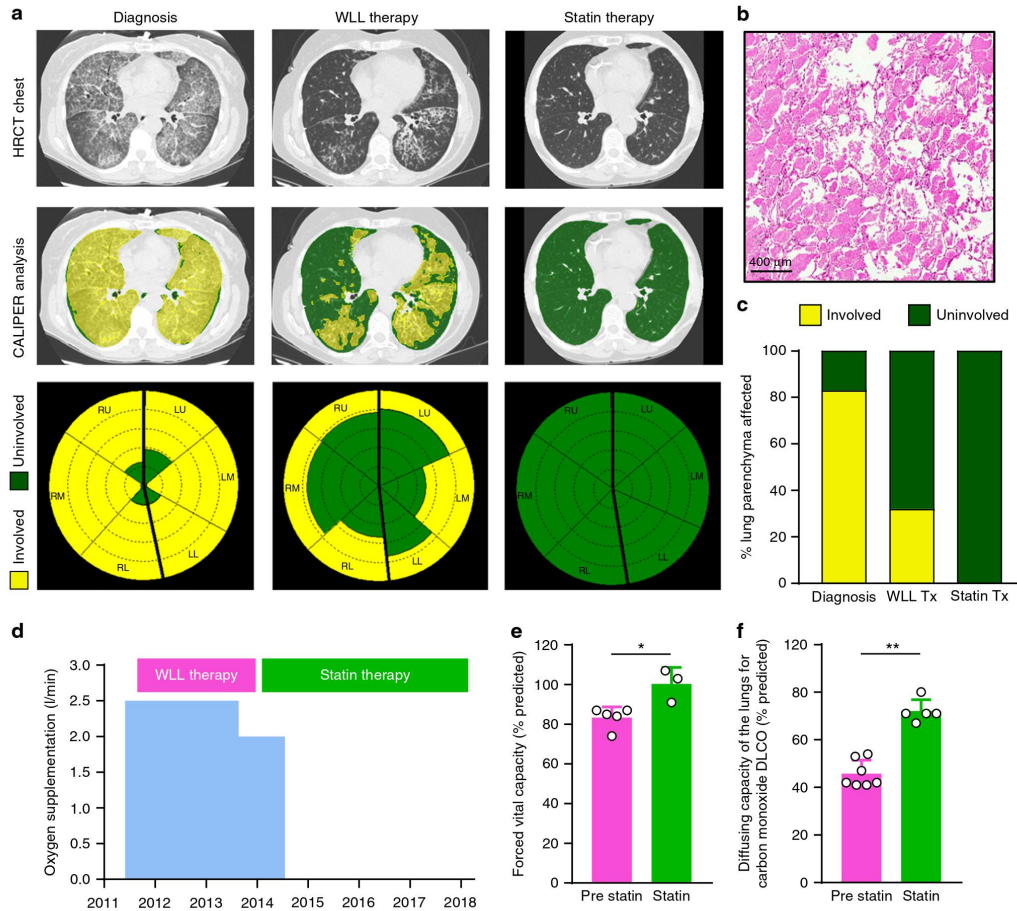


**Fig. 1** Resolution of PAP associated with oral statin therapy. **a** HRCT chest at diagnosis and after WLL therapy or statin therapy. HRCT image illustrating quantitative categorical parenchymal-pattern analysis (green-masking: uninvolved/normal lung parenchyma, yellow-masking: PAP-involved/abnormal lung comprising ground glass and reticular changes). Glyphs showing parenchymal-pattern analysis of total lung parenchyma segmented by right, left; upper, middle, and lower zones. **b** Lung histology at diagnosis. Haematoxylin and eosin. **c** Percentage of lung affected by PAP determined by parenchymal-pattern analysis. Supplemental oxygen requirement (**d**), FVC (**e**), and DLCO (**f**) before and after statin therapy. Data are mean  $\pm$  SD, statistical differences determined by Student's *t* test or Mann-Whitney test.  $P < 0.05$ ,  $**P < 0.01$ ,  $***P < 0.001$ ,  $****P < 0.0001$

and *ABCG1* compared to paired control cells (Fig. 2f). These results indicate statin therapy may act through a direct effect on foamy, cholesterol-laden alveolar macrophages in PAP patients by promoting cholesterol efflux.

**Statins improve PAP lung disease in *Csf2rb*<sup>-/-</sup> mice.** Next, we asked if the clinical benefit of statin therapy could be recapitulated in vivo in a validated PAP model. To address this question, *Csf2rb*<sup>-/-</sup> mice received statin therapy by oral administration for 6 weeks. Compared with age-matched, untreated controls, statin-treated mice had reduced bronchoalveolar lavage (BAL) turbidity (Fig. 3a) (an excellent global measure of PAP sediment accumulation reflecting disease severity<sup>17</sup>) and reduced cholesterol levels in BAL (Fig. 3b) and alveolar macrophages (Fig. 3c) (excellent biochemical measures of PAP disease severity<sup>17</sup>). Similar to results for human alveolar macrophages treated with

statin ex vivo, alveolar macrophages from statin-treated mice had increased mRNA transcript levels in for *Srebp2*, *Nceh*, *Abca1*, and *Abcg1* compared with age-matched, untreated controls (Fig. 3d–g, Supplementary Fig. 2b).

**Statins increase *Csf2rb*<sup>-/-</sup> macrophage cholesterol efflux.** Because statin therapy reduced cholesterol levels in foamy alveolar macrophages from autoimmune PAP patients ex vivo and *Csf2rb*<sup>-/-</sup> mice in vivo (Figs. 2e, 3c), and cholesterol efflux is reduced in macrophages from apoE<sup>-/-</sup>GM-CSF<sup>-/-</sup> mice<sup>27</sup>, we measured the effects of statin on efflux of radiolabelled cholesterol from alveolar macrophages or bone marrow-derived macrophages in the presence of cholesterol acceptors—high-density lipoprotein (HDL) or apolipoprotein-A1 (Apo-A1), which preferentially accept cholesterol from macrophages via *ABCG1* and *ABCA1*, respectively<sup>28</sup>. Compared with untreated



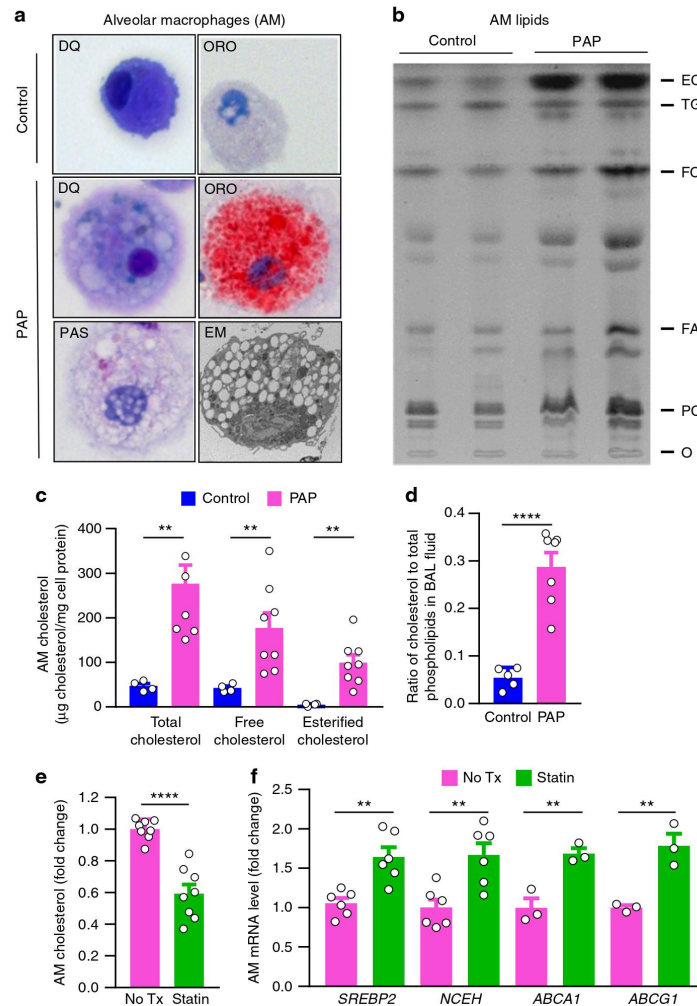


**Fig. 2** Cholesterol accumulation in human PAP alveolar macrophages and correction by statin. **a** Human alveolar macrophages (AMs) stained with Diff-Quick (DQ), Oil-red O (ORO), periodic acid-Schiff (PAS), or electron microscopy (EM). **b** Thin-layer chromatography of AM total lipids from healthy people (control) or PAP patients (PAP). **c** AM cholesterol levels in PAP or controls ( $n = 8$  PAP/4 control). **d** The ratio of cholesterol to total phospholipids in pulmonary surfactant of PAP or controls ( $n = 7$  PAP/5 control). **e** Total cholesterol and **f** mRNA levels for *SREBP2*, *NCEH*, *ABCA1*, *ABCG1* in PAP AMs without and after statin treatment for 24 h ex vivo ( $n = 3$ –6 per group). Data are mean  $\pm$  SD, statistical differences determined by ANOVA with Bonferroni's post hoc test. \* $P < 0.05$ , \*\* $P < 0.01$ , \*\*\* $P < 0.001$ , \*\*\*\* $P < 0.0001$

paired cells, statin-treated alveolar macrophages had increased efflux in the presence of HDL but not Apo-A1 (Fig. 3h, i), whereas statin-treated bone marrow-derived macrophages (BMDMs) had increased efflux in the presence of both Apo-A1 and HDL (Fig. 3j, k). These results support the concept that statin may provide benefit as therapy of PAP by a direct effect on alveolar macrophages by increasing cholesterol clearance.

### Discussion

This study showed that cholesterol—not un-metabolized surfactant or phospholipids—was the predominant material

accumulating in alveolar macrophages in PAP patients and was associated with a marked increase in the ratio of cholesterol to phospholipids in pulmonary surfactant. Statin therapy was associated with improvement in lung disease in autoimmune PAP patients, reduced cholesterol levels in alveolar macrophages from autoimmune PAP patients ex vivo, increased cholesterol efflux from *Csf2rb*<sup>-/-</sup> macrophages ex vivo, and ameliorated lung disease in *Csf2rb*<sup>-/-</sup> mice in vivo. Together, these results identify oral statin therapy as a novel pathogenesis-based pharmacotherapeutic approach for patients with autoimmune PAP.

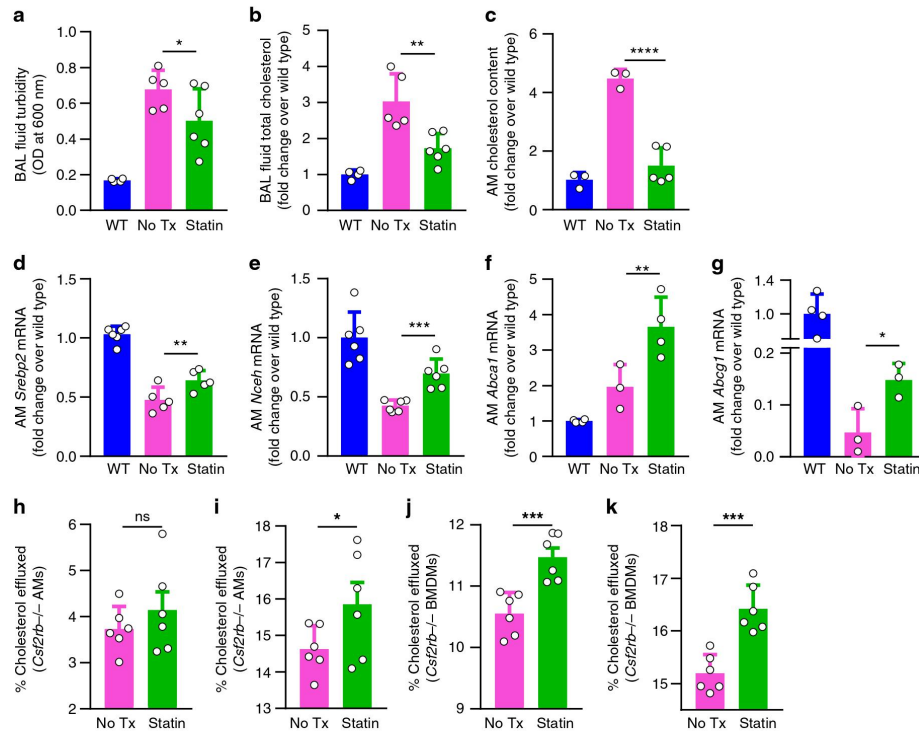


**Fig. 3** Statin therapy improves cholesterol efflux from macrophages and ameliorates PAP in *Csf2rb*<sup>-/-</sup> mice. **a–g** Mice received oral statin therapy for 6 weeks or untreated age-matched *Csf2rb*<sup>-/-</sup> or wild type (WT) mice. Disease severity evaluated by bronchoalveolar lavage **a** turbidity and **b** total cholesterol. **c** Alveolar macrophage cholesterol and mRNA levels for *Srebp2* **d**, *Nceh* **e**, *Abca1* **f**, and *Abcg1* **g**. Cholesterol efflux capacity of *Csf2rb*<sup>-/-</sup> AMs (**h, i**) or BMDMs (**j, k**), treated with statin for 24 hours, measured by percentage of [<sup>3</sup>H]-cholesterol transferred to Apo-A1 (**h, j**) or HDL (**i, k**). Data are mean  $\pm$  SD (3–6 mice/group), statistical differences determined by ANOVA with Bonferroni's post hoc test. \* $P < 0.05$ , \*\* $P < 0.01$ , \*\*\* $P < 0.001$ , \*\*\*\* $P < 0.0001$

The observation that abnormal accumulation of cholesterol in alveolar macrophages and pulmonary surfactant is similar in autoimmune PAP patients and in *Csf2rb*<sup>-/-</sup> mice<sup>16</sup> suggests a similar mechanism may drive PAP pathogenesis. In mice, GM-CSF signaling via PU.1 is required to stimulate differentiation and functions of alveolar macrophages including surfactant clearance<sup>8</sup>. In humans, GM-CSF, PU.1<sup>8</sup>, and PPAR $\gamma$ <sup>9,29</sup> are required for alveolar macrophage differentiation and surfactant clearance. In nonhuman primates, passive transfer of PAP patient-derived GM-CSF autoantibodies reduced expression of GM-CSF signaling axis components in alveolar macrophages in parallel with development of PAP<sup>30</sup>. GM-CSF is critical to cholesterol homeostasis in murine macrophages and stimulates cholesterol clearance in a constitutive, dose-dependent, and reversible fashion<sup>16</sup>. *Csf2rb*<sup>-/-</sup> macrophages readily clear cholesterol-deficient surfactant but clearance is reduced when cholesterol is present. Finally, *ABCA1* and *ABCG1* are vital to cholesterol homeostasis in macrophages and expression of both is abnormal in alveolar macrophages in human and murine PAP<sup>16,25,26,31</sup>. Further, macrophage-specific *Abcg1* gene-ablation causes PAP with accumulation of pulmonary cholesterol<sup>32</sup>. These results suggest a mechanism explaining the pathogenesis of autoimmune PAP (Fig. 4): reduced GM-CSF-PU.1-PPAR $\gamma$  axis signaling in alveolar macrophages  $\rightarrow$  reduced *ABCG1/ABCA1* expression  $\rightarrow$  reduced

cholesterol clearance  $\rightarrow$  secondarily reduced surfactant uptake and clearance (not impaired surfactant phospholipid catabolism)  $\rightarrow$  surfactant accumulation in pulmonary alveoli  $\rightarrow$  clinical manifestations. Several findings suggest the change in *ABCG1* expression may be more important to the pathogenesis of PAP than that of *ABCA1*, which may comprise an incompletely effective compensatory response to increased cholesterol. In *Csf2rb*<sup>-/-</sup> alveolar macrophages, *Abca1* is overexpressed while *Abcg1* is severely reduced (Fig. 3f, g) and a similar pattern seen in primary alveolar macrophages from autoimmune PAP<sup>25</sup>, however, both were reduced in cultured BMDMs in the absence of cholesterol exposure (albeit *Abcg1* more severely)<sup>16</sup>. Despite increased expression of *ABCA1* in PAP alveolar macrophages, these cells remain filled with cholesterol-rich droplets (Fig. 2a, b).

The observation that statin increased cholesterol transporter expression and efflux and reduced cholesterol levels in alveolar macrophages from PAP patients ex vivo and in *Csf2rb*<sup>-/-</sup> mice in vivo suggests a direct therapeutic effect of statins on alveolar macrophages. Indeed, statins have been reported to directly affect alveolar macrophage inflammatory cytokine release, phagocytosis, efferocytosis, and particulate clearance<sup>33,34</sup>. Further, statins increase cholesterol efflux from the macrophage-like cell line THP-1<sup>35</sup> and activate PPAR $\gamma$ <sup>36</sup>, which is known to increase *ABCA1/ABCG1* expression and cholesterol efflux in

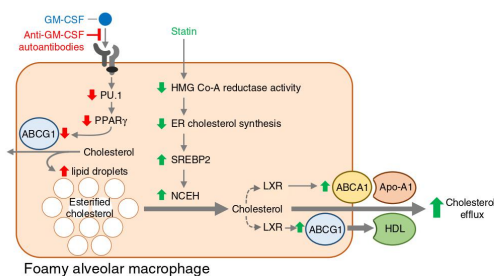


**Fig. 4** Proposed mechanisms for the pathogenesis and statin therapy of PAP. In the absence of GM-CSF signaling, surfactant-derived cholesterol accumulates progressively in lipid droplets resulting in foamy alveolar macrophages (red arrows indicate the effects of reduced GM-CSF signaling). Statin therapy results in increased cholesterol clearance from macrophages in PAP (green arrows represent the effects of statin in foamy alveolar macrophages)

macrophages<sup>25,31</sup>. Our proposed mechanism of action of statin therapy in PAP involves inhibition of HMGCR activity leading to reduced ER cholesterol content, thus increasing *SREBP2* expression. In turn, this increases *NCEH* expression/activity<sup>37,38</sup>, allowing hydrolysis of cholesterol esters and liberation of cholesterol, which increases liver X receptor (LXR) activity, *ABCA1/G1* expression, and subsequent efflux through these transporters primarily to HDL (Fig. 4).

Our results do not exclude the possibility that effects of statin therapy on serum cholesterol and HDL may contribute to therapeutic efficacy in PAP. Indeed, autoimmune PAP patients have an increased serum LDL:HDL ratio and reduced HDL levels<sup>39,40</sup> and the LDL to HDL ratio is inversely correlated with disease severity<sup>39</sup>. This study did not define the optimal dose of statin therapy or the time required to reach maximal treatment effect and additional studies are needed to further determine the specific mechanism of action, pharmacokinetics, and the potential role of statin therapy in autoimmune PAP. We have previously targeted cholesterol homeostasis by oral administration of PPAR $\gamma$  or LXR agonist therapy in *Csf2rb*<sup>-/-</sup> mice<sup>16</sup>. Although both statins and PPAR $\gamma$  agonists are available and commonly used, clinical trials will be needed to determine the relative safety and potential efficacy of these pharmacotherapies in patients with autoimmune PAP.

Finally, these results highlight the potential utility of two novel clinical outcome/diagnostic measures in the differential diagnosis of PAP. First, categorical parenchymal-pattern assessment using CALIPER software and quantitative densitometry of the lung CT scans provide continuous variable-based measures of pulmonary surfactant accumulation, which are useful in assessing PAP disease severity and may be favorable compared to semiquantitative visual assessment<sup>41</sup>. Second, measurement of cholesterol levels (or the cholesterol to phospholipid ratio of surfactant) in BAL could be used to evaluate patients with diffuse ground glass opacification as an adjunct to the bronchoscopic evaluation of PAP, which may reduce the need for a lung biopsy and the associated morbidity.

## Methods

**Ethical approval.** The institutional review boards of the Cincinnati Children's Hospital Medical Center and University of California Los Angeles approved this study. All human participants or their legal guardians gave written informed consent. All animal experiments were approved by the Institutional Animal Care and Use Committee (IACUC) at Cincinnati Children's Hospital Medical Center and the Office of Animal Research Oversight (OARO) at University of California Los Angeles.

**Computed tomography densitometry analysis.** A semi-automated image analysis algorithm was developed to segment the lungs and quantify the change in lung mass over serial CT images. Lung segmentation was performed using a commercially available software program (Amira, Hillsboro Oregon, USA). The whole-lungs were segmented from the body and major vasculature using an initial threshold of <500 Hounsfield units (HU), with user oversight. The average HU values of the left and right lung were quantified along with the respective lung volumes, which were measured by summing the voxel-volumes within the lungs. Based on the average HU of each lung, mean lung tissue densities ( $\rho_{CT}$ ) of both left and right lungs were determined via the following equation.

$$(\rho_{CT}) = \left( \frac{1000 - (HU)}{1000} \right)$$

Studies show that lung density decreases slightly in proportion to height<sup>42</sup>, accordingly, a small correction was used to calculate the total lung mass (TLM) using the following formula: Predicted TLM (g) = height (cm)  $\times$  9.8759 – 1019.1. The data were also expressed as a percentage of the predicted TLM using the following formula: Percent error = (TLM – Predicted TLM)/Predicted TLM  $\times$  100. Predicted TLM was calculated from standard CT in 10 healthy control individuals (Supplementary Table 2). The patient's predicted TLM was calculated based on the height of the patient (Supplementary Table 3).

**CALIPER parenchymal computed tomography analysis.** The CALIPER (Computer-Aided Lung Informatics for Pathology Evaluation and Ratings) image analysis software was developed at Mayo Clinic (Rochester, MN, USA). CALIPER provides automated characterization and quantitative assessment of pulmonary parenchymal disease on high-resolution CT data. Comprehensive description of CALIPER methodology has been previously published<sup>43</sup>. In brief, data processing includes extraction of lung parenchyma from the surrounding thoracic structures (chest wall, central airways and vessels). There is additional segmentation of the lung into 12 regions (left/right with central/peripheral areas within bilateral upper/middle/lower zones) using pre-defined landmarks. Using a 15  $\times$  15  $\times$  15 voxel and sliding box technique, each pixel of the lung parenchyma is mapped to a parenchymal tissue type. The classification is based on the similarity of the sampled voxel histogram to the signature of regions previously determined by consensus agreement of thoracic radiologists and additional morphological characteristics. Through this process, each pixel is labeled as normal parenchyma, low attenuation areas (mild, moderate, and severe subtypes) and increased attenuation areas (ground glass opacity, reticular densities) or honeycombing. The volume of each of these characteristics and percent of total parenchyma for each feature can be quantified. For the assessment of PAP, the sum of high density features (ground glass opacity and reticular densities) was considered "Involved Lung Parenchyma" and the sum of normal and low attenuation areas was considered "Uninvolved Lung Parenchyma". The percent involved vs. uninvolved regions was calculated based on the volume of each characteristic divided by the total segmented lung parenchymal volume.

**Human BAL and alveolar macrophages.** Human BAL fluid and alveolar macrophages were obtained from BAL using flexible bronchoscopy or from discarded material of PAP patients undergoing therapeutic WLL. After the fluid was centrifuged at 283  $\times$  g for 10 minutes, the cellular pellet was resuspended in the culture medium. Human alveolar macrophages were isolated by adherence to tissue culture plastic. Extracellular debris was removed by gentle washing with phosphate-buffered saline (PBS). Cells were maintained in the culture medium of Dulbecco's modified eagle's medium (DMEM) (Life Technologies) plus 10% fetal bovine serum (FBS), 50 U/ml penicillin, and 50  $\mu$ g/ml streptomycin.

**Mice used in this study.** *Csf2rb* gene-deficient (*Csf2rb*<sup>-/-</sup>) mice backcrossed onto a C57BL6/J background were used for this study and the phenotype has been previously reported<sup>44</sup>. C57BL6/J mice (referred to as wild type or WT mice) were purchased from the Jackson Laboratory. All mice were bred and housed at the Cincinnati Children's Research Foundation (CCRF) Vivarium or University of California Los Angeles (UCLA). Mice were maintained on a 12 hour/12 hour light/dark cycle with unlimited access to food and water. All animal experiments were approved by the IACUC at CCRF and the OARO at UCLA.

**Collection of mouse BAL fluid.** Bronchoalveolar lavage (BAL) was performed in mice to acquire epithelial lining fluid and alveolar macrophages. BAL was collected from mice using five 1 ml aliquots of PBS plus 0.5 mM EDTA<sup>17</sup>. The 1 ml aliquots were pooled and the recovered volumes recorded. The turbidity of the fluid was measured as described below. Aliquots of the BAL were taken as pre-spun samples and total BAL lipids were extracted using chloroform and methanol. Cholesterol was measured by the Amplex red cholesterol assay, described in more detail below. Total phosphate and saturated phosphatidylcholine were measured as described below<sup>45,46</sup>. From the remaining BAL fluid alveolar macrophages were isolated by spinning the BAL at 280  $\times$  g for 10 minutes at 4°C to isolate a cellular pellet. The supernatant was removed and the cellular pellets were resuspended in the culture



media (DMEM) for isolation of alveolar macrophages by adherence to tissue culture plastic<sup>16</sup>.

**Diff-Quick staining.** Cells were sedimented and stained with buffered eosin and methylene blue (Diff-Quick, Fisher) and evaluated by light microscopy.

**Oil Red O staining.** Cells were stained with Oil Red O staining using the Oil Red O staining kit (Poly Scientific R&D Corporation) according to the following protocol. Briefly, cells were fixed with 4% PFA and washed twice with distilled water. Cells were placed in absolute propylene glycol for 5 minutes. Propylene glycol was removed and cells were stained in a 0.5% Oil Red O solution in propylene glycol for 30 minutes. Cells were rinsed in an 85% propylene glycol solution for 5 minutes and washed twice with distilled water followed by a hematoxylin counterstain for 2 minutes. Cells were mounted with an aqueous mounting medium (glycerin jelly).

**Electron microscopy.** Alveolar macrophages were collected by centrifugation (3000 rpm, 3 minutes, room temperature), incubated in modified Karnovsky's fixative (2% paraformaldehyde and 2% glutaraldehyde in 0.1 M sodium cacodylate buffer plus 0.1% calcium chloride, pH 7.3) for 2 hours, at room temperature and cell blocks were prepared and evaluated as previously described<sup>47</sup>.

**Lipid extraction from BAL fluid.** A chloroform-methanol extraction was used to extract lipids from cells and BAL for further analysis. 1 ml of BAL was diluted in 1 ml of DPBS, subsequently 2 ml of 100% methanol, and 4 ml of 100% chloroform were added. This was mixed and then centrifuged at 4°C @1000 rpm. The lower phase containing the extracted lipids was transferred to a new glass tube for analysis.

**Cellular lipid analysis.** To collect cellular lipids from primary alveolar macrophages, culture media was aspirated and then 100% isopropanol was added to the tissue culture wells. Cellular lipids were extracted for 2 hours at room temperature or overnight at 4°C. The isopropanol was then transferred into glass tubes and half the volume of new isopropanol was added back to the tissue culture plate for 30 minutes to recover any remaining sample and combined with the original volume. Following removal of isopropanol, a Pierce BCA (bicinchoninic acid assay) protein assay (Thermo Fisher Scientific) was performed on the tissue culture wells to determine the cellular protein concentration.

**Tri-one dimensional thin-layer chromatography (TOD-TLC).** Alveolar macrophages (AMs) were isolated from BALF based on adherence to tissue culture plastic as described above. Cells were repeatedly washed with PBS to remove extracellular surfactant and then 100% isopropanol was added to the tissue culture wells, 1 ml for a 12-well plate and 2 ml for a six-well plate. Cellular lipids were extracted for 2 hours at room temperature or overnight at 4°C. The isopropanol was then transferred into glass tubes and half the volume of new isopropanol was added back into the tissue culture plate for 30 minutes to recover any remaining sample and combined with the original volume. Lipid samples were then evaporated using a stream of nitrogen and a water bath set to 52°C. Cellular lipid samples were then loaded onto high performance thin-layer chromatography plates pre-coated with silica gel 60 (Fisher). Plates were prewashed with chloroform and methanol to remove any contaminants and dried overnight at 120°C. Plates were developed in a solvent system modified from White et al.<sup>48</sup>. In brief, plates were first developed in a solvent mixture of chloroform, ethanol, triethylamine, and water (30:35:35:6) up to 7 cm of a 10 cm plate. Plates are removed from the chamber, dried, and placed in a second solvent of hexane and diethylether (90:10) up to 9 cm of a 10 cm plate. Plates are again removed from the chamber, dried, and then placed in the final solvent of pure hexane and run to the top of the plate. Bands are visualized by spraying with a 0.05% solution of primuline in acetone and water (80:20) and detected as ultraviolet spots at 366 nm on a Typhoon 9500 molecular imager<sup>48</sup>. Lipid band densities were calculated using ImageQuant Software (GE Healthcare Life Sciences) based upon standard curves.

**Cholesterol analysis.** Total and free cholesterol levels were measured by fluorometric enzymatic assay as previously described<sup>16</sup>. Esterified cholesterol was then calculated by subtracting free cholesterol from the total value.

**BAL turbidity.** The turbidity of the fluid was measured as previously described<sup>17,49</sup>. In brief, 250 µl of the BAL were diluted into 750 µl of PBS and the optical density measured at a wavelength of 600 nm and multiplied by the dilution factor.

**BAL phospholipid levels.** Aliquots of the BAL were taken as pre-spun samples and total BAL lipids were extracted using chloroform and methanol. Total phosphate and saturated phosphatidylcholine were measured as previously reported<sup>45,46</sup>.

**Ex vivo human macrophage statin treatment.** After purifying alveolar macrophages as described above, fresh media was added to the adherent alveolar macrophages containing human M-CSF (R&D) (25 ng/ml) only or M-CSF plus simvastatin (Calbiochem) (5 µM) and Mevalonic acid (Sigma Aldrich) (100 µM). After 24 hours of culture, cholesterol analysis or qRT-PCR was performed as described.

**RNA isolation and gene expression analysis.** Total RNA was isolated using Qiazol (Life Technologies) and was converted to complementary DNA (cDNA) using the High Capacity cDNA reverse transcription kit (Applied Biosystems) according to the manufacturer's protocol. Gene expression was determined by quantitative real-time PCR (qRT-PCR) using a Lightcycler480 Real-time qPCR machine and Lightcycler480 mastermix (Roche Diagnostics). Relative gene expression was determined using an efficiency corrected method and efficiency was determined from a 3-log serial dilutions standard curve made from cDNA pooled from all samples. Primers were designed across exon-exon boundaries (Supplementary Data 1). Results were normalized to *36b4* mRNA.

**In vivo statin treatment of *Csf2rb*<sup>-/-</sup> mice.** For oral statin administration studies in mice, simvastatin or pravastatin was incorporated into standard rodent chow (Laboratory Rodent Diet 5001; LabDiet) at a dose expected to deliver 10 mg/kg/BW/Day (Research Diets). BAL turbidity and cholesterol levels were measured as described above. Primary alveolar macrophages were isolated and cholesterol assays and qRT-PCR were performed as described above.

**Bone marrow-derived macrophages.** Bone marrow cells were obtained from 6-week old *Csf2rb*<sup>-/-</sup> mice by crushing the tibias and femurs with the culture media (DMEM (Life Technologies) plus 10% FBS, 50 U/ml penicillin, and 50 µg/ml streptomycin). Mononuclear cells were isolated by centrifugation over a Ficoll-Paque (GE Healthcare Life Sciences) gradient at room temperature for 30 minutes. The buffy coat was washed in PBS and the cellular pellet resuspended in the culture medium with M-CSF (R&D Systems) (10 ng/ml) and cells were cultured in a 10 cm dish overnight at 37°C and the next day non-adherent cells were recovered and transferred to a new dish and cultured under the same conditions for an additional 24 hrs. At this stage, non-adherent cells were discarded and adherent cells cultured for an additional 5 days to allow differentiation of BMDMs.

**Radiolabelled cholesterol efflux analysis.** Alveolar macrophages or bone marrow-derived macrophages were obtained from *Csf2rb*<sup>-/-</sup> mice as described. Macrophages were plated in 24-well plates (1 × 10<sup>5</sup> cells/well) in media (DMEM) containing 10% FBS and allowed to adhere for 2 h. Cells were washed and incubated for an additional 24 h in fresh media containing bovine serum albumin (BSA) (0.2% w/v), M-CSF (10 ng/ml), supplemented with an ACAT inhibitor (58-035; 2 µg/ml) and <sup>3</sup>H-cholesterol (1 µCi/ml). After 24 h, the cells were washed with PBS and incubated in fresh media containing 0.2% BSA and M-CSF (10 ng/ml) for a further 24 h equilibration period, with simvastatin (5 µM) and mevalonic acid (50 µM) or DMSO control. To determine cholesterol efflux, the cells were rinsed and then incubated for 4 h in media containing 0.2% BSA and M-CSF (10 ng/ml) with Apo-AI (15 µg/ml) or HDL (50 µg/ml). The media was removed, the cells washed in PBS, and the radioactive content of the media and cells determined as described<sup>50</sup>. Cholesterol efflux was determined by dividing the radioactive content of the media by the sum of the radioactivity in the cells and media.

**Statistical analysis.** Statistical analysis was performed using GraphPad Prism 7 software. Each data point represents Mean ± SEM. For comparison of two groups, parametric (*t* test) or non-parametric (Mann-Whitney test) tests were done where appropriate. For comparison of three groups or more, statistical analysis was carried out using one-way analysis of variance, followed by Bonferroni's post hoc test. *N* and *P* values are indicated in figure legends, and *P* values < 0.05 was considered statistically significant.

**Data availability.** The authors declare that all data supporting the findings of this study are available within the paper and its supplementary information files or upon reasonable request from the authors.

Received: 7 May 2018 Accepted: 22 June 2018

Published online: 07 August 2018

## References

- Veldhuizen, R., Nag, K., Orgeig, S. & Possmayer, F. The role of lipids in pulmonary surfactant. *Biochim. Biophys. Acta* **1408**, 90–108 (1998).

2. Perez-Gil, J. & Weaver, T. E. Pulmonary surfactant pathophysiology: current models and open questions. *Physiol.* **25**, 132–141 (2010).
3. Trapnell, B. C. & Whitsett, J. A. GM-CSF regulates pulmonary surfactant homeostasis and alveolar macrophage-mediated innate host defense. *Annu. Rev. Physiol.* **64**, 775–802 (2002).
4. Gurel, O., Ikegami, M., Chronoes, Z. C. & Jobe, A. H. Macrophage and type II cell catabolism of SP-A and saturated phosphatidylcholine in mouse lungs. *Am. J. Physiol. Lung Cell Mol. Physiol.* **280**, L1266–L1272 (2001).
5. Griese, M. Pulmonary surfactant in health and human lung diseases: state of the art. *Eur. Respir. J.* **13**, 1455–1476 (1999).
6. Ikegami, M. et al. Surfactant metabolism in transgenic mice after granulocyte macrophage-colony stimulating factor ablation. *Am. J. Physiol.* **270**, L650–L658 (1996).
7. Yoshida, M., Ikegami, M., Reed, J. A., Chronoes, Z. C. & Whitsett, J. A. GM-CSF regulates surfactant protein-A and lipid catabolism by alveolar macrophages. *Am. J. Physiol. Lung Cell Mol. Physiol.* **280**, L379–L386 (2001).
8. Shibata, Y. et al. GM-CSF regulates alveolar macrophage differentiation and innate immunity in the lung through PU.1. *Immunity* **15**, 557–567 (2001).
9. Bonfield, T. L. et al. PU.1 regulation of human alveolar macrophage differentiation requires granulocyte-macrophage colony-stimulating factor. *Am. J. Physiol. Lung Cell Mol. Physiol.* **285**, L1132–L1136 (2003).
10. Kitamura, T. et al. Idiopathic pulmonary alveolar proteinosis as an autoimmune disease with neutralizing antibody against granulocyte/macrophage colony-stimulating factor. *J. Exp. Med.* **190**, 875–880 (1999).
11. Trapnell, B. C., Whitsett, J. A. & Nakata, K. Pulmonary alveolar proteinosis. *N. Engl. J. Med.* **349**, 2527–2539 (2003).
12. Bendtzen, K., Svenson, M. & Hansen, M. B. GM-CSF autoantibodies in pulmonary alveolar proteinosis. *N. Engl. J. Med.* **356**, 2001 (2007).
13. Suzuki, T. et al. Familial pulmonary alveolar proteinosis caused by mutations in CSF2RA. *J. Exp. Med.* **205**, 2703–2710 (2008).
14. Tanaka, T. et al. Adult-onset hereditary pulmonary alveolar proteinosis caused by a single-base deletion in CSF2RB. *J. Med. Genet.* **48**, 205–209 (2011).
15. Martinez-Moczygemba, M. et al. Pulmonary alveolar proteinosis caused by deletion of the GM-CSFRalpha gene in the X chromosome pseudoautosomal region 1. *J. Exp. Med.* **205**, 2711–2716 (2008).
16. Salles, A. et al. Targeting cholesterol homeostasis in lung diseases. *Sci. Rep.* **7**, 10211 (2017).
17. Suzuki, T. et al. Pulmonary macrophage transplantation therapy. *Nature* **514**, 450–454 (2014).
18. Uchida, K. et al. Standardized serum GM-CSF autoantibody testing for the routine clinical diagnosis of autoimmune pulmonary alveolar proteinosis. *J. Immunol. Methods* **402**, 57–70 (2014).
19. Sui, X. et al. Quantitative assessment of pulmonary alveolar proteinosis (PAP) with ultra-dose CT and correlation with pulmonary function tests (PFTs). *PLoS ONE* **12**, e0172958 (2017).
20. Mascialchi, M., Camiciottoli, G. & Diciotti, S. Lung densitometry: why, how and when. *J. Thorac. Dis.* **9**, 3319–3345 (2017).
21. Jacob, J. et al. Predicting outcomes in idiopathic pulmonary fibrosis using automated CT analysis. *Am J Respir. Crit. Care. Med.* <https://doi.org/10.1164/rccm.201711-2174OC> (2018).
22. Daniels, C. B., Barr, H. A., Power, J. H. & Nicholas, T. E. Body temperature alters the lipid composition of pulmonary surfactant in the lizard *Ctenophorus nuchalis*. *Exp. Lung Res.* **16**, 435–449 (1990).
23. Marquart, T. J., Allen, R. M., Ory, D. S. & Baldan, A. miR-33 links SREBP-2 induction to repression of sterol transporters. *Proc. Natl. Acad. Sci. USA* **107**, 12228–12232 (2010).
24. Steinberg, D. Thematic review series: the pathogenesis of atherosclerosis. An interpretive history of the cholesterol controversy, part V: the discovery of the statins and the end of the controversy. *J. Lipid Res.* **47**, 1339–1351 (2006).
25. Thomassen, M. J. et al. ABCG1 is deficient in alveolar macrophages of GM-CSF knockout mice and patients with pulmonary alveolar proteinosis. *J. Lipid Res.* **48**, 2762–2768 (2007).
26. Cavelier, C., Lorenzi, I., Rohrer, L. & von Eckardstein, A. Lipid efflux by the ATP-binding cassette transporters ABCA1 and ABCG1. *Biochim. Biophys. Acta* **1761**, 655–666 (2006).
27. Ditiatkovski, M., Toh, B. H. & Bobik, A. GM-CSF deficiency reduces macrophage PPAR-gamma expression and aggravates atherosclerosis in ApoE-deficient mice. *Arterioscler. Thromb. Vasc. Biol.* **26**, 2337–2344 (2006).
28. Kennedy, M. A. et al. ABCG1 has a critical role in mediating cholesterol efflux to HDL and preventing cellular lipid accumulation. *Cell Metab.* **1**, 121–131 (2005).
29. Moore, K. J. et al. The role of PPAR-gamma in macrophage differentiation and cholesterol uptake. *Nat. Med.* **7**, 41–47 (2001).
30. Sakagami, T. et al. Human GM-CSF autoantibodies and reproduction of pulmonary alveolar proteinosis. *N. Engl. J. Med.* **361**, 2679–2681 (2009).
31. Bonfield, T. L. et al. Peroxisome proliferator-activated receptor-gamma is deficient in alveolar macrophages from patients with alveolar proteinosis. *Am. J. Respir. Cell Mol. Biol.* **29**, 677–682 (2003).
32. de Aguiar Vallim, T. Q. et al. ABCG1 regulates pulmonary surfactant metabolism in mice and men. *J. Lipid Res.* **58**, 941–954 (2017).
33. Miyata, R., Bai, N., Vincent, R., Sin, D. D. & Van Eeden, S. F. Statins reduce ambient particulate matter-induced lung inflammation by promoting the clearance of particulate matter, <10 mum from lung tissues. *Chest* **143**, 452–460 (2013).
34. Morimoto, K. et al. Statins enhance clearance of apoptotic cells through modulation of Rho-GTPases. *Proc. Am. Thorac. Soc.* **3**, 516–517 (2006).
35. Argmann, C. A. et al. Regulation of macrophage cholesterol efflux through hydroxymethylglutaryl-CoA reductase inhibition: a role for RhoA in ABCA1-mediated cholesterol efflux. *J. Biol. Chem.* **280**, 22212–22221 (2005).
36. Yano, M. et al. Statins activate peroxisome proliferator-activated receptor gamma through extracellular signal-regulated kinase 1/2 and p38 mitogen-activated protein kinase-dependent cyclooxygenase-2 expression in macrophages. *Circ. Res.* **100**, 1442–1451 (2007).
37. Natarajan, R., Ghosh, S. & Grogan, W. M. Regulation of the rat neutral cytosolic cholesteryl ester hydrolase promoter by hormones and sterols: a role for nuclear factor-Y in the sterol-mediated response. *J. Lipid Res.* **40**, 2091–2098 (1999).
38. Smith, L. H., Petrie, M. S., Morrow, J. D., Oates, J. A. & Vaughan, D. E. The sterol response element binding protein regulates cyclooxygenase-2 gene expression in endothelial cells. *J. Lipid Res.* **46**, 862–871 (2005).
39. Fang, C. S. et al. Clinical significance of serum lipids in idiopathic pulmonary alveolar proteinosis. *Lipids Health Dis.* **11**, 12 (2012).
40. Tian, X. et al. Impaired lipid metabolism in idiopathic pulmonary alveolar proteinosis. *Lipids Health Dis.* **10**, 54 (2011).
41. Tokura, S. et al. A semiquantitative computed tomographic grading system for evaluating therapeutic response in pulmonary alveolar proteinosis. *Ann. Am. Thorac. Soc.* **14**, 1403–1411 (2017).
42. Hoffman, E. A. et al. Variation in the percent of emphysema-like lung in a healthy, nonsmoking multiethnic sample. The MESA lung study. *Ann. Am. Thorac. Soc.* **11**, 898–907 (2014).
43. Zavaletta, V. A., Bartholmai, B. J. & Robb, R. A. High resolution multidetector CT-aided tissue analysis and quantification of lung fibrosis. *Acad. Radiol.* **14**, 772–787 (2007).
44. Robb, L. et al. Hematopoietic and lung abnormalities in mice with a null mutation of the common beta subunit of the receptors for granulocyte-macrophage colony-stimulating factor and interleukins 3 and 5. *Proc. Natl. Acad. Sci. USA* **92**, 9565–9569 (1995).
45. Bridges, J. P. et al. Orphan G protein-coupled receptor GPR116 regulates pulmonary surfactant pool size. *Am. J. Respir. Cell Mol. Biol.* **49**, 348–357 (2013).
46. Baker, A. D. et al. Targeted PPAR[gamma] deficiency in alveolar macrophages disrupts surfactant catabolism. *J. Lipid Res.* **51**, 1325–1331 (2010).
47. Sakagami, T. et al. Patient-derived granulocyte/macrophage colony-stimulating factor autoantibodies reproduce pulmonary alveolar proteinosis in nonhuman primates. *Am. J. Respir. Crit. Care. Med.* **182**, 49–61 (2010).
48. White, T., Bursten, S., Federighi, D., Lewis, R. A. & Nudelman, E. High-resolution separation and quantification of neutral lipid and phospholipid species in mammalian cells and sera by multi-one-dimensional thin-layer chromatography. *Anal. Biochem.* **258**, 109–117 (1998).
49. Suzuki, T. et al. Hereditary pulmonary alveolar proteinosis: pathogenesis, presentation, diagnosis, and therapy. *Am. J. Respir. Crit. Care. Med.* **182**, 1292–1304 (2010).
50. Venkateswaran, A. et al. Control of cellular cholesterol efflux by the nuclear oxysterol receptor LXR alpha. *Proc. Natl. Acad. Sci. USA* **97**, 12097–12102 (2000).

### Acknowledgements

We thank our patients with PAP, without whose collaboration this work would not have been possible. This work was supported by National Institutes of Health/National Heart, Lung, and Blood Institute grant numbers R01085453 (PI: B.C.T.), HL131634 (PI: J.P.B.), HL118161 and HL136543 (PI: E.J.T.) and National Center for Advancing Translational Science/National Heart, Lung, and Blood Institute grant number HL127672 (PI: B.C.T.).

### Author contributions

C.M., E.L., J.P.B., E.J.T. and B.C.T. designed the study. C.M., E.L., T.W. and B.C.T. provided clinical care for the patients and provided clinical specimens. C.M. and B.C.T. provided case report details. J.C.W. and B.J.B. analyzed radiological data. C.M., E.L., J.P.B., A.S., T.S., J.C.W., B.J.B., T.W., C.C., B.C.C., P.A., K. S., E.J.T. and B.C.T. performed research and analyzed data. C.M., J.P.B., J.C.W., B.J.B., E.J.T. and B.C.T. wrote the



manuscript. All authors contributed to writing and approved the final version of the manuscript.

### Additional information

**Supplementary Information** accompanies this paper at <https://doi.org/10.1038/s41467-018-05491-z>.

**Competing interests:** The authors declare no competing interests.

**Reprints and permission** information is available online at <http://npg.nature.com/reprintsandpermissions/>

**Publisher's note:** Springer Nature remains neutral with regard to jurisdictional claims in published maps and institutional affiliations.



**Open Access** This article is licensed under a Creative Commons Attribution 4.0 International License, which permits use, sharing, adaptation, distribution and reproduction in any medium or format, as long as you give appropriate credit to the original author(s) and the source, provide a link to the Creative Commons license, and indicate if changes were made. The images or other third party material in this article are included in the article's Creative Commons license, unless indicated otherwise in a credit line to the material. If material is not included in the article's Creative Commons license and your intended use is not permitted by statutory regulation or exceeds the permitted use, you will need to obtain permission directly from the copyright holder. To view a copy of this license, visit <http://creativecommons.org/licenses/by/4.0/>.

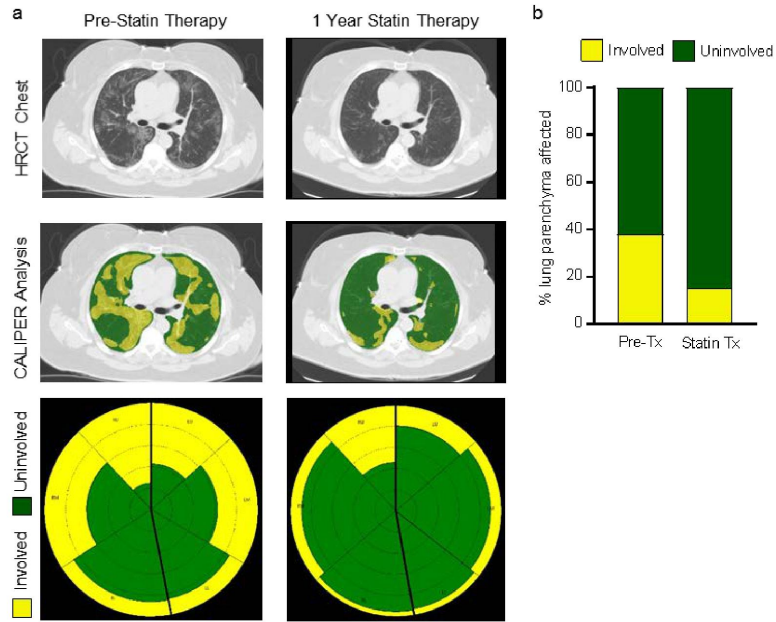
© The Author(s) 2018

**Supplementary Information**

**Statin as a Novel Pharmacotherapy of Pulmonary Alveolar Proteinosis.**

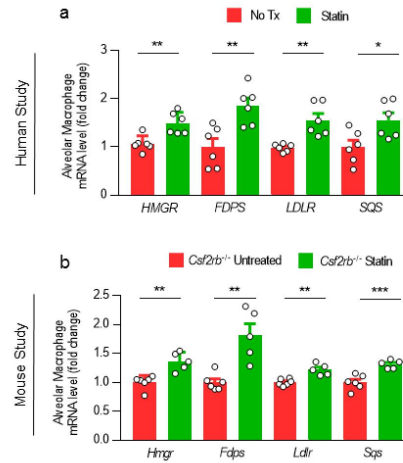
**McCarthy et al.**

**Supplementary Figure 1**



**Supplementary Figure 1. a**, HRCT chest images from Case 2 prior to and 1 year after initiating statin therapy. HRCT image illustrating quantitative categorical parenchymal-pattern, CALIPER analysis (green-masking: uninvolved/normal lung parenchyma, yellow-masking: PAP-involved/abnormal lung comprising groundglass and reticular changes). Glyphs showing parenchymal-pattern analysis of total lung parenchyma segmented by right, left; upper, middle, and lower zones. **b**, Percentage of lung affected by PAP determined by parenchymal-pattern analysis.

## Supplementary Figure 2



**Supplementary Table 1****Serum cholesterol levels of case report patient over a 10 year period (2008-2017)**

| Date       | Total Cholesterol (mg/dL) | HDL (mg/dL) | LDL (mg/dL) | Total Cholesterol:HDL Ratio | Statin Therapy |
|------------|---------------------------|-------------|-------------|-----------------------------|----------------|
| 9/13/2008  | 328                       | 77          | 205         | 4.26                        | -              |
| 3/21/2012  | 214                       | 111         | 87          | 1.93                        | -              |
| 2/12/2013  | 338                       | 194         | 131         | 1.74                        | -              |
| 8/22/2013  | 336                       | 45          | 271         | 7.47                        | -              |
| 7/20/2014  | 270                       | 45          | 183         | 6.00                        | +              |
| 11/28/2014 | 265                       | 44          | 192         | 6.02                        | +              |
| 2/17/2015  | 173                       | 67          | 81          | 2.58                        | +              |
| 4/6/2015   | 194                       | 68          | 104         | 2.85                        | +              |
| 2/23/2016  | 219                       | 88          | 112         | 2.49                        | +              |
| 6/6/2017   | 175                       | 90          | 72          | 1.94                        | +              |

**Supplementary Table 2****Lung mass in healthy people determined by quantitative chest computed tomography densitometry.**

| Subject | Age (y) | Gender | Height (cm) | Left lung mass (g) | Right lung mass (g) | Total lung mass (g) | Predicted Total lung mass (g)* | Percent error† | Percent of predicted total lung mass‡ |
|---------|---------|--------|-------------|--------------------|---------------------|---------------------|--------------------------------|----------------|---------------------------------------|
| 1       | 41      | F      | 154.9       | 255                | 285                 | 540                 | 511                            | 5.7            | 106                                   |
| 2       | 42      | F      | 172.7       | 306                | 360                 | 660                 | 687                            | 3.9            | 96.1                                  |
| 3       | 44      | F      | 165.1       | 244                | 259                 | 503                 | 611                            | 17.7           | 82.3                                  |
| 4       | 44      | F      | 162.5       | 307                | 327                 | 634                 | 586                            | 8.2            | 108                                   |
| 5       | 45      | F      | 160.0       | 302                | 352                 | 654                 | 561                            | 14.2           | 117                                   |
| 6       | 46      | M      | 177.8       | 306                | 347                 | 653                 | 737                            | 11.4           | 88.6                                  |
| 7       | 46      | F      | 165.1       | 313                | 339                 | 652                 | 611                            | 6.7            | 107                                   |
| 8       | 49      | M      | 200.6       | 506                | 558                 | 1064                | 962                            | 10.6           | 111                                   |
| 9       | 54      | F      | 172.7       | 313                | 365                 | 678                 | 687                            | 1.3            | 98.7                                  |
| 10      | 62      | M      | 180.3       | 314                | 349                 | 663                 | 762                            | 13.0           | 87.0                                  |

\* Predicted TLM (g) = height (cm) x 9.8759 – 1019.1

† Percent error = ((TLM – Predicted TLM) ÷ Predicted TLM) x 100

‡ Percent predicted TLM = (TLM (g) ÷ Predicted TLM) x 100

Abbreviations: TLM, total lung mass.

**Supplementary Table 3****Lung mass in the patient (Case 1) determined by quantitative chest computed tomography densitometry.**

| Date      | Left lung mass (g) | Right lung mass (g) | Total lung mass (g) | Predicted total lung mass (g)*‡ | Percent of predicted total lung mass†‡ |
|-----------|--------------------|---------------------|---------------------|---------------------------------|--|
| 5/6/2011  | 727                | 862                 | 1589                | 587                             | 271                                    |
| 2/20/2012 | 685                | 685                 | 1370                | 587                             | 233                                    |
| 2/23/2013 | 497                | 513                 | 1010                | 587                             | 172                                    |
| 6/5/2017  | 310                | 351                 | 661                 | 587                             | 113                                    |

\* Predicted TLM (g) = height (cm) x 9.8759 – 1019.1

† Percent error = ((TLM – Predicted TLM) ÷ Predicted TLM) x 100

‡ Median age of the control cohort (Supplementary Table 2) was younger than that of the case, however, CT measurements were normalized to body height, as described in the methods section. A marked improvement in relative lung weight was appreciable over time.

## **CHAPTER 4**

**Alveolar macrophage lipid levels and plasma anti-GM-CSF antibodies correlate with disease improvement in patients with pulmonary alveolar proteinosis**



**Alveolar macrophage lipid levels and plasma anti-GM-CSF antibodies correlate with disease improvement in patients with Pulmonary Alveolar Proteinosis**

Elinor Lee<sup>1,2,3</sup>, Kevin J. Williams<sup>4,5</sup>, Cormac McCarthy<sup>6</sup>, Claudia Chalk<sup>7,8</sup>, Brenna Carey<sup>7,8</sup>, Bruce C. Trapnell<sup>7,8,9</sup>, Thomas Q. de Aguiar Vallim<sup>1,3,5,10,11</sup>, Tisha Wang<sup>1,2</sup>, Elizabeth J. Tarling<sup>1,3,10,11</sup>

<sup>1</sup>Department of Medicine, David Geffen School of Medicine, University of California, Los Angeles

<sup>2</sup>Division of Pulmonary and Critical Care Medicine, University of California, Los Angeles

<sup>3</sup>Department of Molecular, Cellular, & Integrative Physiology, University of California, Los Angeles

<sup>4</sup>UCLA Lipidomics Lab, University of California, Los Angeles

<sup>5</sup>Department of Biological Chemistry, University of California, Los Angeles

<sup>6</sup>School of Medicine, University College Dublin

<sup>7</sup>Translational Pulmonary Science Center, Cincinnati Children's Hospital Medical Center

<sup>8</sup>Division of Pulmonary Biology, Cincinnati Children's Hospital Medical Center

<sup>9</sup>Division of Pulmonary, Critical Care, and Sleep Medicine, University of Cincinnati College of Medicine

<sup>10</sup>Molecular Biology Institute, University of California, Los Angeles

<sup>11</sup>Jonsson Comprehensive Cancer Center, University of California, Los Angeles

**Abstract:**

Pulmonary surfactant is essential for the maintenance of alveolar structure and surface tension required for gas exchange and breathing. Surfactant synthesis, secretion, and metabolism are dependent upon two primary cell types, alveolar type II epithelial cells and alveolar macrophages. Pulmonary Alveolar Proteinosis (PAP) is a rare lung syndrome characterized by the accumulation of surfactant and lipid-loaded macrophages within the alveoli due to disruption of granulocyte-macrophage colony stimulating factor (GM-CSF) signaling in alveolar macrophages. This results in alveolar macrophages that are deficient in surfactant catabolism. Early studies suggested that PAP resulted from dysfunction in phospholipid homeostasis that led to the accumulation of phospholipid-enriched surfactant. However, more recent studies suggest that PAP pathogenesis is driven by changes in cholesterol homeostasis that may be linked to alveolar macrophages. We now report on the use of mass spectrometry to define the lipid signature of alveolar macrophages obtained from PAP patients. In addition, we quantify how these macrophage-associated lipids change during clinical treatment of these patients. Our studies demonstrate that compared to non-PAP macrophages, PAP alveolar macrophages are significantly enriched in both phosphatidylcholines (PC), especially PC16:0/16:0, and cholesterol esters (CE). Importantly, clinical improvement in treated PAP patients is associated with a decrease in PC and CE species, indicating that levels of these macrophage-associated lipids correlate with the severity of the disease. Lastly, we identify plasma antibodies to GM-CSF as a previously unrecognized clinical biomarker that correlates with regression of disease in treated patients.

## Introduction

Pulmonary Alveolar Proteinosis (PAP) is a rare lung disorder with no cure or FDA approved therapies (1). The pathogenesis of this syndrome is heterogenous with various biochemical defects that lead to the accumulation of surfactant within the alveoli. It is categorized into primary, secondary, and congenital etiologies (2). Primary PAP occurs due to altered GM-CSF signaling from either high levels of neutralizing antibodies to GM-CSF or hereditary causes due to mutations in the GM-CSF receptor (CSF2RA or CSF2RB, which encode the alpha and beta chain peptides of the GM-CSF receptor, respectively). Secondary PAP is associated with underlying diseases that secondarily affect alveolar macrophage number or function such as hematologic malignances, immunologic syndromes, infections, or toxic inhalational exposures. Congenital PAP is the rarest type and caused by mutations in genes that are essential for surfactant production. About 90% of patients have primary PAP, specifically autoimmune PAP (aPAP), characterized by the presence of autoantibodies against GM-CSF, leading to the disruption of GM-CSF signaling in alveolar macrophages (1). GM-CSF has been identified as a key mediator of alveolar macrophage maturation, self-renewal, and population size (3, 4). In the absence of GM-CSF signaling, alveolar macrophages are impaired in their ability to regenerate, mature, and catabolize surfactant (4). Furthermore, mice deficient in GM-CSF (*Csf2<sup>-/-</sup>*) or its receptor (*Csf2ra<sup>-/-</sup>* and *Csf2rb<sup>-/-</sup>*) develop PAP-like pulmonary histopathology and are utilized as mouse models to study PAP (5-9). Current treatment is limited and focused on controlling symptoms and preventing progression of disease. The standard of care is whole lung lavage (WLL), which is relatively ineffective and not widely available; however, there are multiple experimental therapies including administration of inhaled GM-CSF (2).

Surfactant is comprised of 80% phospholipids, most of which is dipalmitoyl phosphatidylcholine (DPPC; PC16:0/16:0), 10% neutral lipids (mostly cholesterol ester), and 10% proteins (10). Surfactant homeostasis is maintained by the actions of alveolar type II epithelial cells and alveolar macrophages. Alveolar type II cells synthesize and secrete surfactant. About 20-30% of surfactant is taken up and catabolized by alveolar macrophages, while the majority is recycled for additional rounds of secretion or degraded by type II epithelial cells (10). It was originally proposed that PAP was the result of impaired catabolism of phospholipids in alveolar macrophages (11-13). However, more recent studies comparing WT mice and *Csf2<sup>-/-</sup>* mice have demonstrated that the relative proportion of cholesterol in surfactant was elevated in *Csf2<sup>-/-</sup>* mice, while the relative proportion of saturated to total phospholipids remained comparable in both groups (14). Additionally, alveolar macrophages isolated from PAP patients and *Csf2<sup>-/-</sup>* or *Csf2rb<sup>-/-</sup>* mice have increased levels of both esterified and free/unesterified cholesterol but minimal changes in the level of triglycerides, free fatty acids, and phospholipid species compared to macrophages obtained from controls (14, 15).

It has also been reported that alveolar macrophages isolated from PAP patients or mouse models of PAP have significantly lower expression of the ATP binding cassette transporter G1 (ABCG1) and peroxisome proliferator-activated receptor gamma (PPAR $\gamma$ ), important mediators of cholesterol and lipid efflux from macrophages (5, 16-20). Furthermore, we recently reported that treatment of a subset of PAP patients with a statin, a drug that targets HMG-CoA reductase leading to reductions in plasma cholesterol levels, which markedly reduced pulmonary abnormalities in PAP lung disease (15). These data are consistent with the concept that alterations in cholesterol homeostasis have a significant role in the pathogenesis of PAP(14, 15).

Surprisingly, to date, the lipidomic profile of alveolar macrophages in PAP remains unknown. Given the key role of alveolar macrophages in the catabolism of surfactant and in cholesterol metabolism, we hypothesized that defining the lipid composition of these cells might provide new mechanistic insight into PAP and identify novel therapeutic targets. Here, we report on studies that utilized mass spectrometry to quantify and characterize the lipidome of alveolar macrophages from nonPAP and PAP patients. Further, we report on the lipid profile of alveolar macrophages from two PAP patients during their clinical course. Based on these data, we have identified an association between specific macrophage lipids and the severity of PAP disease. We also identify a potential novel biomarker that may prove useful in predicting the response of individual PAP patients to treatment.

## **Materials and Methods**

### **Patient selection and ethical approval**

All patients included in this study are male and female adults who have autoimmune PAP and are being treated at University of California, Los Angeles and Cincinnati Children's Hospital Medical Center. Ages range from 21 to 66 years old. The institutional review boards of University of California, Los Angeles and of Cincinnati Children's Hospital Medical Center approved this study. All human participants gave their written informed consent.

### **Measurement of GM-CSF antibody levels**

GM-CSF autoantibody levels were measured at Cincinnati Children's Hospital Medical Center as described by Uchida et al (21).

### **Collection of human bronchoalveolar fluid and isolation alveolar macrophages**

Human bronchoalveolar (BAL) fluid was collected from discarded material of PAP patients undergoing therapeutic WLL. Alveolar macrophages were isolated by centrifugation at 200 g for 5 minutes. Cells were resuspended with Ammonium-Chloride-Potassium (ACK) lysing buffer to lyse red blood cells. Cells were counted and aliquoted at  $2 \times 10^6$  or  $5 \times 10^6$  cells in 200  $\mu\text{L}$  of phosphate-buffered solution (PBS). Macrophage purity was  $>95\%$  as previously described (17, 20, 22). For frozen samples, cells were frozen immediately at  $-80^\circ\text{C}$  and counted after being thawed and prior to lipid extraction. The duration of the cells in the freezer ranged from 0.1-8 years before analysis. Long-term stability of the lipids in human lavage fluid for these lengths of time has been previously described (23).

### **Lipid extraction and analysis for lipidizer**

A modified Bligh and Dyer extraction was performed on human alveolar macrophages (24). For alveolar macrophages, we used  $5 \times 10^6$  cells in 200  $\mu\text{L}$  of PBS. Prior to the biphasic extraction, a 13 lipid class Lipidizer Internal Standard Mix (AB Sciex, 5040156) was added to each sample. Two successive extractions were done, and the resulting organic layers were pooled and dried down in a Genevac EZ-2 Elite. Lipid samples were then resuspended in 1:1 methanol/dichloromethane with 10 mM ammonium acetate and transferred to robovials (Thermo, 10800107) for analysis.

Samples were analyzed on the Sciex Lipidizer Platform for targeted quantitative measurement of 1,100 lipid species across 13 classes including cholesterol esters (CE), ceramides (CER), dihydroceramides (DCER), diacylglycerols (DAG), free fatty acids (FFA), hexosylceramides (HCER), lactosylceramides (LCER), lysophosphatidylcholines (LPC),

lysophosphatidylethanolamines (LPE), phosphatidylcholines (PC), phosphatidylethanolamines(PE), sphingomyelins (SM), and triacylglycerols (TAG). The quantification processing has been well described previously (25). Differential Mobility Device on the Lipidyzer was tuned with SelexION tuning kit (Sciex, 5040141). The instrument settings, tuning settings, and multiple reaction monitoring (MRM) list are available upon request. The data was analyzed on the Lipidyzer software with the quantitative values being normalized to cell counts.

### **Processing and analysis of samples for gas chromatography/mass spectrometry (GC-MS)**

For alveolar macrophages, we used  $2 \times 10^6$  cells in 200  $\mu$ L of PBS to perform acid methanolysis with methanol, toluene, and hydrochloric acid (HCl). Standards were created from a stock cholesterol standard (Avanti Polar Lipids, 700000P-100mg) and diluted with hexane. Prior to adding the acid methanolysis mix, a stigmasterol internal standard lipid was added to each sample and standard. Once the mix was added, the samples were incubated at 45°C for 8-12 hours. Then, lipids were extracted by adding 1:1 0.4M NaCl and hexane, mixing, spinning, and transferring the top layer to new tubes. This then underwent cholesterol derivatization via silylation reaction with pyridine (Sigma, 270970-100 mL) and N,O-Bis(trimethylsilyl)trifluoroacetamide with trimethylchlorosilane (BSTFA+TMCS; Supelco, 33155-4) before being run on the GC-MS machine to measure total cholesterol. The instrument settings and tuning settings are available upon request. The data was analyzed on the MassHunter software with quantitative values being normalized to cell counts.

## Statistical analysis

Results are represented as mean  $\pm$  SEM. Statistical analysis was done with GraphPad Prism 8 software. Paired t-tests were performed for comparison of two time points in an individual's clinical course. Two-way ANOVA followed by Bonferroni correction was done for comparison of three groups. N and P values are reported in the figure legends. A *P* value of  $<0.05$  was considered statistically significant.

## Results

### Alveolar macrophages from PAP patients show broad changes in lipid homeostasis

In order to define the lipid signature in alveolar macrophages, we performed whole lung lavages and/or bronchoscopy with bronchoalveolar lavage (BAL) on PAP patients and on one nonPAP patient (Table 1). The nonPAP patient had a bronchoscopy with BAL performed to evaluate for infection. Macrophages were isolated from whole lung lavage fluid by centrifugation, and lysed red blood cells were removed by subsequent centrifugation. Lipids were extracted from the enriched macrophages and analyzed by mass spectrometry.

As expected, the major lipids recovered from the macrophages of the nonPAP patient were phosphatidylcholine (PC) and phosphatidylethanolamine (PE) (Figure 1A). These cells contained lower levels of other major lipid classes, which included free fatty acid (FFA), sphingomyelin (SM), triglyceride (TAG), and cholesterol ester (CE) (Figure 1A). In contrast, analysis of alveolar macrophages from PAP patients demonstrated an overall increase in most lipid classes compared to the nonPAP patient; PC and CE were the most abundant lipid classes in the majority of PAP patients (Figure 1B-C). PC levels were increased by 50- to 140- fold in the PAP alveolar macrophages compared to the nonPAP alveolar macrophages, and CE levels were



increased by 40- to 130- fold (Figure 1B-C). In contrast, PE was only increased by 1.5- to 3- fold in the PAP macrophages (Figure 1B-C). Furthermore, total cholesterol content as measured by gas chromatography-mass spectrometry (GC-MS) was significantly elevated by 20- to 80- fold in PAP alveolar macrophages compared to the nonPAP alveolar macrophages (Figure 1D).

Unexpectedly, although the major surfactant lipid in both nonPAP and PAP patients is PC16:0/16:0, the PC species in the alveolar macrophages differed significantly; in nonPAP/control cells, the PC containing 16:0/16:0 and 16:0/18:1 fatty acids represented approximately 15% and 30% of the total cellular PC, respectively (Figure 1E) (23, 26). In contrast, in PAP cells, PC16:0/16:0 and PC16:0/18:1 represented 40-50% and 10-15% of the total cellular PC, respectively (Figure 1E). Cholesterol ester (CE) represented the other major lipid class that differed between macrophages derived from control versus PAP patients (Fig. 1B-C). The saturated (16:0) and unsaturated (18:2) fatty acids present in the CE of nonPAP cells represented approximately 10% and 40% of the total CE, respectively (Figure 1F). In contrast, the corresponding values from the PAP patient macrophages were 20-30% and 10-20% (Figure 1F). Together, these data suggest that alveolar macrophages from PAP patients can take up surfactant lipid effectively, but further metabolism/catabolism of cholesterol and fatty acid is defective.

### **Lipid profile of alveolar macrophages changes during patients' clinical courses**

Because PAP is a disease of lipid accumulation, we next determined whether the lipid profile of alveolar macrophages correlated with disease progression. Here, we provide examples of two autoimmune PAP (aPAP) patients, who were not included in the prior analyses (Table 2). The first patient, patient A, an otherwise healthy 47 year old male, was diagnosed with aPAP in

early 2014. He required 2-3 whole lung lavages per year before being initiated on inhaled GM-CSF in February 2016. After being on inhaled GM-CSF for 9 months, his clinical status improved markedly, and he has not required any additional whole lung lavages (Figure 2A). His clinical improvement was evidenced by the improvement of his lung disease on imaging. CT images were obtained at diagnosis in 2014 when the patient had received no treatment (Figure 2B, No Tx) and in 2018 after receiving multiple whole lung lavages (WLL) and inhaled GM-CSF for 33 months (Figure 2B; WLL+Tx). Improvement in lung disease was characterized by less ground glass opacifications and septal thickening on his CT scan in 2018 compared to his initial CT scan in 2014 (Figure 2B). Interestingly, his plasma GM-CSF antibody level also decreased, corresponding to the improvement in his disease; however, the level was still elevated in the abnormal range compared to healthy individuals (Figure 2C). Alveolar macrophages were obtained in 2014 shortly after diagnosis and after initiation on inhaled GM-CSF (Figure 2A; blue boxes). Lipidomics of the alveolar macrophages in 2014, shortly after diagnosis, revealed that the most abundant lipid classes included phosphatidylcholine, free fatty acid, and cholesterol ester (Figure 2D-E). The levels of these three lipids were greatly elevated compared to the corresponding levels from nonPAP alveolar macrophages. Interestingly, the overall levels of the major lipid classes in the alveolar macrophages of the patient decreased 10 months after being initiated on inhaled GM-CSF (Figure 2D-E). These data demonstrate that the macrophages present in the alveolar space after 10 months of GM-CSF have lipid profiles that are more similar to those seen in nonPAP cells, consistent with normal, or near-normal, macrophage lipid metabolism. Indeed, total cholesterol levels as measured by GC-MS were significantly decreased in his alveolar macrophages 10 months after being on inhaled GM-CSF, indicating improvement in surfactant lipid catabolism (Figure 2F). Furthermore, PC and CE species compositions were

altered in alveolar macrophages before and after GM-CSF inhalation (Figure 2G-H). The overall amount of PC and CE species significantly decreased after the patient was placed on inhaled GM-CSF (Figure 2G-H). Specifically, PC 16:0/16:0 was increased, but PC 16:0/18:1 was decreased (Figure 2G). CE16:0 and CE 18:2 species were increased, while CE18:0 and CE 18:1 species were decreased after GM-CSF initiation (Figure 2H).

In contrast, the second patient, patient B, had a much different clinical course (Figure 3A). A 34 year old female diagnosed with aPAP in late 2017, she had two whole lung lavages before developing severe hypoxic respiratory failure, requiring admission to the intensive care unit. She was initiated on inhaled GM-CSF but continued to require intermittent whole lung lavages (Figure 3A). Because of the severe nature of her disease, she received rituximab and was started on a statin (Figure 3A). Despite these interventions, the patient remained short of breath and oxygen-dependent. She was then started on pioglitazone, plasmapheresed, and received additional doses of rituximab (Figure 3A). The patient currently remains on supplemental oxygen (5-6L/min) and is awaiting lung transplantation due to declining respiratory status in spite of multiple therapies (Figure 3A). Recent CT imaging of the chest in 2020 (Figure 3B; WLL+Tx) confirmed a lack of clinical improvement with evidence of ongoing diffuse ground glass opacifications and septal thickening with new subpleural fibrotic changes when compared to her CT scan 2 years earlier following two whole lung lavages (Figure 3B; WLL). Her GM-CSF antibody levels also remained elevated despite all the interventions (Figure 3C). However, as shown in Figure 3C, her plasma GM-CSF antibody levels did decrease markedly after the physical removal of the antibodies by plasmapheresis. Interestingly, the frequency of WLL decreased following the reduction in plasma levels of antibodies to GM-CSF (Figure 3A), suggesting that plasmapheresis was effective as a temporizing measure although her overall

clinical condition has not significantly improved. Alveolar macrophages were obtained when the patient was initiated on inhaled GM-CSF and after initiation on a statin (Figure 3A; blue boxes). Analysis of the lipid profile of the patient's alveolar macrophages indicated that the most abundant lipid classes were PC and CE, which differed from both the nonPAP patient and patient A (Figure 3D-E compared with Figures 1A and 2D-E, respectively). Both total PC and CE cellular levels increased in the later timepoint of the patient's clinical course. In contrast, total macrophage cholesterol levels were only modestly increased following multiple therapies (Figure 3F). The fatty acid composition of PC and CE species in the alveolar macrophages also changed as the patient's disease progressed. In contrast to patient A where there was a decrease in most fatty acid species, the proportion of PC16:0/16:0 species decreased, while the proportion of other PC species increased (Figure 3G; pie chart). Additionally, the proportion of CE 16:0 and CE 18:1 species decreased, while CE 18:2 species increased (Figure 3H). These data are consistent with continued impaired macrophage surfactant lipid metabolism and worsening PAP disease.

### **GM-CSF antibody levels change during patients' clinical courses and correlate to disease severity**

Because it is difficult and invasive to obtain lavage fluid and analyze the lipidomics of alveolar macrophages from PAP patients, we looked for other surrogate markers that may be able to assess the disease severity. We identified a reduction in GM-CSF antibody levels in three different PAP patients who demonstrated clinical improvement, requiring less frequent whole lung lavages (Figure 4), which was similar to what we saw in patient A (Figure 2C). This

suggests that the relative level of GM-CSF antibody for an individual patient correlates to his or her disease severity, and a decline in the antibody levels is associated with clinical improvement.

## **Discussion**

This is the first report defining in depth the lipidome of PAP alveolar macrophages and examining how the lipidome changes with treatment. In comparison to the alveolar macrophages recovered from a nonPAP patient, the alveolar macrophages from all PAP patients prior to treatment exhibited increased levels of numerous lipids, including total cholesterol, PC, CE, LPC, SM and FFA. We focused on analyzing PC and CE in more detail since they displayed the most significant changes in lipidomic analyses. PC 16:0/16:0 was the predominant lipid species and enriched in the macrophages of all PAP patient samples, where it comprised around 40-50% of all PC species. In contrast, PC 16:0/16:0 represented just 15% of PC species in the nonPAP macrophages. Compared to CEs in the nonPAP macrophages, the CEs of PAP patient macrophages were also all enriched in C16:0. However, the composition of CE species varied for each patient, demonstrating the heterogeneity of the lipid accumulation in this disease.

Surprisingly, lipid profiles of alveolar macrophages in PAP have not been previously defined. However, Griese and colleagues, recently performed the first broad lipidomic analysis of bronchoalveolar lavage fluid of patients with various types of PAP (23). In this sample preparation, whole lung lavage fluid was centrifuged to remove cellular content, and the remaining lavage fluid was analyzed. They reported an overall increase of total lipid concentration within the lavage fluid recovered from the alveolar airspace with free cholesterol being increased the most by 60-fold followed by CE and PC that increased by 24-fold and 17-fold, respectively. Since lavage fluid is a mixture of surfactant, alveolar macrophages,

proteinaceous material, and other cell types and because in these latter studies, alveolar macrophages were removed prior to lipidomic analysis, it is not possible to directly compare the results of Griese et al. with those reported in the current study.

In order to determine if there was any relationship between the macrophage lipid profile and disease progression or regression, we followed the lipid profile of alveolar macrophages throughout the treatment course of individual PAP patients. We noted that the absolute abundance of lipids, specifically PC and CE, correlated with disease severity. Alveolar macrophage PC, CE and total cholesterol levels decreased by 13%, 47% and 37%, respectively, in one autoimmune PAP patient who had clinical improvement in his lung disease after being initiated on inhaled GM-CSF. In contrast, a second patient who failed to improve clinically but rather exhibited progression and worsening of lung disease despite initiation of various experimental therapies, exhibited a 2-fold increased levels of PC and CE in her alveolar macrophages. Additional studies will be required to determine if the alveolar macrophage lipidome or a specific combination of lipids could be used as a biomarker to determine severity of disease.

Notably, it is challenging, expensive, and invasive to obtain lavage fluid and evaluate the lipid profile of alveolar macrophages from PAP patients. Therefore, we sought to find alternative approaches to assess disease severity since there are no specific validated biomarkers currently available for PAP. We analyzed anti-GM-CSF antibody levels in our autoimmune PAP patients and discovered that the patient with clinical improvement also had a reduction in his anti-GM-CSF antibody titer. Consistent with unremitting PAP disease, the patient with progressive and worsening disease did not show a decline in anti-GM-CSF antibody level until she underwent plasmapheresis to physically remove circulating antibodies. Interestingly, after plasmapheresis,

the patient did require less frequent whole lung lavages. Prior studies have suggested that there is no significant correlation between serum levels of anti-GM-CSF antibody and disease severity among cohorts of PAP patients (27-30). Seymour and colleagues reported an overall decrease in anti-GM-CSF antibody levels in patients who received subcutaneous GM-CSF treatment regardless of their response to treatment. Response was defined as greater than or equal to 50% improvement in A-a gradient,  $T_{LCO}$ , and/or radiographically defined volume of pulmonary abnormalities. Interestingly, there was a trend for having a larger difference in the change in anti-GM-CSF antibody level before and after therapy in responders versus non-responders (median change = -90  $\mu\text{g/mL}$  vs -60  $\mu\text{g/mL}$ , respectively), consistent with our observations (27). More studies that follow autoimmune PAP patients with different clinical courses and on different therapies longitudinally will be needed to see if there is a true relationship between the anti-GM-CSF antibody levels and the disease process in individual patients.

In conclusion, here, we define the first detailed report of the lipidome of PAP alveolar macrophages. We report that PC and CE are the most abundant lipid classes in PAP alveolar macrophages. While PC(16:0/16:0) is the predominant PC species in all PAP patients, the most abundant CE species varies for each patient, demonstrating the heterogenous nature of the disease. Furthermore, increased concentrations of PC and CE in alveolar macrophages appear to correlate with more severe or progressive PAP disease. Our recent study demonstrated that treatment of a subset of PAP patients with statins led to a remarkable improvement in their clinical symptoms (15). Whether statins affect the macrophage CE species in the responsive patients is currently unknown. Elucidation of the lipidome in PAP, particularly from patients on different therapies, will provide further insight into the pathogenesis of PAP, assist in

discovering new biomarkers to predict severity of disease and response to treatment, and identify novel therapeutic targets.

### **Acknowledgement/grant support**

We would like to thank members of the Tarling and Vallim lab for critical and thoughtful discussion. We thank Dr. Peter Edwards for review and comment of the manuscript. EL is supported by HL072752 and HL007895. BCT is supported by HL085453 and HL118342. TQdeAV is supported by HL122677, DK119112, and DK118064. EJT is supported by HL116181, HL136543, HL122677, HL152156, and UL1TR001881.



## FIGURE LEGENDS

**Figure 1. High-resolution lipidomic profiling reveals an overall increase of all lipid classes in alveolar macrophages of PAP patients compared to nonPAP patients with phosphatidylcholine and cholesterol ester being the most abundant lipid classes in the majority of PAP patients.**

All of the analysis was done on an ABSciex Lipidyzer Platform. (a) The quantitative measurement of lipid classes (nmol/10<sup>7</sup> cells) in the alveolar macrophage of a nonPAP patient. (b) The quantitative measurement of lipid classes (nmol/10<sup>7</sup> cells) in the alveolar macrophages of PAP patients compared to a nonPAP patient. (c) The quantitative measurement of the most abundant lipid classes (nmol/10<sup>7</sup> cells) apart from phosphatidylcholine in the alveolar macrophages of PAP patients compared to a nonPAP patient. (d) Total cholesterol content (nmol/10<sup>6</sup> cells) measured by GC/MS in the alveolar macrophages of PAP patients compared to a nonPAP patient. (e) Lipid measurement of the most abundant PC species (nmol/10<sup>7</sup> cells), including PC(16:0/14:0), PC(16:0/16:0), PC(16:0/16:1), PC(16:0/18:0), PC(16:0/18:1), PC(16:0/18:2), and PC(16:0/20:4), in alveolar macrophages from PAP patients compared to nonPAP patient. Compositional analysis of PC species of alveolar macrophages from PAP patients compared nonPAP patient. (f) Lipid measurement of the most abundant CE species (nmol/10<sup>7</sup> cells), including CE(14:0), CE(16:0), CE(16:1), CE(18:0), CE(18:1), CE(18:2), and CE(20:4), in alveolar macrophages from PAP patients compared to nonPAP patient. All samples are run in duplicate or triplicate. Data are mean ± SEM. CE = cholesterol esters; CER= ceramides; DCER= dihydroceramides; DAG= diacylglycerols (DAG); FFA= free fatty acids; HCER= hexosylceramides; LCER= lactosylceramides; LPC= lysophosphatidylcholines; LPE=

lysophosphatidylethanolamines; PC= phosphatidylcholines; PE= phosphatidylethanolamines; SM= sphingomyelins; TAG= triacylglycerols.

**Figure 2. There is a decreased amount of phosphatidylcholine and cholesterol ester in the alveolar macrophages of PAP patient who have received therapy, which appears to be related to improving disease.**

(a) Clinical course of a 47 year old patient with an improvement in disease after being initiated on inhaled GM-CSF. Red stars indicate whole lung lavages that were performed at UCLA. Green triangles denote when CT chest scans were taken and shown in part b. Boxes represent whole lung lavages used for analysis in parts d-g. (b) CT chest scans of the patient at the time of presentation to UCLA (March 2014) and after inhaled GM-CSF therapy (November 2018). Red stars indicate ground glass opacities, and red arrowheads indicate septal thickening. (c) GM-CSF antibody levels (mcg/mL) measured throughout patient's clinical course. (d and e) Two representations of the quantitative measurement of lipid classes (nmol/10<sup>7</sup> cells) in alveolar macrophages of the patient before and after initiation of inhaled GM-CSF. (f) Total cholesterol content (nmol/10<sup>6</sup> cells) measured by GC/MS before and after patient has been on inhaled GM-CSF. (g and h) Lipid measurement of the most abundant PC species (nmol/10<sup>7</sup> cells) (g) and of the most abundant CE species (nmol/10<sup>7</sup> cells) (h) in alveolar macrophages of the patient before and after being placed on inhaled GM-CSF. Samples are run in triplicate. Data are mean ± SEM. Statistical significance determined by student's t test. \* p<0.05, \*\* p<0.01, \*\*\* p<0.001, \*\*\*\* p<0.0001. WLL= whole lung lavage; Tx = treatment, which includes inhaled GM-CSF. CE = cholesterol esters; CER= ceramides; DCER= dihydroceramides; DAG= diacylglycerols (DAG); FFA= free fatty acids; HCER= hexosylceramides; LCER= lactosylceramides; LPC=

lysophosphatidylcholines; LPE= lysophosphatidylethanolamines; PC= phosphatidylcholines; PE= phosphatidylethanolamines; SM= sphingomyelins; TAG= triacylglycerols.

**Figure 3. There is an increased amount of phosphatidylcholine and cholesterol ester in the alveolar macrophages of PAP patient despite receiving therapy, which appears to be associated with worsening, unremitting disease.**

(a) Clinical course of a 34 year old patient with worsening PAP disease and unresolving hypoxia despite multiple therapies. Stars indicate whole lung lavages. Red stars indicate whole lung lavages that were performed at UCLA. Green triangles denote when CT chest scans were taken and shown in part b. Boxes represent when the whole lung lavages from patients were used for analysis in parts d-g. (b) CT chest scans of the patient at the time of presentation to UCLA (April 2018) and after multiple therapies (January 2020). Red stars indicate ground glass opacities, and red arrowheads indicate septal thickening. (c) GM-CSF antibody levels (mcg/mL) measured throughout patient's clinical course. (d and e) Two representations of the quantitative measurement of lipid classes (nmol/10<sup>7</sup> cells) in alveolar macrophages of the patient before and after being initiated on multiple therapies. (f) Total cholesterol content (nmol/10<sup>6</sup> cells) measured by GC/MS before and after being started on multiple therapies. (g and h) Lipid measurement of the most abundant PC species (nmol/10<sup>7</sup> cells) (g) and of the most abundant CE species (nmol/10<sup>7</sup> cells) (h) in alveolar macrophages of the patient before and after being placed on multiple therapies. Samples are run in duplicate (samples from only whole lung lavage) or triplicate (samples after patient has been initiated on multiple therapies). Data are mean ± SEM. Statistical significance determined by student's t test. \* p<0.05, \*\* p<0.01, \*\*\* p<0.001, \*\*\*\* p<0.0001. WLL= whole lung lavage; Tx = treatment, which includes inhaled GM-CSF, statin,

pioglitazone, rituximab, and plasmapheresis. CE = cholesterol esters; CER= ceramides; DCER= dihydroceramides; DAG= diacylglycerols (DAG); FFA= free fatty acids; HCER= hexosylceramides; LCER= lactosylceramides; LPC= lysophosphatidylcholines; LPE= lysophosphatidylethanolamines; PC= phosphatidylcholines; PE= phosphatidylethanolamines; SM= sphingomyelins; TAG= triacylglycerols.

**Figure 4. A decline in GM-CSF antibody levels correlates with clinical improvement in PAP patients.**

(a) Clinical course of a 21 year old patient who had improvement in PAP disease after being initiated on inhaled GM-CSF therapy. Stars indicate whole lung lavages. (b) GM-CSF antibody levels (mcg/mL) measured throughout patient's clinical course. (c) Clinical course of a 60 year old patient who had improvement in PAP disease after being initiated on statin therapy. Stars indicate whole lung lavages. (d) GM-CSF antibody levels (mcg/mL) measured throughout patient's clinical course. (e) Clinical course of a 66 year old patient who had worsening of PAP disease after being taken off of statin and then improvement in PAP disease after being re-initiated on statin therapy and given a dose of rituximab. Stars indicate whole lung lavages. Red stars indicate whole lung lavages that were performed at UCLA. (f) GM-CSF antibody levels (mcg/mL) measured throughout patient's clinical course. Stars indicate whole lung lavages. WLL= whole lung lavage. Rx= treatment, which includes statin.

Figure 1

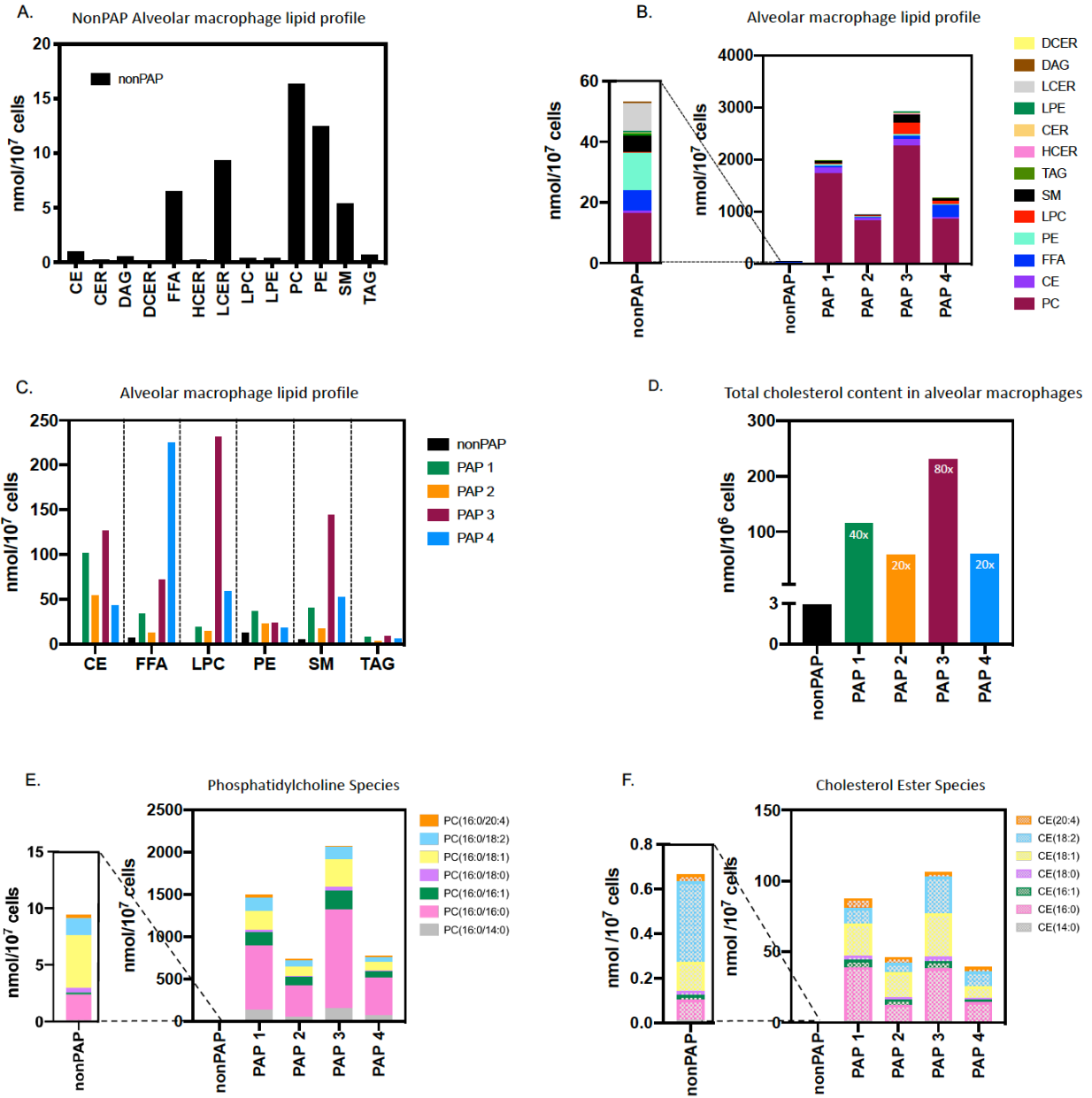


Figure 2

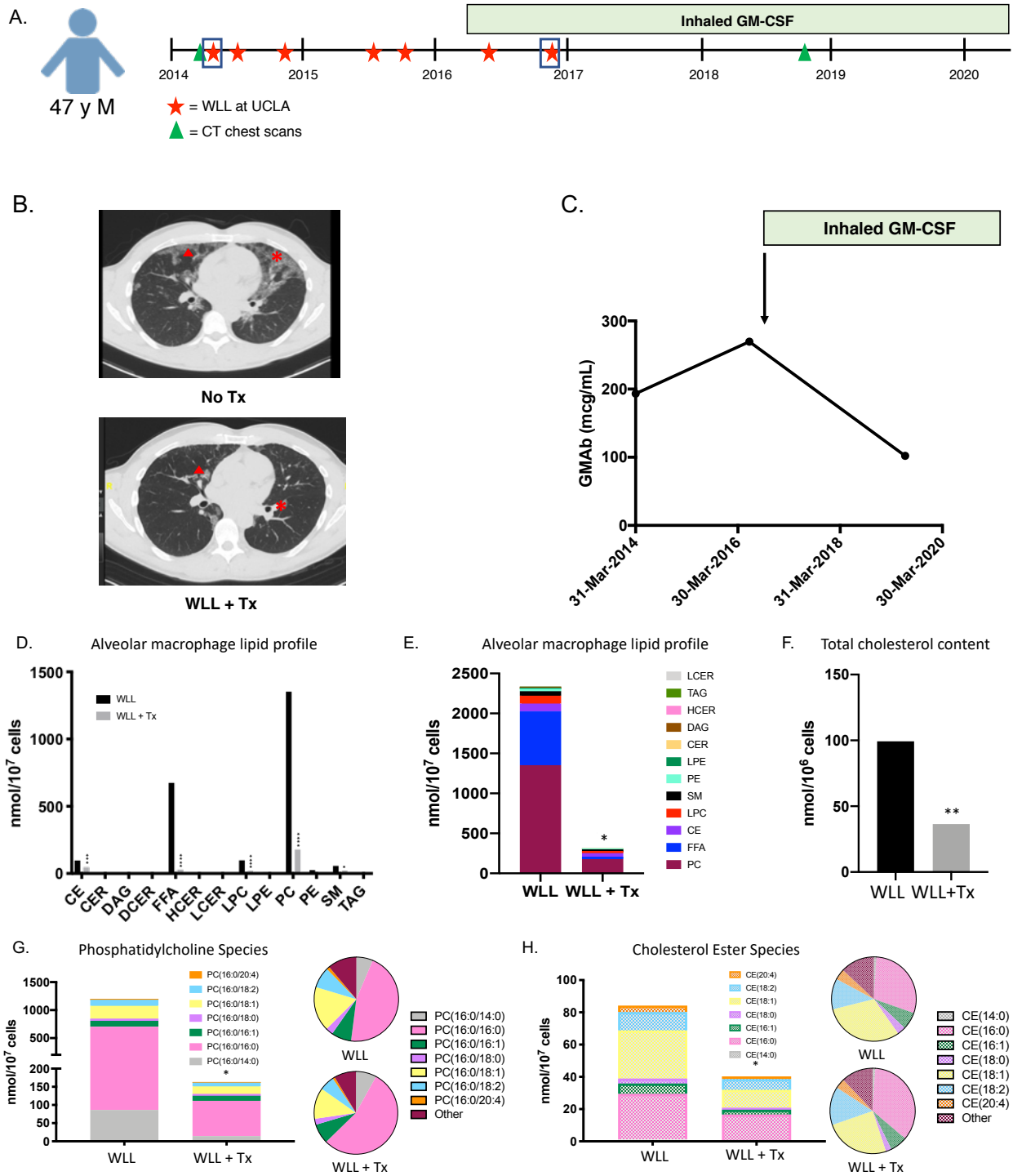


Figure 3

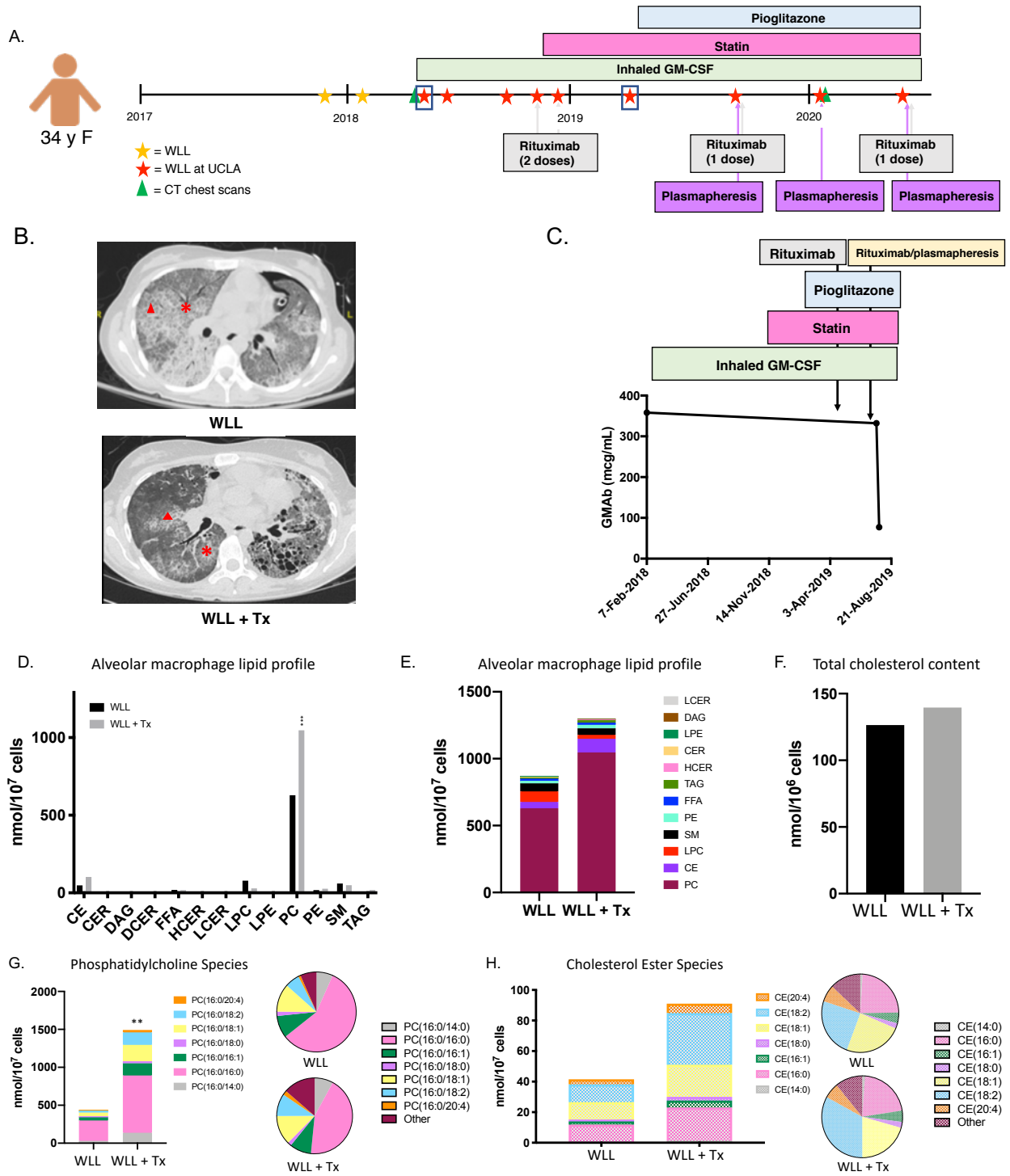


Figure 4

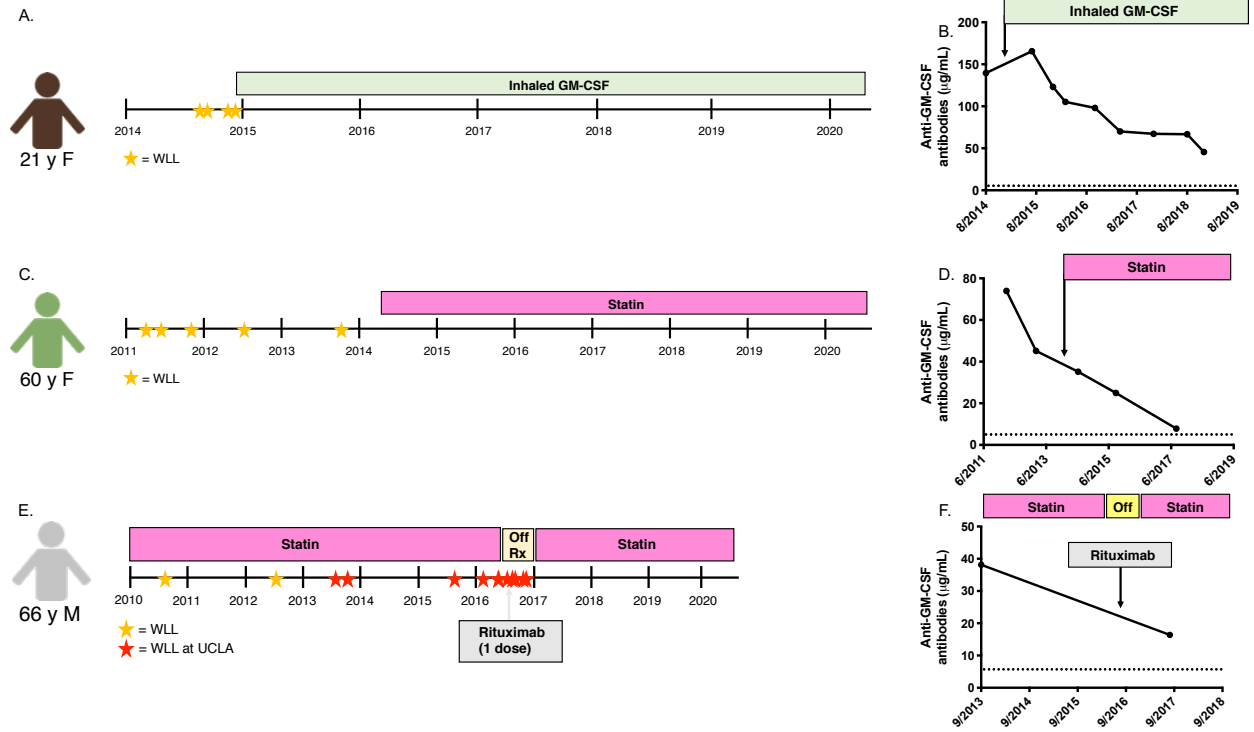




Table 1. Baseline characteristics of nonPAP and 4 individual PAP patients.

| Characteristics       | NonPAP                | PAP patient 1      | PAP patient 2         | PAP patient 3      | PAP patient 4         |
|-----------------------|-----------------------|--------------------|-----------------------|--------------------|-----------------------|
| Age                   | 61 yo                 | 28 yo              | 55 yo                 | 66 yo              | 50 yo                 |
| Sex                   | Male                  | Female             | Female                | Male               | Male                  |
| Race and ethnic group | White                 | Black              | Black                 | Asian              | Black                 |
| Body-mass index       | 25-29.9               | 25-29.9            | ≥40                   | 18.5-24.9          | 25-29.9               |
| Imaging               | No pulmonary fibrosis | Pulmonary fibrosis | No pulmonary fibrosis | Pulmonary fibrosis | No pulmonary fibrosis |
| Insurance             | Commercial            | Commercial         | Commercial            | Commercial         | Commercial            |
| Smoking status        | Never smoker          | Never smoker       | Never smoker          | Never smoker       | Never smoker          |
| Co-morbidities        |                       |                    |                       |                    |                       |
| Hyperlipidemia        | No                    | No                 | Yes                   | Yes                | Yes                   |
| Hypertension          | No                    | Yes                | Yes                   | Yes                | Yes                   |
| Diabetes              | No                    | No                 | No                    | Yes                | Yes                   |
| Cancer                | No                    | No                 | No                    | No                 | No                    |

Table 2. Baseline characteristics of patients with autoimmune PAP on various experimental therapies.

| Characteristics       | Patient A             | Patient B          |
|-----------------------|-----------------------|--------------------|
| Age                   | 47 yo                 | 34 yo              |
| Sex                   | Male                  | Female             |
| Race and ethnic group | Non-Hispanic white    | Hispanic           |
| Body-mass index       | 18.5-24.9             | 18.5-24.9          |
| Imaging               | No pulmonary fibrosis | Pulmonary fibrosis |
| Insurance             | Commercial            | Medicaid           |
| Smoking status        | Never smoker          | Never smoker       |
| Co-morbidities        |                       |                    |
| Hyperlipidemia        | No                    | No                 |
| Hypertension          | No                    | No                 |
| Diabetes              | No                    | No                 |
| Cancer                | No                    | No                 |

## References

1. Trapnell BC, Whitsett JA, Nakata K. Pulmonary Alveolar Proteinosis. *N Engl J Med*. 2003;349:2527-39.
2. Trapnell BC, Nakata K, Bonella F, Campo I, Griese M, Hamilton J, et al. Pulmonary alveolar proteinosis. *Nat Rev Dis Primers*. 2019;5(1).
3. Hamilton JA. GM-CSF in inflammation and autoimmunity. *Trends Immunol*. 2002;23(8):403-8.
4. Guilliams M, De Kleer I, Henri S, Post S, Vanhoutte L, De Prijck S, et al. Alveolar macrophages develop from fetal monocytes that differentiate into long-lived cells in the first week of life via GM-CSF. *J Exp Med*. 2013;210(10):1977-92.
5. Thomassen MJ, Barna BP, Malur AG, Bonfield TL, Farver CF, Malur A, et al. ABCG1 is deficient in alveolar macrophages of GM-CSF knockout mice and patients with pulmonary alveolar proteinosis. *J Lipid Res*. 2007;48(12):2762-8.
6. Robb L, Drinkwater CC, Metcalf D, Li R, Kontgen F, Nicola NA, et al. Hematopoietic and lung abnormalities in mice with a null mutation of the common beta subunit of the receptors for granulocyte-macrophage colony-stimulating factor and interleukins 3 and 5. *Proc Natl Acad Sci USA*. 1995;92(21):9565-9.
7. Suzuki T, Shima K, Arumugam P, Ma Y, Black D, Chalk C, et al. Development and validation of *Csf2ra* gene-deficient mice as a clinically relevant model of children with hereditary pulmonary alveolar proteinosis. *Am J Respir Crit Care Med*. 2017;195:A4837.
8. Arumugam P, Suzuki T, Shima K, McCarthy C, Sallese A, Wessendarp M, et al. Long-Term Safety and Efficacy of Gene-Pulmonary Macrophage Transplantation Therapy of PAP in *Csf2ra*<sup>-/-</sup> Mice. *Mol Ther*. 2019;27(9):1597-611.
9. Suzuki T, Arumugam P, Sakagami T, Lachmann N, Chalk C, Sallese A, et al. Pulmonary macrophage transplantation therapy. *Nature*. 2014;514(7523):450-4.
10. Lopez-Rodriguez E, Gay-Jordi G, Mucci A, Lachmann N, Serrano-Mollar A. Lung surfactant metabolism: early in life, early in disease and target in cell therapy. *Cell Tissue Res*. 2017;367(3):721-35.
11. Griese M. Pulmonary surfactant in health and human lung diseases: state of the art. *Eur Respir J*. 1999;13(6):1455-76.
12. Ikegami M, Ueda T, Hull W, Whitsett JA, Mulligan RC, Dranoff G, et al. Surfactant metabolism in transgenic mice after granulocyte macrophage-colony stimulating factor ablation. *Am J Physiol*. 1996;270(4 Pt 1):L650-8.

13. Pison U, Wright JR, Hawgood S. Specific binding of surfactant apoprotein SP-A to rat alveolar macrophages. *Am J Physiol.* 1992;262:L412-7.
14. Sallese A, Suzuki T, McCarthy C, Bridges J, Filuta A, Arumugam P, et al. Targeting cholesterol homeostasis in lung diseases. *Sci Report.* 2017;7(1):10211-4.
15. McCarthy C, Lee E, Bridges JP, Sallese A, Suzuki T, Woods JC, et al. Statin as a novel pharmacotherapy of pulmonary alveolar proteinosis. *Nat Commun.* 2018;9(1):3127.
16. Cavelier C, Lorenzi I, Rohrer L, von Eckardstein A. Lipid efflux by the ATP-binding cassette transporters ABCA1 and ABCG1. *Biochim Biophys Acta.* 2006;1761(7):655-66.
17. Baldan A, Tarr P, Vales CS, Frank J, Shimotake TK, Hawgood S, et al. Deletion of transmembrane transporter ABCG1 results in progressive pulmonary lipidosis. *J Biol Chem.* 2006;281:29401-10.
18. Bonfield TL, Farver CF, Barna BP, Malur A, Abraham S, Raychaudhuri B, et al. Peroxisome proliferator-activated receptor-gamma is deficient in alveolar macrophages from patients with alveolar proteinosis. *Am J Respir Cell Mol Biol.* 2003;29(6):677-82.
19. Kennedy MA, Barrera GC, Nakamura K, Baldan A, Tarr P, Fishbein MC, et al. ABCG1 has a critical role in mediating cholesterol efflux to HDL and preventing cellular lipid accumulation. *Cell Metab.* 2005;1(2):121-31.
20. de Aguiar Vallim TQ, Lee E, Merriott DJ, Goulbourne CN, Cheng J, Cheng A, et al. ABCG1 regulates pulmonary surfactant metabolism in mice and men. *J Lipid Res.* 2017;58(5):941-54.
21. Uchida K, Nakata K, Carey B, Chalk C, Suzuki T, Sakagami T, et al. Standardized serum GM-CSF autoantibody testing for the routine clinical diagnosis of autoimmune pulmonary alveolar proteinosis. *J Immunol Methods.* 2014;402(1-2):57-70.
22. Baldán A, Gomes AV, Ping P, Edwards PA. Loss of ABCG1 results in chronic pulmonary inflammation. *J Immunol.* 2008;180(5):3560-8.
23. Griese M, Bonella F, Costabel U, de Blic J, Tran NB, Liebisch G. Quantitative lipidomics in pulmonary alveolar proteinosis. *Am J Respir Crit Care Med.* 2019;200(7):881-7.
24. Bligh EG, Dyer WJ. A rapid method of total lipid extraction and purification. *Can J Biochem Physiol.* 1959;37(8):911-7.
25. Contrepois K, Mahnoudi S, Ubhi BK, Papsdorf K, Hornburg D, Brunet A, et al. Cross-platform comparison of untargeted and targeted lipidomics approaches on aging mouse plasma. *Sci Rep.* 2018;8(1):17747.

26. Veldhuizen R, Nag K, Orgeig S, Possmayer F. The role of lipids in pulmonary surfactant. *Biochim Biophys Acta*. 1998;1408(2-3):90-108.
27. Seymour JF, Doyle IR, Nakata K, Presneill JJ, Schoch OD, Hamano E, et al. Relationship of anti-GM-CSF antibody concentration, surfactant protein A and B levels, and serum LDH to pulmonary parameters and response to GM-CSF therapy in patients with idiopathic alveolar proteinosis. *Thorax*. 2003;58(3):252-7.
28. Arai T, Hamano E, Inoue Y, Tazawa R, Nukiwa T, Sakatani M, et al. Serum neutralizing capacity of GM-CSF reflects disease severity in a patient with pulmonary alveolar proteinosis successfully treated with inhaled GM-CSF. *Respir Med*. 2004;98(12):1227-30.
29. Lin FC, Chang GD, Chern MS, Chen YC, Chang SC. Clinical significance of anti-GM-CSF antibodies in idiopathic pulmonary alveolar proteinosis. *Thorax*. 2006;61(6):528-34.
30. Inoue Y, Trapnell BC, Tazawa R, Arai T, Takada T, Hizawa N, et al. Characteristics of a large cohort of patients with autoimmune pulmonary alveolar proteinosis in Japan. *Am J Respir Crit Care Med*. 2008;177(7):752-62.

## **CHAPTER 5**

### **Conclusion**

## **The study of PAP has led to important discoveries**

A disease is labeled as “rare” if it has a prevalence of <200,000 persons in America. Using this definition, there is an estimate of over 7000 rare diseases that affect an estimated 25-30 million people in the US (1). Because of their low prevalence, rare diseases have often been neglected and deemed less economical to study than more common diseases. Therefore, it is often challenging to generate interest and acquire funding for rare diseases. It is also difficult to recruit large numbers of patients to studies involving rare diseases and obtain samples. Contrary to the popular misconception that the study of rare diseases has low impact, research on rare diseases has provided many insights into common disorders and the human body as a whole. This holds true for PAP.

PAP is a rare lung disorder that occurs due to the accumulation of pulmonary surfactant in the alveolar space due to a disruption in GM-CSF signaling. There is currently no FDA-approved therapy or cure. In the past, GM-CSF was thought to be an important hematopoietic growth factor that stimulates the survival, proliferation, and differentiation of myeloid cells and their precursors (2). Recent studies have shown that GM-CSF is more than simply a hematopoietic growth factor. The development of GM-CSF-deficient mice models has elucidated the importance of GM-CSF in surfactant homeostasis, which is critical for proper lung physiology and protection from infection. These mice were found to have accumulation of surfactant in the alveolar space; interestingly, they did not have any major perturbation of hematopoiesis (3). This was also true of mice deficient in the GM-CSF receptor (4, 5). These results suggested that surfactant catabolism required GM-CSF, particularly in alveolar macrophages, and led to extensive research on the role of GM-CSF signaling in alveolar macrophages. GM-CSF has been identified as a key regulator of alveolar macrophage

maturation, self-renewal, and population (6, 7). In the absence of GM-CSF signaling, the alveolar macrophages have impairment in their ability to self-maintain, mature, and catabolize surfactant as well as to phagocytose organisms and release reactive oxygen species (7-9). Interestingly, surfactant uptake was unaffected by the lack of GM-CSF (10, 11). Many advances have been made in the field of lung lipid biology due to the discovery and understanding of PAP. However, much still remains to be discovered.

### **A dysregulation in phospholipid and cholesterol metabolism leads to PAP**

In the past, there was a widely-held belief that the accumulation of surfactant in PAP was due to the impaired catabolism of phospholipids in alveolar macrophages. Early studies demonstrated an increased content of total lipid and phospholipid in the lung tissue and BAL washings from patients with PAP compared to patients without this disease; however, the relative proportions of the phospholipid and fatty acids were similar in the non-PAP and PAP patient groups (12). Furthermore, there was no difference in phospholipid synthesis by the lung between non-PAP and PAP patients based on radiolabeled palmitic acid experiments, but there was delayed dissipation of radiolabeled phospholipid in the washings from PAP patients compared to the non-PAP patients, thus suggesting that there was an impairment in the removal or degradation of alveolar phospholipid. This was also demonstrated in GM-CSF-deficient mice (10). Therefore, it was thought that PAP resulted from impaired clearance of phospholipids; however, such mechanism has yet to be identified (10, 12, 13).

More recent studies have suggested that a disruption in cholesterol homeostasis underlies the pathogenesis of PAP. Salles and colleagues demonstrated that alveolar macrophages from GM-CSF-deficient mice had markedly increased levels of free and esterified cholesterol and



minimally increased levels of phospholipid compared to WT mice, which was determined by thin-layer chromatography and colorimetric assay (14). The relative proportion of cholesterol was elevated in the surfactant of GM-CSF-deficient mice, while the relative composition of PC, which is the predominant phospholipid class in surfactant, remained the same between WT and GM-CSF-deficient mice. Furthermore, the addition of PAP patient-derived surfactant to BMDM from WT and GM-CSF-deficient mice led to higher levels of total, free, and esterified cholesterol in the macrophages of GM-CSF-deficient mice. There was marked impairment of cholesterol clearance in the macrophages of the GM-CSF-deficient mice. Other studies have also shown that PAP alveolar macrophages have abnormal expression of ABCA1, ABCG1, and PPAR $\gamma$ , important mediators in cholesterol transport in macrophages (15-17). This suggests that a dysregulation in cholesterol metabolism, possibly due to a defect in cholesterol clearance in alveolar macrophages, leads to PAP.

To evaluate this novel paradigm, we decided to further explore the role of ABCG1, a known lipid transporter involved in cholesterol efflux which has been shown to be downregulated in patients with PAP (16). Previous studies using ABCG1 whole body knockout mice demonstrated a build-up of lipid-laden, foamy alveolar macrophages and large type 2 epithelial cells filled with lamellar bodies (LB) as well as extracellular lipid accumulation within the lungs (18-20). Because both alveolar macrophages and type 2 epithelial cells are involved in surfactant homeostasis and because they both express ABCG1, we created macrophage-specific and type 2 epithelial cell-specific ABCG1-deficient mice (*Abcg1<sup>MAC-KO</sup>* and *Abcg1<sup>T2-KO</sup>*, respectively) to evaluate each cell's role in the development of pulmonary lipidosis and in surfactant homeostasis. As expected, *Abcg1<sup>MAC-KO</sup>* mice had large, foamy alveolar macrophages with increased lipid deposition in the lungs compared to *Abcg1<sup>fllox/fllox</sup>* mice. Interestingly, there

was also an increase in the number of type 2 epithelial cells, but these type 2 epithelial cells were enlarged with increased amount of LB within the cells, suggesting that alveolar macrophages may be modulating type 2 epithelial cells and their role in surfactant metabolism (21).

*Abcg1*<sup>T2-KO</sup> mice also demonstrated an increase in the number of type 2 epithelial cells with increased amount of LB within these cells in the lungs compared to *Abcg1*<sup>flox/flox</sup> mice; however, the alveolar macrophages appeared normal. Further, the lipid content of surfactant was altered with increased levels of PC, CE, and total cholesterol, thus suggesting that ABCG1 may be playing an important role in type 2 epithelial cells to maintain surfactant homeostasis. Even though the alveolar macrophages appear normal in the *Abcg1*<sup>T2-KO</sup> mice, it remains unclear whether or not their ability to clear surfactant is impacted, thus contributing to the changes seen in the lipid content of surfactant. Together, our data suggest that an important communication between alveolar macrophages and type 2 epithelial cells exist and is integral to maintain surfactant homeostasis. More studies need to be done to elucidate the connection between these two cells.

We also decided to examine the cholesterol content in the alveolar macrophages and BAL fluid of PAP patients, because prior studies were mostly done in mouse models. Cholesterol, measured by thin-layer chromatography and colorimetric assay, was the predominant material accumulating in the alveolar macrophages and was associated with an increase in the ratio of cholesterol to phospholipids in pulmonary surfactant (22). Additionally, we treated *Csfrb*<sup>2-/-</sup> mice with statin, an already available medication known to decrease plasma cholesterol by inhibiting HMG-CoA reductase, the rate limiting enzyme of cholesterol synthesis, and found a reduction of cholesterol levels in alveolar macrophages as well as lavage fluid. These mice also had improvement in their lung disease, which was shown by a decrease in BAL

fluid turbidity, a marker that has been shown to reflect disease severity in mice (23). Excitingly, we were also able to identify PAP patients who were started on a statin for dyslipidemia and found to have improvement in their disease based on their improvement in symptoms and imaging, lack of need for oxygen, and no longer requiring whole lung lavage therapies. We were also able to demonstrate that their alveolar macrophages had a reduction in cholesterol levels after statin therapy. Furthermore, we were able to show that statin increased cholesterol efflux in the PAP alveolar macrophages by ultimately increasing the expression of ABCA1 and ABCG1, the two lipid transporters involved in cholesterol efflux. Our discovery supports the feasibility of statin as a new pharmacotherapy for PAP patients; however, clinical trials need to be done to evaluate the efficacy and safety of statin in these patients. Additionally, we may be able to measure cholesterol in BAL fluid as an adjunct to imaging for patients who are undergoing evaluation for PAP and minimize the need for lung biopsy. Our data support the hypothesis that impaired cholesterol clearance in alveolar macrophages is driving PAP pathophysiology.

After demonstrating the importance of cholesterol homeostasis in PAP, we wanted to investigate the lipidome of PAP alveolar macrophages to not only further corroborate this novel paradigm but also identify other lipids that may be contributing to the disease pathology. We were able to utilize mass spectrometry, a sophisticated and sensitive technology that enables us to quantify over 600 lipid species, to evaluate the lipid composition of alveolar macrophages in PAP. Surprisingly, the lipid profiles of PAP alveolar macrophages have not been previously defined. Griese and colleagues did recently perform the first broad lipidomic analysis on the lavage fluid of patients with various types of PAP and demonstrated an overall increase of total lipid concentration within the lavage fluid; however, the alveolar macrophages were removed prior to their analysis (24). In comparison to the alveolar macrophages from a non-PAP patient,

the alveolar macrophages from PAP patients had an overall marked increase in the lipid content. PC and CE were the most abundant lipid classes in the majority of patients. Additionally, total cholesterol content, as measured by GC-MS, was significantly elevated in the PAP alveolar macrophages compared to the non-PAP alveolar macrophages. These data suggest that PAP alveolar macrophages can take up surfactant lipid effectively; however, metabolism of cholesterol and fatty acid may be defective. We also examined the lipid profile of alveolar macrophages throughout patients' clinical courses to see if it reflects patients' disease severity. Levels of PC and CE decreased in the alveolar macrophages of a PAP patient who had improvement in his clinical disease after being started on inhaled GM-CSF. In contrast, levels of PC and CE increased in the alveolar macrophages of a PAP patient who has progressing disease despite multiple therapies and is currently undergoing lung transplant evaluation. The absolute abundance of PC and CE appears to correlate with disease severity, but additional studies need to be done to see if the alveolar macrophage lipidome or a specific combination of lipids could be used as a biomarker to determine severity of disease. Further, our analysis of the PAP alveolar macrophage lipidome suggests that both phospholipid and cholesterol are playing important roles in the pathogenesis of PAP, not just one or the other; they were the most abundant lipid classes in the PAP alveolar macrophages, and a reduction in both phospholipid and cholesterol content led to disease improvement in clinical setting. More studies need to be done to investigate the mechanisms underlying the dysregulation of phospholipid and cholesterol metabolism that leads to impaired surfactant clearance in PAP.

## **Future directions**

Our data suggest that a disruption in both phospholipid and cholesterol homeostasis leads to surfactant accumulation in PAP. We have demonstrated that PC and CE species are the predominant lipid classes in PAP alveolar macrophages. Additionally, increased concentrations of PC, CE, and total cholesterol appeared to correlate with more severe or progressive disease. We plan to repeat this analysis on more non-PAP and PAP patients to validate our current findings. This will also enable us to better understand the heterogeneity of the disease and see if a specific lipid or combination of lipids could be used as a biomarker to determine severity of disease or response to treatment. Because lavage samples can be challenging, invasive, and expensive to obtain, we will also examine the lipid content of non-PAP and PAP patients' plasma to see if there is a particular lipid or a combination of lipids that could be used as a surrogate marker to correlate disease severity or response to therapy. PC 16:0/22:6 and PC 18:0/22:6 have been found to be significantly elevated in the plasma of GM-CSF knockout mice compared to control mice; however, this has not yet been studied in patients (25).

Although the majority of PAP patients have a good prognosis of  $94\% \pm 2\%$  survival rate at 5 years with WLL therapy, about 20% of PAP patients develop fibrosis that can lead to end-stage lung disease and ultimately death (26, 27). There is currently no assay or biomarker available that can identify which patients will develop fibrosis. We will divide the PAP patients into groups with or without fibrosis and analyze the lipid profile of their alveolar macrophages and BAL fluid to see if a difference exists between the groups (27). In our preliminary analysis of lung tissue from patients with and without idiopathic pulmonary fibrosis, a different, more common pulmonary condition that results in lung scarring for an unknown reason, we have noticed that there is a larger amount of triglycerides in patients with fibrosis; however, we have

not seen that trend in our PAP patients who develop fibrosis compared to those who do not develop fibrosis. We did see that PAP patients with fibrosis had higher amounts of CE in their alveolar macrophages compared to PAP patients without fibrosis. We also want to measure oxidized lipids in these patients, because prior studies have shown how they may play a role in driving fibrosis in the lungs (28, 29). One study demonstrated an increased amount of oxidized phosphatidylcholine (oxPC) in the alveolar macrophages and BAL fluid of mice that underwent bleomycin-induced fibrosis (28). The direct instillation of oxPC into mouse lung stimulated foam cell formation and initiated a fibrotic response. Further, the deletion of ABCG1 in mice that were treated with bleomycin resulted in an increase in the size of the foamy macrophages and exacerbation of lung fibrosis (28). Treating with GM-CSF decreased the lipid accumulation within the alveolar macrophages and attenuated the fibrotic response. Additionally, our lab has shown in the past that *Abcg1*<sup>-/-</sup> mice accrued oxidized lipids in the lungs (30). These mice also develop fibrosis in their lungs (unpublished data). If we are able to identify a certain quantity and/or a specific set of oxidized lipids associated with patients who develop fibrosis, especially in the BAL fluid of patients prior to the development of fibrosis, we may be able to utilize it in the clinical setting to predict who might develop fibrosis. By identifying this set of patients sooner, we may be able to intervene more aggressively with more frequent whole lung lavages to remove these lipids or even start patients on anti-fibrotic therapies sooner to halt or slow down the progression of their disease. Our findings may also provide insight into the mechanism of more common pulmonary diseases, such as idiopathic pulmonary fibrosis, or other medical conditions, like sarcoidosis and rheumatoid arthritis, where patients have the potential to develop pulmonary fibrosis, and help identify novel therapeutic strategies for these other disease processes.

Much of the research on PAP has been focused on the clearance of surfactant by the alveolar macrophages. This may be due to the fact that *Csf2rb*<sup>-/-</sup> mice had reversal of their PAP phenotype after WT bone marrow transplantation or after instillation of WT bone-marrow-derived macrophages into the lungs, suggesting that the lack of GM-CSF in alveolar macrophages is responsible for PAP (23, 31). However, our lab has shown that *Abcg1*<sup>-/-</sup> mice, which develop an age-dependent pulmonary lipidosis, not only have an increase in lipid deposition in alveolar macrophages but also an increase in lamellar body and lipid content in type 2 epithelial cells (20). This was also true in macrophage-specific-ABCG1-deficient mice, suggesting that alveolar macrophage-type 2 epithelial cross talk may be influencing type 2 epithelial cell function and its role in surfactant homeostasis (21). Type 2 epithelial cell-specific-ABCG1-deficient mice also develop enlarged type 2 epithelial cells with increased numbers of LB within the cells and higher amounts of phospholipids and cholesterol in the surfactant compared to control *Abcg1*<sup>fllox/fllox</sup> mice, yet their alveolar macrophages appeared normal. Our data suggest that type 2 epithelial cells may be playing an unappreciated role in impaired surfactant clearance that underlies PAP. Therefore, if possible, we want to obtain explanted lung tissue from PAP patients who underwent lung transplantation and perform electron microscopy to better characterize the appearance of type 2 epithelial cells. If these cells have an increase in lamellar bodies and/or are lipid laden, it will be important to elucidate the mechanism underlying this. We want to understand if this is (i) the result of increased uptake of surfactant by the type 2 epithelial cells in an attempt to remove the overabundance of surfactant in the alveolar space via recycling, (ii) if the cells are unable to release the recycled or *de novo* surfactant due to the overabundance of surfactant in the alveolar space, (iii) if there is an increase in surfactant, especially lipid, synthesis, or (iv) if there is some other process. Because isolating type 2

epithelial cells from PAP patients is extremely challenging, we may need to employ an *ex vivo* system and generate alveolospheres containing induced type 2 epithelial cells from pluripotent stem cells (PSC) (32). We can generate alveolospheres from disease-specific iPSC from patients with *CSF2*, *CSF2RA*, or *CSF2RB* mutation and evaluate what happens to the lipid content and lamellar bodies. We can also utilize CRISPR/Cas9 technology to correct the *CSF2*, *CSF2RA*, or *CSF2RB* alleles, resulting in a corrected line to differentiate into alveolospheres and do comparisons with the diseased alveolospheres. Then, we could theoretically expose the alveolospheres to surfactant from non-PAP and PAP patients and measure the lipid content. We may also utilize mouse models of PAP to evaluate lipid synthesis in the lungs *in vivo* by using isotope-labeled water and measuring lipids by GC-MS and Lipidyzer. Hunt and colleagues previously observed an increase in the absolute rate of PC synthesis within the lungs of GM-CSF knockout mice compared to control animals; however, they were unable to assess the rate of PC secretion into the BAL fluid (25). The study of type 2 epithelial cells will provide more insight into the pathogenesis of PAP and possibly identify novel pharmacotherapy targets.

Although studying lipid profiles has enabled us to better understand PAP, we also plan to perform RNA sequencing (RNA-seq) on alveolar macrophages and plasma RNA to investigate the molecular mechanisms underlying the disease process of PAP. This will enable us to look at the transcriptome and identify possibly new pathways that may be involved with the disease. This will also help us find novel drug targets. Because this disease is so heterogenous and because there is currently no specific biomarker available, we additionally want to see if there is an association with a specific transcriptomic profile and a patient's improving or worsening clinical course. We want to identify novel biomarkers that may predict those who may have spontaneous resolution of disease, those who may have stable, chronic disease, those who may



have progressive disease, and those who may develop fibrosis. With this information, we can help prognosticate a patient's clinical trajectory and appropriately tailor a patient's treatment plan. Additionally, we may be able to find novel therapeutic targets. We also plan to perform RNA-seq on patients who are on various therapies. Once again, we hope to find biomarkers that may help predict responders and non-responders to specific therapies so that we can provide personalized medicine to the patients in order to prevent adverse reactions from ineffective therapies. Furthermore, we may consider to do single cell RNA-seq on lung tissues from PAP mouse models, which would enable us to identify other cell populations that may be playing a role in the disease. For example, Hunt and colleagues discovered neutral-lipid droplet accumulations in alveolar lipofibroblasts in the lungs of *Csf2*<sup>-/-</sup> mice, suggesting that other cells might be involved in PAP (25).

Another area of interest is the role of lipids and the immune response. Autoimmune PAP is characterized by high levels of neutralizing GM-CSF autoantibodies in patients (33, 34). Transfer of highly purified, human GM-CSF antibodies to primates caused the development of PAP in the non-human primates (35). Interestingly, low levels of GM-CSF autoantibodies exist in healthy individuals; however, patients with aPAP have concentrations of autoantibodies that cross a "critical threshold" and result in the inhibition of GM-CSF signaling (36-38). These antibodies are composed of polyclonal immunoglobulin G (predominantly subclasses 1 and 2) and appear to target multiple non-overlapping epitopes throughout the GM-CSF molecule, suggesting that the autoantibody formation is not likely due to a pathogen-related, cross-reacting epitope (33, 39). Furthermore, there are numerous somatic mutations in GM-CSF autoantibodies, suggesting that T cells are involved and that B cells have re-entered germinal centers and undergone somatic mutation and affinity selection (40). It is unclear why patients develop these

antibodies. Notably, our lab has demonstrated in the past that specific lipids, like oxidized phospholipids and/or sterols, elicit a lung-specific response in *Abcg1*<sup>-/-</sup> mice (19, 30). There is an increase in natural antibody (Nab)-secreting B-1 B cells in response to the lipid accumulation that is associated with an increase in titers of IgM, IgA, and IgG against oxidation specific epitopes in the lungs. This was also seen in *Abcg1*<sup>T2-KO</sup> mice, where there were increased titers of IgG, IgG2c, and IgA in the BAL fluid compared to the *Abcg1*<sup>flox/flox</sup> mice (21). This may also be true in PAP where specific lipids are homing B-1 B cells to the lungs. We want to measure B-1 B cells and immunoglobulins in the BAL fluid of aPAP patients in addition to the oxidized lipid species as mentioned previously, especially since B-1 B cells have been implicated in other autoimmune diseases (41, 42). An increase in B-1 B cell population may be contributing to the high levels of GM-CSF autoantibodies in autoimmune PAP. Although B-1 B cells tend to secrete IgM or IgG3, they may be serving as antigen presenting cells to T cells, thus triggering an adaptive immune response (43, 44). More studies need to be done to better understand the role of B-1 B cells in PAP if they are indeed present.

### **Concluding remarks**

PAP is a life-threatening, rare lung disease that is caused by an accumulation of surfactant in the alveolar space and has no cure. In the past, the dysregulation of phospholipid metabolism was thought to drive the pathogenesis of PAP and result in the accrual of surfactant in the lungs. More recent studies have shifted the paradigm and suggested that the impairment of cholesterol clearance is the primary defect that causes PAP. This dissertation investigated molecular mechanisms that lead to impaired surfactant clearance in PAP and discovered that in fact, it is the disruption in both phospholipid and cholesterol homeostasis that leads to PAP. We

were also able to identify possible novel biomarkers, specifically PC and CE levels in alveolar macrophages and relative plasma titers of GM-CSF antibody, that can be used to correlate with disease severity. Finally, we demonstrated that statin, a medication that is currently available to decrease plasma cholesterol, improved disease severity in PAP mice and patients, thus proposing it as a possible new pharmacotherapy for PAP. Although advances in research have vastly improved our understanding of PAP in recent years, more studies need to be done to better understand the pathophysiology of PAP and ultimately find a cure for these patients.

## References

1. Griggs RC, Batshaw M, Dunkle M, Gopal-Srivastava R, Kaye E, Krischer J, et al. Clinical research for rare disease: opportunities, challenges, and solutions. *Mol Genet Metab.* 2009;96(1):20-6.
2. Gasson JC. Molecular physiology of granulocyte-macrophage colony-stimulating factor. *Blood.* 1991;77(6):1131-45.
3. Stanley E, Lieschke GJ, Grail D, Metcalf D, Hodgson G, Gall JA, et al. Granulocyte/macrophage colony-stimulating factor-deficient mice show no major perturbation of hematopoiesis but develop a characteristic pulmonary pathology. *Proc Natl Acad Sci U S A.* 1994;91(12):5592-6.
4. Robb L, Drinkwater CC, Metcalf D, Li R, Köntgen F, Nicola NA, et al. Hematopoietic and lung abnormalities in mice with a null mutation of the common beta subunit of the receptors for granulocyte-macrophage colony-stimulating factor and interleukins 3 and 5. *Proc Natl Acad Sci U S A.* 1995;92(21):9565-9.
5. Suzuki T, Shima K, Arumugam P, Ma Y, Black D, Chalk C, et al. Development and validation of *Csf2ra* gene-deficient mice as a clinically relevant model of children with hereditary pulmonary alveolar proteinosis. *Am J Respir Crit Care Med.* 2017;195:A4837.
6. Hamilton JA. GM-CSF in inflammation and autoimmunity. *Trends Immunol.* 2002;23(8):403-8.
7. Guillemins M, De Kleer I, Henri S, Post S, Vanhoutte L, De Prijck S, et al. Alveolar macrophages develop from fetal monocytes that differentiate into long-lived cells in the first week of life via GM-CSF. *J Exp Med.* 2013;210(10):1977-92.
8. Paine R, 3rd, Preston AM, Wilcoxon S, Jin H, Siu BB, Morris SB, et al. Granulocyte-macrophage colony-stimulating factor in the innate immune response to *Pneumocystis carinii* pneumonia in mice. *J Immunol.* 2000;164(5):2602-9.
9. LeVine AM, Reed JA, Kurak KE, Cianciolo E, Whitsett JA. GM-CSF-deficient mice are susceptible to pulmonary group B streptococcal infection. *J Clin Invest.* 1999;103(4):563-9.
10. Ikegami M, Ueda T, Hull W, Whitsett JA, Mulligan RC, Dranoff G, et al. Surfactant metabolism in transgenic mice after granulocyte macrophage-colony stimulating factor ablation. *Am J Physiol.* 1996;270(4 Pt 1):L650-8.
11. Yoshida M, Ikegami M, Reed JA, Chronos ZC, Whitsett JA. GM-CSF regulates protein and lipid catabolism by alveolar macrophages. *Am J Physiol Lung Cell Mol Physiol.* 2001;280(3):L379-L86.

12. Ramirez J, Harlan WR, Jr. Pulmonary alveolar proteinosis. Nature and origin of alveolar lipid. *Am J Med.* 1968;45(4):502-12.
13. Griese M. Pulmonary surfactant in health and human lung diseases: state of the art. *Eur Respir J.* 1999;13(6):1455-76.
14. Sallese A, Suzuki T, McCarthy C, Bridges J, Filuta A, Arumugam P, et al. Targeting cholesterol homeostasis in lung diseases. *Sci Report.* 2017;7(1):10211-4.
15. Bonfield TL, Farver CF, Barna BP, Malur A, Abraham S, Raychaudhuri B, et al. Peroxisome proliferator-activated receptor-gamma is deficient in alveolar macrophages from patients with alveolar proteinosis. *Am J Respir Cell Mol Biol.* 2003;29(6):677-82.
16. Thomassen MJ, Barna BP, Malur AG, Bonfield TL, Farver CF, Malur A, et al. ABCG1 is deficient in alveolar macrophages of GM-CSF knockout mice and patients with pulmonary alveolar proteinosis. *J Lipid Res.* 2007;48(12):2762-8.
17. Cavelier C, Lorenzi I, Rohrer L, von Eckardstein A. Lipid efflux by the ATP-binding cassette transporters ABCA1 and ABCG1. *Biochim Biophys Acta.* 2006;1761(7):655-66.
18. Kennedy MA, Barrera GC, Nakamura K, Baldan A, Tarr P, Fishbein MC, et al. ABCG1 has a critical role in mediating cholesterol efflux to HDL and preventing cellular lipid accumulation. *Cell Metab.* 2005;1(2):121-31.
19. Baldán A, Gomes AV, Ping P, Edwards PA. Loss of ABCG1 results in chronic pulmonary inflammation. *J Immunol.* 2008;180(5):3560-8.
20. Baldan A, Tarr P, Vales CS, Frank J, Shimotake TK, Hawgood S, et al. Deletion of transmembrane transporter ABCG1 results in progressive pulmonary lipidosis. *J Biol Chem.* 2006;281:29401-10.
21. de Aguiar Vallim TQ, Lee E, Merriott DJ, Goulbourne CN, Cheng J, Cheng A, et al. ABCG1 regulates pulmonary surfactant metabolism in mice and men. *J Lipid Res.* 2017;58(5):941-54.
22. McCarthy C, Lee E, Bridges JP, Sallese A, Suzuki T, Woods JC, et al. Statin as a novel pharmacotherapy of pulmonary alveolar proteinosis. *Nat Commun.* 2018;9(1):3127.
23. Suzuki T, Arumugam P, Sakagami T, Lachmann N, Chalk C, Sallese A, et al. Pulmonary macrophage transplantation therapy. *Nature.* 2014;514(7523):450-4.
24. Griese M, Bonella F, Costabel U, de Blic J, Tran NB, Liebisch G. Quantitative lipidomics in pulmonary alveolar proteinosis. *Am J Respir Crit Care Med.* 2019;200(7):881-7.

25. Hunt AN, Malur A, Monfort T, Lagoudakis P, Mahajan S, Postle AD, et al. Hepatic steatosis accompanies pulmonary alveolar proteinosis. *Am J Respir Cell Mol Biol.* 2017;57(4):448-58.
26. Seymour JF, Presneill JJ. Pulmonary alveolar proteinosis: progress in the first 44 years. *Am J Respir Crit Care Med.* 2002;166(2):215-35.
27. Akira M, Inoue Y, Arai T, Sugimoto C, Tokura S, Nakata K, et al. Pulmonary Fibrosis on High-Resolution CT of Patients With Pulmonary Alveolar Proteinosis. *AJR Am J Roentgenol.* 2016;207(3):544-51.
28. Romero F, Shah D, Duong M, Penn RB, Fessler MB, Madenspacher J, et al. A pneumocyte-macrophage paracrine lipid axis drives the lung toward fibrosis. *Am J Respir Cell Mol Biol.* 2015;53(1):74-86.
29. Hou X, Summer R, Chen Z, Tian Y, Ma J, Cui J, et al. Lipid Uptake by Alveolar Macrophages Drives Fibrotic Responses to Silica Dust. *Sci Rep.* 2019;9(1):399.
30. Baldan A, Gonen A, Choung C, Que X, Marquart TJ, Hernandez I, et al. ABCG1 is required for pulmonary B-1 B cell and natural antibody homeostasis. *J Immunol.* 2014;193(11):5637-48.
31. Nishinakamura R, Wiler R, Dirksen U, Morikawa Y, Arai K, Miyajima A, et al. The pulmonary alveolar proteinosis in granulocyte macrophage colony-stimulating factor/interleukins 3/5 beta c receptor-deficient mice is reversed by bone marrow transplantation. *J Exp Med.* 1996;183(6):2657-62.
32. Jacob A, Morley M, Hawkins F, McCauley KB, Jean JC, Heins H, et al. Differentiation of Human Pluripotent Stem Cells into Functional Lung Alveolar Epithelial Cells. *Cell Stem Cell.* 2017;21(4):472-88.
33. Kitamura T, Tanaka N, Watanabe J, Uchida K, Kanegasaki S, Yamada Y, et al. Idiopathic pulmonary alveolar proteinosis as an autoimmune disease with neutralizing antibody against granulocyte/macrophage colony-stimulating factor. *J Exp Med.* 1999;190(6):875-80.
34. Tanaka N, Watanabe J, Kitamura T, Yamada Y, Kanegasaki S, Nakata K. Lungs of patients with idiopathic pulmonary alveolar proteinosis express a factor which neutralizes granulocyte-macrophage colony stimulating factor. *FEBS Lett.* 1999;442(2-3):246-50.
35. Sakagami T, Beck D, Uchida K, Suzuki T, Carey BC, Nakata K, et al. Patient-derived granulocyte/macrophage colony-stimulating factor autoantibodies reproduce pulmonary alveolar proteinosis in nonhuman primates. *Am J Respir Crit Care Med.* 2010;182(1):49-61.
36. Uchida K, Nakata K, Suzuki T, Luisetti M, Watanabe M, Koch DE, et al. Granulocyte/macrophage-colony-stimulating factor autoantibodies and myeloid cell immune functions in healthy subjects. *Blood.* 2009;113(11):2547-56.

37. Bendtzen K, Svenson M, Hansen MB. GM-CSF autoantibodies in pulmonary alveolar proteinosis. *N Engl J Med.* 2007;356(19):2001-2.
38. Uchida K, Nakata K, Carey B, Chalk C, Suzuki T, Sakagami T, et al. Standardized serum GM-CSF autoantibody testing for the routine clinical diagnosis of autoimmune pulmonary alveolar proteinosis. *J Immunol Methods.* 2014;402(1-2):57-70.
39. Uchida K, Nakata K, Trapnell BC, Terakawa T, Hamano E, Mikami A, et al. High-affinity autoantibodies specifically eliminate granulocyte-macrophage colony-stimulating factor activity in the lungs of patients with idiopathic pulmonary alveolar proteinosis. *Blood.* 2004;103(3):1089-98.
40. Wang Y, Thomson CA, Allan LL, Jackson LM, Olson M, Hercus TR, et al. Characterization of pathogenic human monoclonal autoantibodies against GM-CSF. *Proc Natl Acad Sci U S A.* 2013;110(19):7832-7.
41. Sato T, Ishikawa S, Akadegawa K, Ito T, Yurino H, Kitabatake M, et al. Aberrant B1 cell migration into the thymus results in activation of CD4 T cells through its potent antigen-presenting activity in the development of murine lupus. *Eur J Immunol.* 2004;34(12):3346-58.
42. Duan B, Morel L. Role of B-1a cells in autoimmunity. *Autoimmun Rev.* 2006;5(6):403-8.
43. Baumgarth N. A Hard(y) Look at B-1 Cell Development and Function. *J Immunol.* 2017;199(10):3387-94.
44. Popi AF, Longo-Maugéri IM, Mariano M. An Overview of B-1 Cells as Antigen-Presenting Cells. *Front Immunol.* 2016;7:138.